

SECOND CLASS PARTICLES AND LIMIT SHAPES OF EVACUATION AND SLIDING PATHS FOR RANDOM TABLEAUX

ŁUKASZ MAŚLANKA AND PIOTR ŚNIADY

ABSTRACT. We investigate two closely related setups. In the first one we consider a TASEP-style system of particles with specified initial and final configurations. The probability of each history of the system is assumed to be equal. We show that the rescaled trajectory of the *second class particle* converges (as the size of the system tends to infinity) to a random arc of an ellipse.

In the second setup we consider a uniformly random Young tableau of square shape and look for typical (in the sense of probability) *sliding paths* and *evacuation paths* in the asymptotic setting as the size of the square tends to infinity. We show that the probability distribution of such paths converges to a random *meridian* connecting the opposite corners of the square. We also discuss analogous results for non-square Young tableaux.

1. INTRODUCTION

This article is the full version of a 12-page extended abstract [MŚ20] which was published in the proceedings of the *32nd International Conference on Formal Power Series and Algebraic Combinatorics, FPSAC 2020*.

The results of the current paper concern two distinct setups which are closely connected. The first one, presented in Section 1.1, involves a certain interacting particle system. The second one, presented in Section 1.3, involves random Young tableaux.

1.1. TASEP system with the uniform distribution over histories.

1.1.1. The setup. For given integers $N, M \geq 1$ we consider the particle system depicted on Figure 1. There are $N + M - 1$ nodes, labeled by the

2020 *Mathematics Subject Classification.* 60C05 (Primary), 05E10, 60K35, 82C22 (Secondary).

Key words and phrases. second class particles, interacting particle systems, TASEP, random Young tableaux, limit shape, jeu de taquin, promotion, Schützenberger’s evacuation, square Young tableaux.

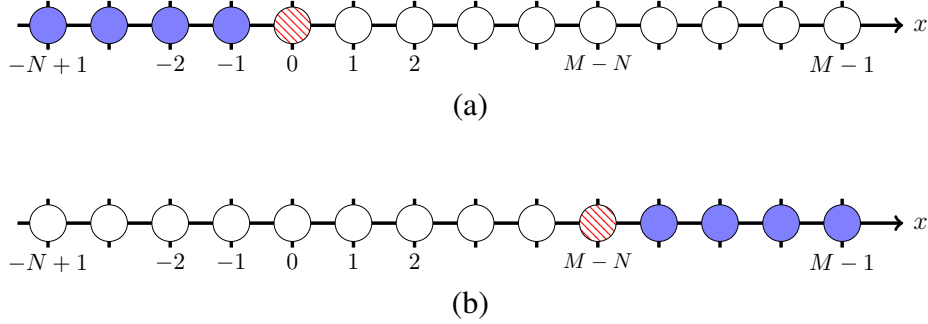


Figure 1. (a) The initial configuration of the particle system. The first class particles are depicted as filled blue circles, the holes are depicted as empty circles. The striped red circle denotes the second class particle. (b) The final configuration of the particle system.

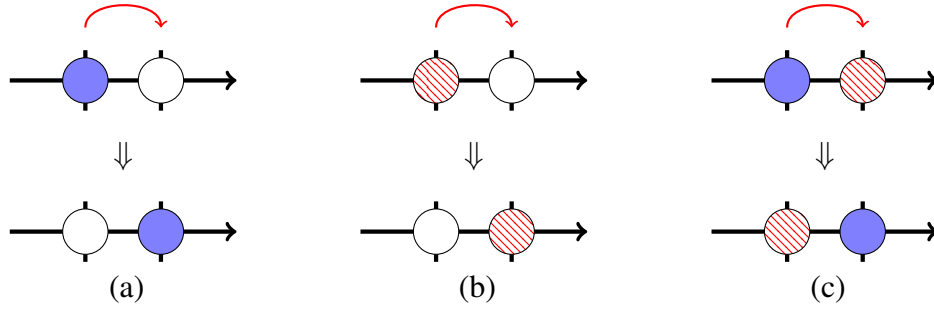


Figure 2. Three allowed types of transitions: (a) a first class particle can jump to the right if the next node is free, (b) the second class particle can jump to the right if the next node is free, (c) the first class particle can jump to the right if the next node is occupied by the second class particle; in this case the second class particle has to yield and the particles exchange their places.

integers from the set

$$(1.1) \quad \{-N+1, \dots, 0, 1, \dots, M-1\}.$$

In the initial configuration (which corresponds to the time $t = 1$) the $N - 1$ nodes which correspond to the negative integers are occupied by *the first class particles*, the $M - 1$ nodes which correspond to the positive integers are empty (or, equivalently, are occupied by *holes*), and the node which corresponds to zero is occupied by *the second class particle*, see Figure 1a.

In each step exactly one of the following transitions occurs:

- any particle (first or second class) may jump right to the next node provided that this node is empty, see Figures 2a and 2b, or
- a first class particle may jump right to the next node provided that this node is occupied by the second class particle. In this case the second class particle has to yield and jumps one node to the left, see Figure 2c.

The *second class particle* is an analogue of a passenger with a cheap second class ticket who has to yield the seat to any passenger with a more expensive first class ticket.

It is not very difficult to show that no matter which transitions occur, the system terminates at time $t_{\max} = MN$ (that is after $MN - 1$ transitions) in the configuration shown on Figure 1b in which no additional transition is allowed.

By the *history* we will understand the information about the state of the particle system over all values of the time $t \in \{1, \dots, t_{\max}\}$, see Figure 3 for an example. We consider the finite set of all possible histories of the particle system and associate to each such a history equal probability. In other words, we consider a version of the TASEP (which is an acronym for Totally Asymmetric Simple Exclusion Process) system [Spi70] with modified transition probabilities.

1.1.2. Why second class particles? Macroscopic quantities describing an interacting particle system (such as particle density) are usually described by nonlinear partial differential equations (PDEs for short). For example, the famous Burgers equation [Bur48] describes the density profile in the hydrodynamical limit for the asymmetric simple exclusion process [BF87]. Weak solutions of nonlinear PDEs can develop singularities, often referred to as *shocks*. The shocks can be found by looking for the crossings of the characteristic lines of the PDE.

Ferrari [Fer92] discovered that a second class particle, depending on the place in which it begins its journey, can identify microscopically the location of the shock or describe the behavior of the characteristic lines of the limiting hydrodynamic equation. Ferrari and Fontes showed in [FF94] that this hydrodynamical limit converges to the traveling wave solution of the inviscid Burgers equation. This connection was later transferred to more general settings by Rezakhanlou [Rez95], Ferrari and Kipnis [FK95], Sepäläinen [Sep01] and others. Furthermore, the second class particle enters naturally in the study of the fluctuations of the current of particles [FF94].

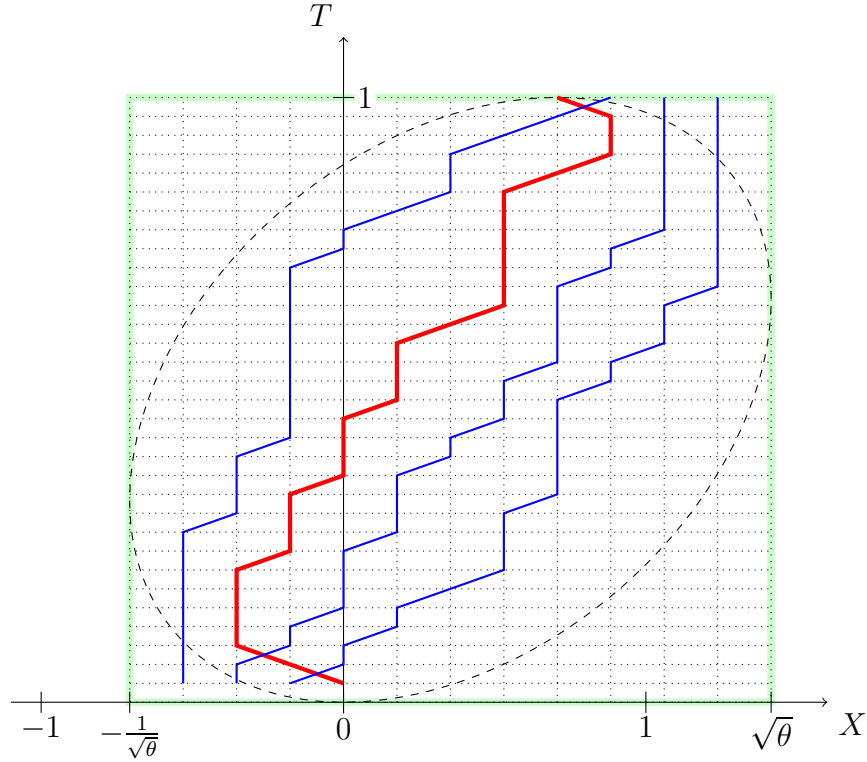


Figure 3. Sample history of the particle system for $N = 4$ and $M = 8$. The trajectories of the first class particles are shown as solid blue lines, the trajectory of the second class particle is shown as the thick red line. The thick green rectangle indicates the *bounding box*. The dashed line indicates the *arctic ellipse* which corresponds to the shape parameter $\theta = \frac{M}{N} = 2$.

A pictorial interpretation of TASEP as a traffic model is given in [MG05]. The particles are interpreted as cars on a single-line highway with no possibility of passing (which corresponds to the exclusion rule) and the shock corresponds to the front of the traffic jam. The motion of the shock is referred to as the *propagation of the shock* or the *rarefaction wave* (or *rarefaction fan*) depending whether the shock moves to the left or is being resorpted. The second class particle identifies the shock and allows to qualitatively describe its motion.

Mountford and Guiol [MG05] studied in fact a more advanced physical interpretation of the TASEP model as a moving interface on the plane (space-time). This gave them a powerful tool to analyze the shocks in the TASEP process in terms of the last passage percolation.

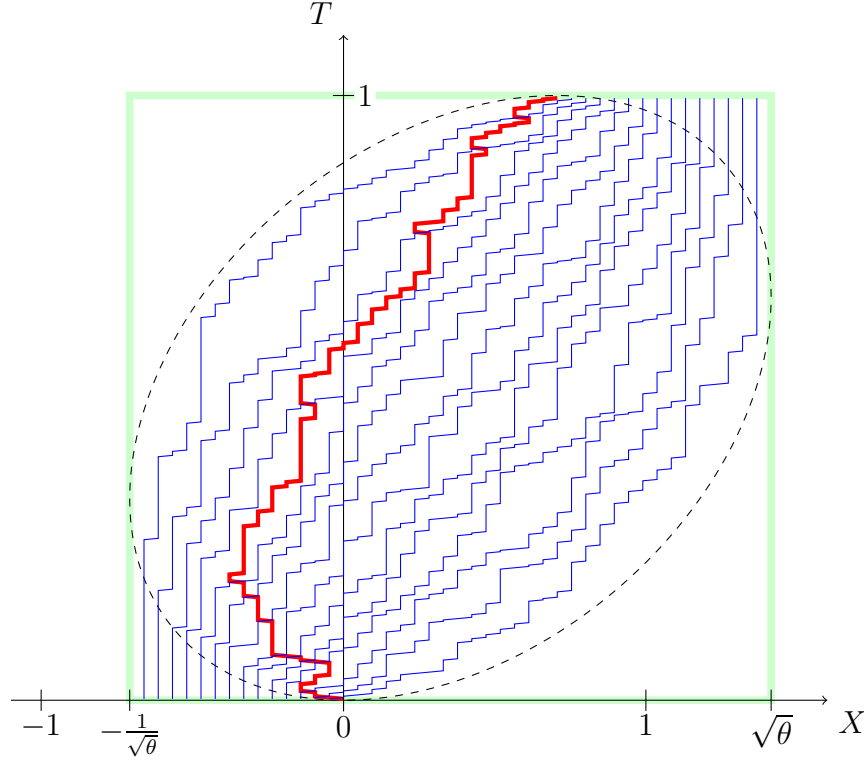


Figure 4. An analogue of Figure 3 for $N = 15$ and $M = 30$.

A nice heuristic (as well as rigorous) explanation of the shocks behavior and the importance of the second class particles in this context can be found in the book of Liggett [Lig99, Part III].

1.1.3. *The asymptotic setup.* We assume that (M_i) and (N_i) are two sequences of positive integers which tend to infinity and such that their ratio

$$\lim_{i \rightarrow \infty} \frac{M_i}{N_i} = \theta > 0$$

converges to some positive limit which we call *the shape parameter*. For $t \in \{1, \dots, M_i N_i\}$ we denote by $u_i(t) \in \{-N_i + 1, \dots, M_i - 1\}$ the position of the second class particle at time t . In order to keep the notation lightweight we will sometimes omit the index i and instead of $M_i, N_i, u_i(t)$ we will write shortly $M, N, u(t)$.

Until now we parameterized the space using the integer parameter $x \in \{-N+1, \dots, M-1\}$ and the time using the integer parameter $t \in \{1, \dots, MN\}$, however for asymptotic questions it is more convenient to pass to the rescaled

coordinates

$$X = \frac{x}{\sqrt{MN}} \in \left[-\frac{1}{\sqrt{M/N}}, \sqrt{M/N} \right],$$

$$T = \frac{t}{t_{\max}} \in [0, 1],$$

see Figures 3 and 4. The rectangle

$$(1.2) \quad B_\theta = \left\{ (X, T) : X \in \left[-\frac{1}{\sqrt{\theta}}, \sqrt{\theta} \right], \quad T \in [0, 1] \right\}$$

which shows the range in which the coordinates X and T vary asymptotically will be called *the bounding box*; on Figures 3 to 5 it is shown as the green rectangle.

For each value of the parameter $s \in [-1, 1]$ we define a function

$$\Xi_s : [0, 1] \rightarrow \left[-\frac{1}{\sqrt{\theta}}, \sqrt{\theta} \right]$$

given by

$$\Xi_s(T) = 2\sqrt{T(1-T)} s + \frac{\theta - 1}{\sqrt{\theta}} T,$$

see Figure 5.

1.1.4. The main result 1: the trajectory of the second class particle.

Theorem 1.1. *We keep the assumptions and notations from Section 1.1.3.*

Then there exists a sequence (S_i) of random variables with the property that the supremum distance

$$\sup_{T \in [0, 1]} \left| \frac{1}{\sqrt{M_i N_i}} u_i(\lceil T M_i N_i \rceil) - \Xi_{S_i}(T) \right|$$

converges in probability to zero, as $i \rightarrow \infty$.

The probability distribution of S_i is supported on the interval $[-1, 1]$ and for $i \rightarrow \infty$ it converges to the standard semicircular distribution with the density

$$(1.3) \quad f_{\text{SC}}(x) = \frac{2}{\pi} \sqrt{1 - x^2} \quad \text{for } x \in [-1, 1].$$

This theorem is illustrated on Figure 5. Its proof is postponed to Section 11. This result is analogous to the results of Ferrari and Kipnis [FK95], as well as Mountford and Guiol [MG05] for the usual TASEP system starting from a decreasing shock profile.

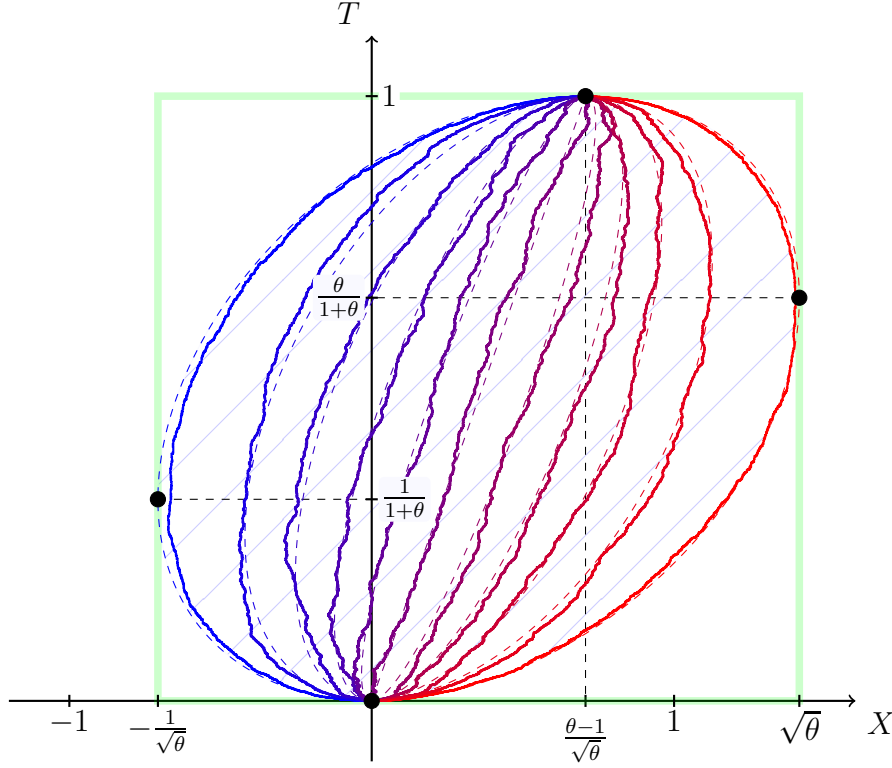


Figure 5. The dashed lines are arcs of ellipses Ξ_s for the shape parameter $\theta = 2$. The shown values of the parameter $s \in F_{SC}^{-1} \{0/10, 1/10, \dots, 10/10\}$ are the deciles of the semicircle distribution (above $F_{SC}: [-1, 1] \rightarrow [0, 1]$ denotes the cumulative distribution function of the semicircle distribution (1.3)). The shaded region forms *the arctic ellipse*. The four black dots are the points where the arctic ellipse is tangent to the bounding box. The solid zigzag lines are trajectories of the second class particle for $N = 500$ and $M = 1000$. These trajectories were selected from a sample of 1000 simulations; each of them corresponds to an appropriate empirical decile of the distribution of the second class particle at time $T = \frac{1}{2}$.

1.1.5. *The limit trajectories.* Each curve Ξ_s for the parameter $s \in [-1, 1] \setminus \{0\}$ is an arc of an ellipse which fits into the bounding box B_θ , passes through the points

$$(1.4) \quad (0, 0), \quad \left(\frac{\theta - 1}{\sqrt{\theta}}, 1 \right),$$

and is tangent there to the bottom and the top edge of the bounding box B_θ . In the degenerate case $s = 0$ the curve Ξ_0 is a straight line connecting the aforementioned two points (1.4). The union of the two extreme curves Ξ_{-1} and Ξ_1 is the unique ellipse (which we call *the arctic ellipse*) which is inscribed into the bounding box B_θ and is tangent to its bottom and its top side in the aforementioned two points (1.4), see Figure 5. In the special case $\theta = 1$ the scaling of the axes can be chosen in such a way that the arctic ellipse becomes a circle which we call the “*the arctic circle*”. Our use of this name is not a coincidence since it turns out to be indeed related to the celebrated *arctic circle theorem* [Rom12].

1.2. Random sorting networks. Theorem 1.1 can be regarded as the solution to a toy version of the problem of *random sorting networks* considered by Angel, Holroyd, Romik, and Virág [AHRV07]. More specifically, we consider the symmetric group \mathfrak{S}_{N+M-1} viewed as the set of permutations of the set of nodes (1.1) and the permutation $\rho_{N,M} \in \mathfrak{S}_{N+M-1}$ defined as

$$\rho_{N,M}(i) = \begin{cases} i + M & \text{if } i \in \{-N + 1, \dots, -1\}, \\ M - N & \text{if } i = 0, \\ i - N & \text{if } i \in \{1, \dots, M - 1\} \end{cases}$$

which describes the change of the positions of the particles and holes during the passage from the initial configuration shown on Figure 1a to the final configuration shown on Figure 1b. For an integer $s \in \{-N + 1, \dots, M - 2\}$ denote the adjacent transposition at location s by $\tau_s = (s, s + 1) \in \mathfrak{S}_{N+M-1}$.

Any history of the particle system considered in Section 1.1.1 can be encoded by the sequence $s_1, \dots, s_{t_{\max}-1} \in \{-N + 1, \dots, M - 2\}$, where s_t and $s_t + 1$ are the nodes which are interchanged in t -th transition. It is easy to check that

$$(1.5) \quad \rho_{N,M} = \tau_{s_{t_{\max}-1}} \tau_{s_{t_{\max}-2}} \cdots \tau_{s_2} \tau_{s_1}$$

and the corresponding sequence of partial products

$$(1.6) \quad \text{id}, \quad \tau_{s_1}, \quad \tau_{s_2} \tau_{s_1}, \quad \dots, \quad \tau_{s_{t_{\max}-1}} \tau_{s_{t_{\max}-2}} \cdots \tau_{s_2} \tau_{s_1}$$

is a shortest path from the identity permutation id to $\rho_{N,M}$ in the Cayley graph of the symmetric group \mathfrak{S}_{N+M-1} generated by adjacent transpositions.

Conversely, each shortest path (1.6) in the Cayley graph gives a valid history of the particle system. Any such a shortest path will be called a *sorting network*. The trajectory of the second class particle

$$(1.7) \quad (u(t) : t \in \{1, \dots, t_{\max}\}) = (0, \quad \tau_{s_1}(0), \quad \tau_{s_2} \tau_{s_1}(0), \quad \dots, \quad \tau_{s_{t_{\max}-1}} \cdots \tau_{s_2} \tau_{s_1}(0))$$

corresponds in this language to the sequence of images of 0 under the action of the entries of the sequence (1.6).

Angel, Holroyd, Romik, and Virág [AHRV07] considered a more difficult version of this setup in which the permutation $\rho_{N,M}$ is replaced by the *reverse permutation* $\rho \in \mathfrak{S}_{N+M-1}$ given by

$$\rho(i) = M - N - i$$

and—among several other results—stated some conjectures concerning the asymptotic behavior of the right-hand side of (1.7) for a *random sorting network*, i.e., a random shortest path from the identity permutation id to the reverse permutation ρ , sampled with the uniform distribution. We focus today on [AHRV07, Conjecture 1] which is a direct analogue of our Theorem 1.1. A minor difference is that the limit curves which appear in Theorem 1.1 form a one-parameter family of arcs of ellipses while the limit curves which appear in [AHRV07, Conjecture 1] form a one-parameter family of *sine curves*. (At first sight it might appear that the family of curves in [AHRV07] has two parameters, but one of these parameters can be eliminated by the requirement about the positions of the endpoints.)

The aforementioned conjecture [AHRV07, Conjecture 1] was proved only very recently by Dauvergne and Virág [DV20] who used methods quite different from those which we use in the current paper.

1.3. Sliding paths and evacuation paths in random tableaux. As promised, we turn now to the second interest area of the current paper, namely to random Young tableaux.

1.3.1. Notations related to Young diagrams and tableaux. We assume the reader's basic knowledge of tableaux theory, including partitions, (skew) Young diagrams, standard (skew) Young tableaux, RSK algorithm, jeu de taquin, rectification, Littlewood–Richardson coefficients and basics of the representation theory of the symmetric groups.

We denote the set of partitions of n by \mathbb{Y}_n . We draw Young diagrams on the Cartesian plane using the French convention, that is, we draw them from the bottom to the top, see Figure 6a.

For any Young diagram λ we denote the set of standard Young tableaux of shape λ by \mathcal{T}_λ . The *shape* of a tableau T will be denoted by $\text{sh}(T)$ and its size by $|\text{sh}(T)|$, or shortly $|T|$.

Let T be a tableau. If p is a number which appears exactly once in T (which will always be the case in our considerations), we define the *position of the box with the number p* as the Cartesian coordinates of the bottom-left corner of the unique square which contains p ; we denote this position by $\text{pos}_p(T)$. For example, for T from Figure 6b, $\text{pos}_5(T) = (2, 0)$.

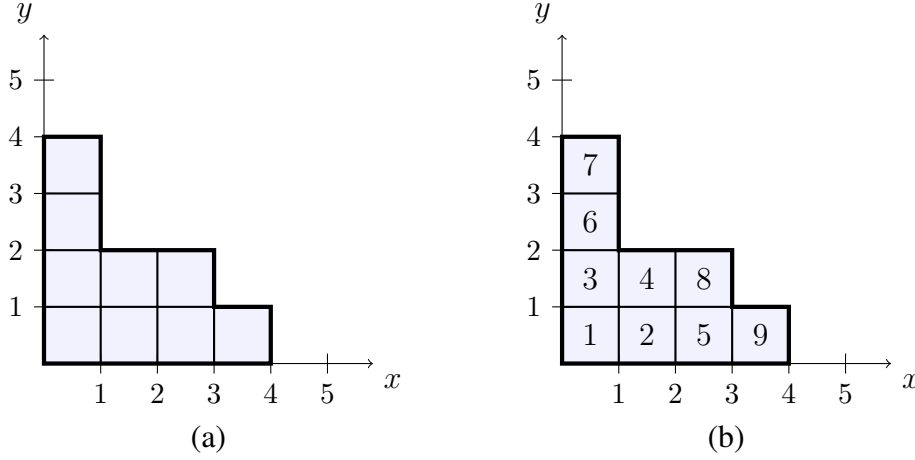


Figure 6. (a) The Young diagram $\lambda = (4, 3, 1, 1)$ shown in the Cartesian coordinate system. (b) Example of a standard Young tableau of shape λ .

We will have a particular interest in Young diagrams and tableaux of square shape. By $\square_N \in \mathbb{Y}_{N^2}$ we denote the square diagram with side of length N .

1.3.2. Sliding paths and evacuation paths. One of the operations heavily used in the study of Young tableaux is *jeu de taquin* [Ful97, Section 1.2], which acts on Young tableaux in the following way (see Figures 8a and 8b): we remove the bottom-left box of the given tableau T and obtain a *hole* in its place. Then we look at the two boxes: the one to the right and the one above the hole, and choose the one which contains the smaller number. We slide this smaller box into the location of the hole, see Figure 7. As a result, the hole moves in the opposite direction. We continue this operation as long as there is some box to the right or above the hole. The path which was traversed by the ‘traveling hole’ will be called the *sliding path*, see Figure 8a. The result of *jeu de taquin* applied to a tableau T will be denoted by $j(T)$, see Figure 8b.

If T is a standard tableau then $j(T)$ is no longer standard because the numbering of its boxes starts with 2; however, if we decrease each entry of $j(T)$ by 1 then it becomes standard. This observation allows us to define the *dual promotion* $\partial^*: \mathcal{T}_\lambda \rightarrow \mathcal{T}_\lambda$ which is a bijection on the set of standard Young tableaux of any fixed shape λ . The idea is to put once again the box with the number $|T|$ to the aforementioned standardized version of the tableau $j(T)$ in the place where we removed a box during *jeu de taquin*, see Figure 8c.

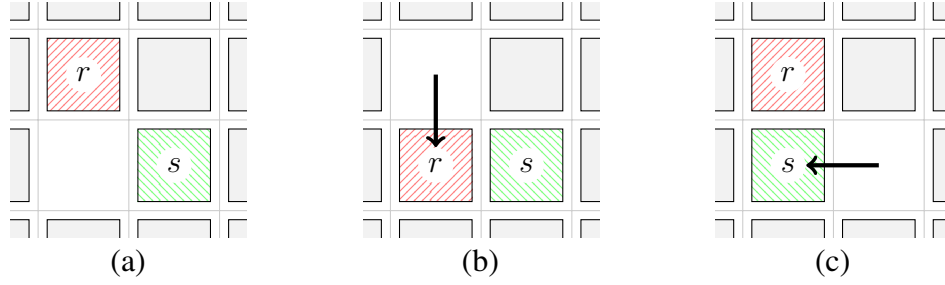


Figure 7. Elementary step of the jeu de taquin transformation: (a) the initial configuration of boxes, (b) the outcome of the slide in the case when $r < s$, (c) the outcome of the slide in the case when $s < r$. Copyright ©2014 Society for Industrial and Applied Mathematics. Reprinted from [Śni14] with permission. All rights reserved.

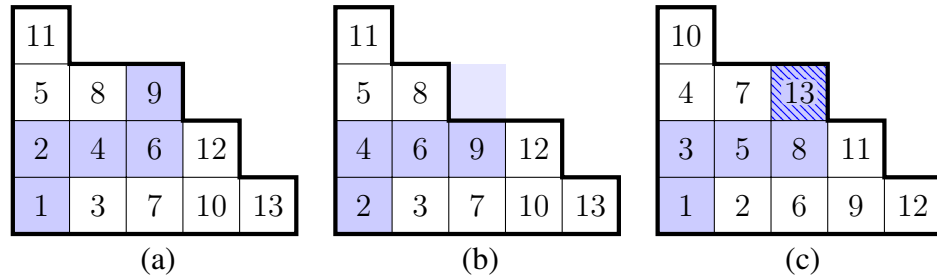


Figure 8. (a) A standard Young tableau T of shape $\lambda = (5, 4, 2, 1)$. The highlighted boxes form the *sliding path*. (b) The outcome $j(T)$ of the jeu de taquin transformation. (c) The result $\partial^*(T)$ of the *dual promotion* applied to T .

For a given tableau $T \in \mathcal{T}_\lambda$ with $n = |\lambda|$ boxes the jeu de taquin transformation j can be iterated n times until we end with the empty tableau. During each iteration the box with the biggest number n either moves one node left or down, or stays put. Its trajectory

$$(1.8) \quad \text{evac}(T) = \left(\text{pos}_n(T), \text{pos}_n(j(T)), \dots, \text{pos}_n(j^{n-1}(T)) \right)$$

will be called the *evacuation path*.

1.3.3. *The main results 2 and 3: asymptotics of sliding paths and evacuation paths.* Observe that if we draw the boxes of a given square tableau $T \in \mathcal{T}_{\square_N}$ as little squares of size $\frac{1}{N}$ then the corresponding sliding path is a zigzag line connecting the opposite corners of the unit square $[0, 1]^2$.

Let $T \in \mathcal{T}_{\square_N}$ be a random standard Young tableau of square shape (sampled with the uniform probability distribution on \mathcal{T}_{\square_N} which will be denoted \mathbb{P}_N). Our goal is to find asymptotics of such random zigzag lines in the limit as $N \rightarrow \infty$, see Figure 9. We will show that there exists a family of smooth lines, called *meridians*, which connect the opposite corners of the unit square, with the property that the probability distribution of the scaled sliding path for a random tableau converges, as $N \rightarrow \infty$, to a random meridian.

An analogous result holds true for the scaled evacuation path for a random square tableau: during iteratively applied jeu de taquin operations j , the biggest box of the tableau asymptotically moves along a random meridian.

A version of this result applies also to the other boxes of the tableau; it follows that the time evolution of the tableau in the iterated applications of jeu de taquin

$$(1.9) \quad T, j(T), j^2(T), \dots, j^{N^2}(T)$$

converges in probability, as $N \rightarrow \infty$, to dynamics of an incompressible liquid which flows along the meridians.

For the details of our results, see Theorems 2.3 and 2.4 in Section 2.

1.3.4. Not only squares. For simplicity and concreteness we stated our main results concerning random Young tableaux only for large random Young tableaux of *square shape*. However, analogous results hold true also for random tableaux of shape which is a *balanced Young diagram* (see Section 3 for the definition and Figure 10 for a teaser). In Section 10 we present a way in which the results obtained in this paper can be used (or generalized) in order to cover the class of balanced Young diagrams.

1.4. The content of the paper. The paper is organized as follows.

In Section 2 we state the main results (Theorems 2.3 and 2.4) about the typical shapes of the evacuation paths and sliding paths in square Young tableaux.

In Section 3 we give basic definitions on permutations and representation theory.

In Section 4 we introduce a ‘surfers’ language which we will use to describe dynamics of the box with the biggest entry (which we will call ‘the surfer’) and the smaller boxes (‘the water’). In this spirit we also introduce the story of the *multisurfers* which will play a crucial role in our proofs and considerations. We will use this new multisurfer story later as a point of reference for the original problem of the (single) surfer in order to prove

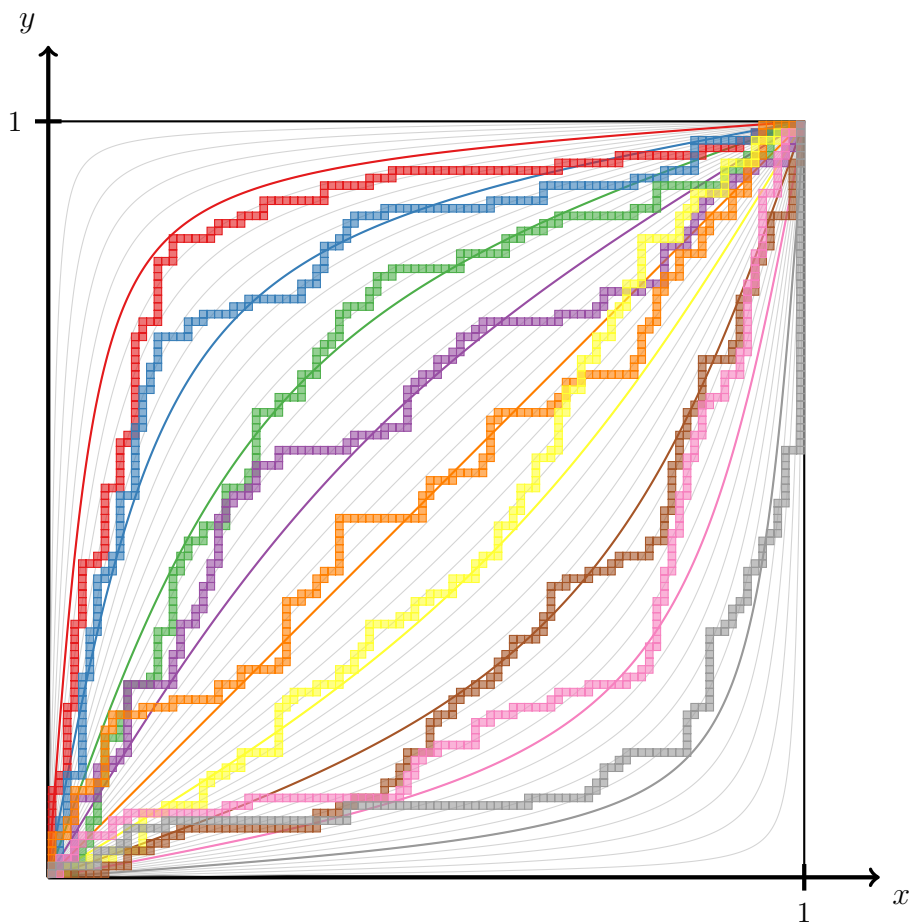


Figure 9. The nine zigzag lines are sample sliding paths for random square tableaux of size $N = 100$, selected so that they cross the anti-diagonal near the corresponding meridians (smooth thick curves) with the longitudes $\psi \in \{1/10, 2/10, \dots, 9/10\}$. The gray lines are the meridians with the longitudes $\psi \in \{2/100, 4/100, \dots, 98/100\}$. See also the blue-to-red family of curves on Figure 13.

Theorem 4.1 concerning the position of the surfer along its journey. We sketch the proof in Section 4.4.

In Section 5 we show the way in which we will embed simultaneously both the story of the single surfer and the story of the multisurfers into a common universe.

In Section 6 we provide Theorem 6.2 concerning the distribution of the multisurfers on the water. We use here the Jucys–Murphy elements to give a direct link between the statistical properties of the multisurfers and the

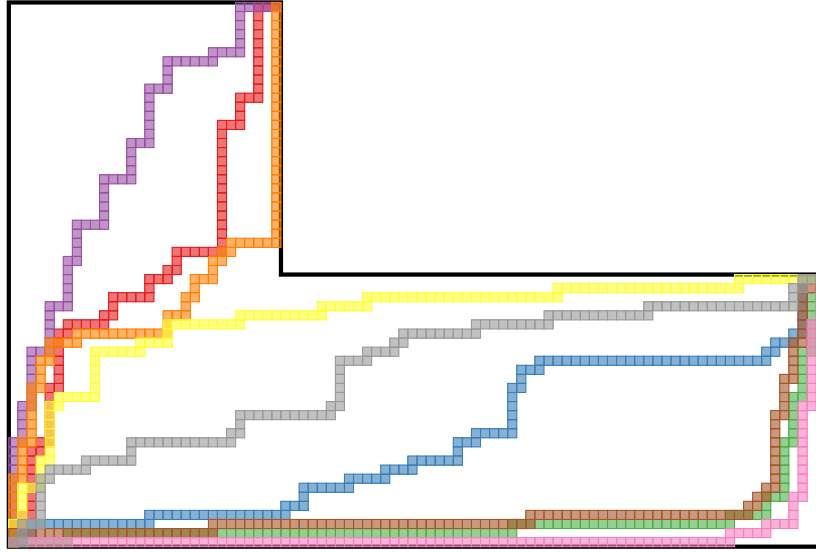


Figure 10. Sample sliding paths in random Young tableaux of an L -shape with 3600 boxes.

symmetric group characters evaluated on certain polynomials in the Jucys–Murphy elements.

In Section 7 we use the aforementioned results from Sections 5 and 6 to prove Theorem 4.1.

In Section 8 we prove Theorem 2.3 concerning typical evacuation paths.

Section 9 is devoted to the proof of Proposition 9.1 which shows the equivalence between the problems of finding the sliding paths and the evacuation paths in random Young tableaux of given shape.

In Section 10 we extend our main results (Theorem 10.5) concerning typical evacuation and sliding paths to some subset of C -balanced Young tableaux.

In Section 11 we provide the link between the trajectory of the second class particle in an interacting particle system and the sliding path for a random Young tableau and prove Theorem 1.1.

2. THE LIMIT SHAPE OF SLIDING PATHS AND EVACUATION PATHS

2.1. Asymptotics of a single box in the evacuation trajectory. As we mentioned in Section 1.3, we will focus on random standard Young tableaux of square shape \square_N sampled according to the uniform measure \mathbb{P}_N . The symbol T_N will be reserved for such a uniformly random square Young tableau of shape \square_N .

The position of each of the boxes in the evacuation path (1.8) coincides with the position of a specific box in the standard Young tableau obtained

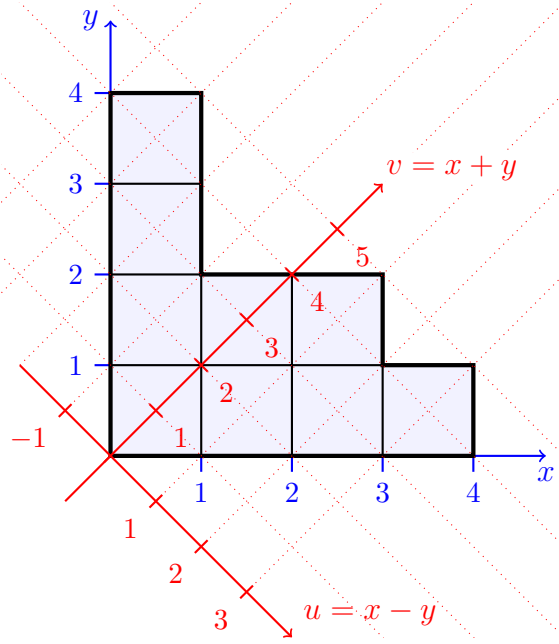


Figure 11. The Cartesian and the Russian coordinate systems on the plane.

by iterating the dual promotion ∂^* :

$$(2.1) \quad \text{pos}_{N^2} (j^i(T_N)) = \text{pos}_{N^2-i} (\partial^{*i}(T_N)).$$

Since $\partial^*: \mathcal{T}_{\square_N} \rightarrow \mathcal{T}_{\square_N}$ is a bijection, for each $i \geq 0$ the latter standard tableaux $\partial^{*i}(T_N)$ is also a uniformly random square Young tableau. It follows that the solution to the (much simpler) problem of understanding the asymptotics of a *single* element of the evacuation trajectory (1.8) follows from the work of Pittel and Romik [PR07], see also Section 2.3 below. In the current section we will recall the details of their work and we will use it to state our second main result, Theorem 2.3 (which addresses the more complex problem of understanding the *whole* evacuation trajectory (1.8)) and the third main result, Theorem 2.4.

2.2. The circles of latitude g_α . The *Russian coordinate system* is given by the following transformation of the Cartesian plane (warning: our notations differ from those of Pittel and Romik [PR07] who scale the coordinates below by an additional factor $1/\sqrt{2}$):

$$u := x - y, \quad v := x + y,$$

see Figure 11.

For each $0 \leq \alpha \leq 1$ and $u \in \left[-2\sqrt{\alpha(1-\alpha)}, 2\sqrt{\alpha(1-\alpha)}\right]$ define

$$k_{\alpha,u} := \sqrt{4\alpha(1-\alpha) - u^2}$$

and for any $0 < \alpha < 1$ the function

$$h_\alpha: \left[-2\sqrt{\alpha(1-\alpha)}, 2\sqrt{\alpha(1-\alpha)}\right] \rightarrow \mathbb{R}$$

given by

(2.2)

$$h_\alpha(u) := \begin{cases} \frac{2u}{\pi} \arctan\left(\frac{1-2\alpha}{k_{\alpha,u}} \cdot u\right) + \frac{2}{\pi} \arctan\left(\frac{k_{\alpha,u}}{1-2\alpha}\right) & \text{if } 0 < \alpha < \frac{1}{2}, \\ 2 - \frac{2u}{\pi} \arctan\left(\frac{2\alpha-1}{k_{\alpha,u}} \cdot u\right) - \frac{2}{\pi} \arctan\left(\frac{k_{\alpha,u}}{2\alpha-1}\right) & \text{if } \frac{1}{2} < \alpha < 1, \\ 1 & \text{if } \alpha = \frac{1}{2}. \end{cases}$$

In the expression above there may occur $k_{\alpha,u} = 0$ in the denominator; in such case (for fixed $\alpha \in (0, 1)$) we consider the appropriate limit: if $u_0 = \pm 2\sqrt{\alpha(1-\alpha)}$ then

$$h_\alpha(u_0) := \lim_{u \rightarrow u_0} h_\alpha(u) = \begin{cases} u_0 & \text{for } 0 < \alpha < \frac{1}{2}, \\ 2 - u_0 & \text{for } \frac{1}{2} < \alpha < 1. \end{cases}$$

Additionally we define the one-point functions $h_0(0) := 0$ and $h_1(0) := 2$.

For any $\alpha \in [0, 1]$ we consider the curve which in the Russian coordinate system is defined as

$$(2.3) \quad g_\alpha^{\text{Rus}} := \left\{ (u, h_\alpha(u)) : |u| \leq 2\sqrt{\alpha(1-\alpha)} \right\} \subset \mathbb{R}^2$$

and, equivalently, in the Cartesian coordinates is given by (see Figures 12 and 13)

$$g_\alpha := \left\{ \left(\frac{u + h_\alpha(u)}{2}, \frac{h_\alpha(u) - u}{2} \right) : |u| \leq 2\sqrt{\alpha(1-\alpha)} \right\} \subset [0, 1]^2.$$

We call g_α **the circle of latitude** with the latitude α .

Roughly speaking, for each $\alpha \in [0, 1]$ the (scaled down) α -level curve (which separates the boxes with entries $\leq \alpha N^2$ from the boxes bigger than this threshold, see Figure 12) in a uniformly random square tableau T_N converges in probability, as $N \rightarrow \infty$, to the circle of latitude g_α , see [PR07, Theorem 1] for a precise statement.

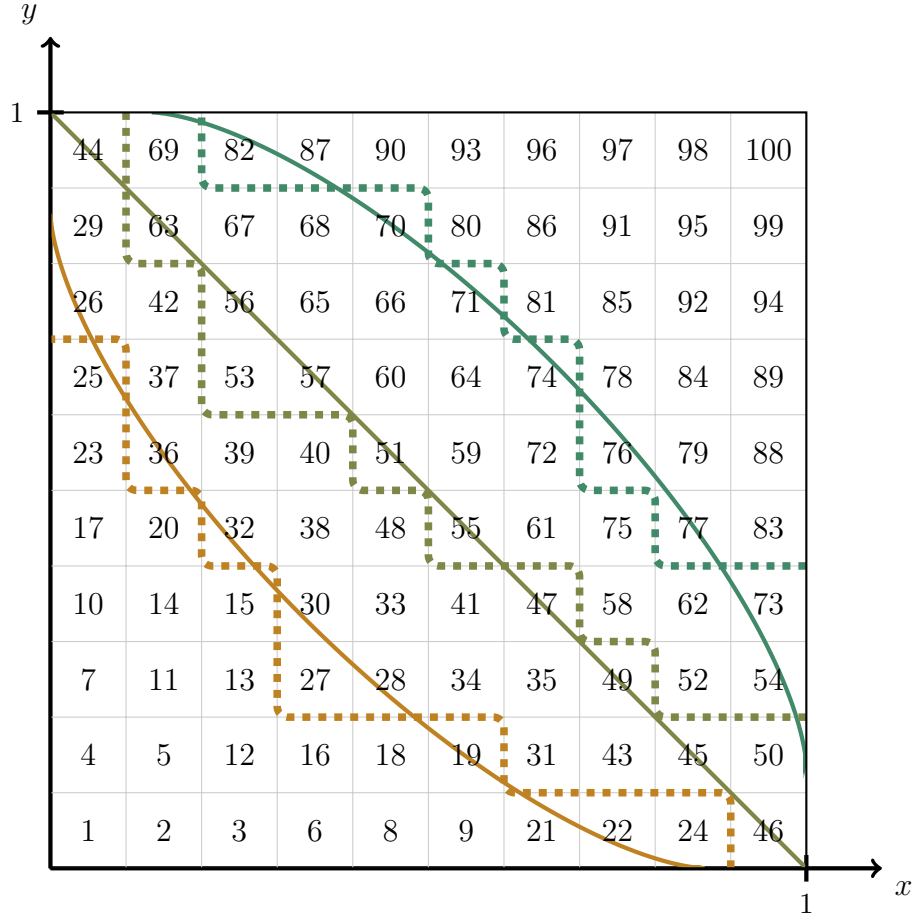


Figure 12. A scaled down sample random square tableau of size $N = 10$. The zigzag lines are the level curves for $\alpha \in \{1/4, 2/4, 3/4\}$. The smooth lines are the corresponding circles of latitude g_α , see also the orange-to-green family of curves on Figure 13.

2.3. The random position of the box $\lfloor \alpha N^2 \rfloor$, the limit measure ν_α . Pittel and Romik [PR07, Theorem 2] also found the explicit formula for the limit distribution of the scaled down location

$$\frac{1}{N} \text{pos}_{\lfloor \alpha N^2 \rfloor} (T_N)$$

of the entry $\lfloor \alpha N^2 \rfloor$ in a uniformly random square Young tableau T_N , as $N \rightarrow \infty$. This limit distribution turns out to be supported on the circle of latitude g_α and thus it is uniquely determined by the probability distribution

of the u -coordinate. The latter, denoted by ν_α , turns out to be the semicircular distribution on the interval $\left[-2\sqrt{\alpha(1-\alpha)}, 2\sqrt{\alpha(1-\alpha)}\right]$ with the density

$$(2.4) \quad f_{\nu_\alpha}(u) := \frac{k_{\alpha,u}}{2\pi\alpha(1-\alpha)}.$$

2.4. Geographic coordinates on the square. For any point $p = (x, y) \in [0, 1]^2$ of the unit square there is exactly one $\alpha = \alpha(p) \in [0, 1]$ such that p lies on the curve g_α . We say that *the latitude of p* is equal to α . With the notations of Pittel and Romik [PR07] the latitude $\alpha(x, y) = L(x, y)$ is just the limit height function of random square standard Young tableaux.

The *longitude of p* , which we denote by

$$\psi(p) = \nu_\alpha((-\infty, x - y]) = F_{\nu_\alpha}(x - y),$$

is defined as the mass of the points on the curve g_α which have their u -coordinate not greater than the u -coordinate of the point p or, equivalently, in terms of the cumulative distribution function F_{ν_α} of the measure ν_α . Notice that $\psi((0, 0)) = \psi((1, 1)) = 1$. The set of points of the unit square $[0, 1]^2$ with equal longitude ψ is a curve called the *meridian ψ* , see Figures 9 and 13.

For given $\alpha \in (0, 1)$ and $\psi \in [0, 1]$ we denote by

$$P_{\alpha,\psi} = (x_\alpha^\psi, y_\alpha^\psi) \in [0, 1]^2$$

the unique point of the unit square $[0, 1]^2$ with the latitude α and the longitude ψ . We set additionally $P_{0,\psi} = (0, 0)$ and $P_{1,\psi} = (1, 1)$ for any $\psi \in [0, 1]$. We denote by

$$u_\alpha^\psi := x_\alpha^\psi - y_\alpha^\psi \quad \text{and} \quad v_\alpha^\psi := x_\alpha^\psi + y_\alpha^\psi$$

the u - and v -coordinate of the point $(x_\alpha^\psi, y_\alpha^\psi) = P_{\alpha,\psi}$.

Remark 2.1. We will not use the following observation, but fans of cartography may find it interesting: for reasons which will hopefully become obvious later on, the map

$$[0, 1]^2 \ni (\alpha, \psi) \mapsto P_{\alpha,\psi} \in [0, 1]^2$$

is *equiareal* which manifests by equality of the areas of the curvilinear rectangles on Figure 13.

Remark 2.2. The result of Pittel and Romik [PR07, Theorem 2] is a special case of a general phenomenon of existence of the level curves (circles of latitudes) for random Young tableaux of specified shape. Biane [Bia98] proved that such level curves exist for any balanced sequence of Young diagrams, see Section 10 for more information.

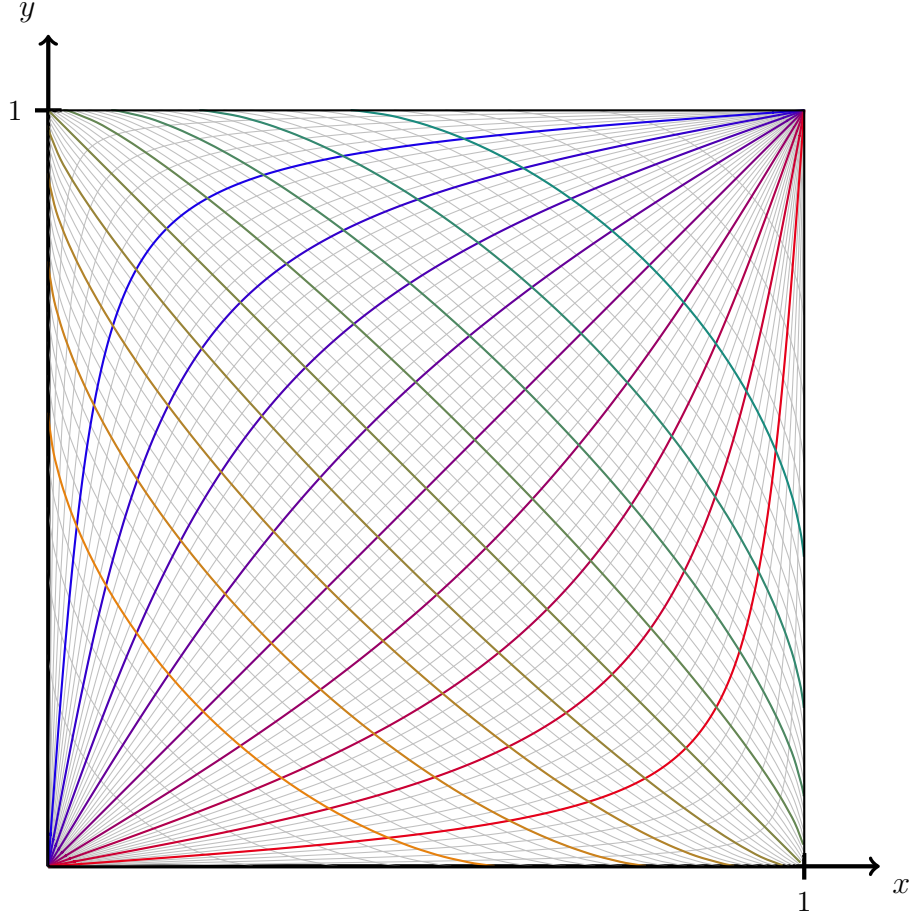


Figure 13. The geographic coordinate system on the unit square $[0, 1]^2$. The blue-to-red family of thick colored curves connecting the bottom left and the upper right corner are the meridians with the longitudes $\psi \in \{1/10, 2/10, \dots, 9/10\}$. The gray lines are the meridians with the longitudes $\psi \in \{2/100, 4/100, \dots, 98/100\}$, cf. Figure 9. The orange-to-green family of thick colored curves are the circles of latitudes g_α with the latitudes $\alpha \in \{1/10, 2/10, \dots, 9/10\}$. The thin, gray lines are the circles of latitude g_α with the latitudes $\alpha \in \{2/100, 4/100, \dots, 98/100\}$, see Figure 12. The shown meridians and circles of latitude split the square into a 50×50 grid of curvilinear rectangles with equal areas.

2.5. The second main result. Typical evacuation path. For a given tableau $T_N \in \mathcal{T}_{\square_N}$ and $t \in [0, 1)$ we denote by

$$(2.5) \quad X_t = X_t(T_N) = \frac{1}{N} \text{pos}_{N^2} \left(j^{\lfloor tN^2 \rfloor}(T_N) \right) \in [0, 1]^2$$

the scaled down position of the point from the evacuation path $\text{evac}(T_N)$, cf. (1.8). Clearly, the parameter t indicates how many boxes were removed so far and therefore we can relate to it as the *time*.

Our second main result states that, asymptotically, *the scaled evacuation path in a random square tableau is a random meridian*, see Figure 9.

Theorem 2.3. *For each $N \in \mathbb{N}$ there exists a random variable $\Psi_N : \mathcal{T}_{\square_N} \rightarrow [0, 1]$ such that the supremum distance*

$$(2.6) \quad \sup_{t \in [0, 1]} |X_t(T_N) - P_{1-t, \Psi_N(T_N)}|$$

converges in probability to zero, as $N \rightarrow \infty$. More explicitly: for each $\varepsilon > 0$

$$\lim_{N \rightarrow \infty} \mathbb{P}_N \left\{ T_N \in \mathcal{T}_{\square_N} : \sup_{t \in [0, 1]} |X_t(T_N) - P_{1-t, \Psi_N(T_N)}| > \varepsilon \right\} = 0.$$

The probability distribution of the random variable Ψ_N converges, as $N \rightarrow \infty$, to the uniform distribution on the unit interval $[0, 1]$.

In other words (with a small abuse of notation), the random trajectory $(X_t(T_N))_{t \in [0, 1]}$ with respect to the supremum norm converges in distribution to a random meridian $(P_{1-t, \psi})_{t \in [0, 1]}$ when $N \rightarrow \infty$, that is shortly,

$$(X_t(T_N))_{t \in [0, 1]} \xrightarrow[N \rightarrow \infty]{d} (P_{1-t, \psi})_{t \in [0, 1]},$$

where ψ is a random variable with the uniform $U(0, 1)$ distribution.

The proof is postponed to Section 8 and the preparations to it will take the majority of time.

2.6. The third main result. Typical sliding path. Let T be a standard Young tableau with n boxes. Sometimes when investigating the sliding path, we are concerned not only about its shape, but also we would like to be able to tell which entries were placed in the rearranged boxes. This motivates the notion of *the sliding path in the lazy parametrization* (or shortly *the lazy sliding path*) which is a sequence of boxes $\mathbf{q}(T) := (\mathbf{q}_1, \dots, \mathbf{q}_n) \subset \mathbb{N}^2$ where \mathbf{q}_i is the last box along the sliding path corresponding to T (cf. Figure 8a) which contains a number $\leq i$, cf. [RS15, Section 3.3].

Our third main result is stated in the language of lazy sliding path and says that, asymptotically, *the scaled sliding path in a random square tableau is, just like in Theorem 2.3, a random meridian*, see Figure 9.

Theorem 2.4. *For each $N \in \mathbb{N}$ there exists a random variable $\tilde{\Psi}_N: \mathcal{T}_{\square_N} \rightarrow [0, 1]$ such that the supremum distance*

$$\sup_{t \in [0,1]} \left| \frac{1}{N} \mathbf{q}_{[tN^2]}(T_N) - P_{t, \tilde{\Psi}_N(T_N)} \right|$$

converges in probability to zero, as $N \rightarrow \infty$.

The probability distribution of the random variable $\tilde{\Psi}_N$ converges, as $N \rightarrow \infty$, to the uniform distribution on the unit interval $[0, 1]$.

In other words (with a small abuse of notation), the lazy sliding path $(\mathbf{q}_{[tN^2]}(T_N))_{t \in [0,1]}$ with respect to the supremum norm converges in distribution to a random meridian $(P_{t,\psi})_{t \in [0,1]}$ when $N \rightarrow \infty$, that is shortly,

$$\frac{1}{N} \mathbf{q}_{[tN^2]}(T_N) \xrightarrow[N \rightarrow \infty]{d} P_{t,\psi}$$

where ψ is a random variable with the uniform $U(0, 1)$ distribution.

The proof is postponed to Section 9.2 and is based on showing that the random lazy sliding path and the (reversed) random evacuation path have the same distribution, cf. Proposition 9.1. In other words, we show that the problem of finding typical sliding paths is equivalent to the problem of finding typical evacuation paths from Theorem 2.3.

2.7. Conjecture on the independence of the iterated sliding paths. Recall from Section 1.3.2 that the dual promotion ∂^* is a bijection defined by a two-step procedure in which first we apply the jeu de taquin and then we add the box which was removed from the initial tableau T . We can iterate ∂^* on the random tableau T_N and get *the sequence of iterated sliding paths*

$$(2.7) \quad \mathbf{q}(T_N), \quad \mathbf{q}(\partial^*(T_N)), \quad \mathbf{q}((\partial^*)^2(T_N)), \quad \dots$$

Since ∂^* is a bijection, Theorem 2.4 provides asymptotics of the distribution of each element of the sequence (2.7) separately. The following conjecture aims to provide asymptotic information about their *joint* distribution.

Conjecture 2.5. *For each integer $k \geq 1$ the probability distribution of the random vector*

$$\left(\tilde{\Psi}_N(T_N), \quad \tilde{\Psi}_N(\partial^*(T_N)), \quad \dots, \quad \tilde{\Psi}_N((\partial^*)^{k-1}(T_N)) \right)$$

converges, as $N \rightarrow \infty$, to the uniform distribution on the unit cube $[0, 1]^k$.

Romik and the second named author proved an analogue of this conjecture in the case of the Plancherel-distributed random infinite tableaux, see [RS15, the comment below Theorem 1.5] and Section 2.8 for more details.

2.8. Something old, something new, something borrowed: sliding paths for random infinite tableaux. The problem of the asymptotic shape of a sliding path (analogous to the one from Theorem 2.4) was studied before by Romik and the second named author [RŚ15, Section 1.3] for a certain *infinite* random Young tableau, more specifically for the recording tableau $Q(x_1, x_2, \dots)$ obtained by applying the Robinson–Schensted correspondence to an infinite sequence (x_1, x_2, \dots) of independent, identically distributed random variables with the uniform distribution on the unit interval $[0, 1]$. Such a choice corresponds to sampling the random Young tableau according to, so called, *the Plancherel measure*.

In such a setting the sliding path happens to converge almost surely to a straight line with a random direction [RŚ15, Theorem 1.1], in other words the analogue of our meridians in the context of the Plancherel measure is given by the straight lines emanating from the origin of the coordinate system.

One of the main difficulties in the proof of Theorem 2.4 will be the construction of the random variables $\tilde{\Psi}_N$ which provide the longitude of the meridian along which the sliding path travels. This difficulty is absent in [RŚ15] because in that context the analogue of the longitude turns out to be simply equal to x_1 , the first entry of the random sequence to which the Robinson–Schensted correspondence is applied.

It would be tempting to repeat the approach from [RŚ15] in our context, for example one could proceed as follows. Let

$$\pi^{(N)} = \left(\pi_1^{(N)}, \dots, \pi_{N^2}^{(N)} \right)$$

be a uniformly random element of the set of *extremal Erdős–Szekeres permutations*, i.e., permutations with the property that the corresponding tableaux associated via the Robinson–Schensted correspondence have the square shape \square_N . Then the corresponding recording tableau $T_N = Q(\pi^{(N)})$ is, as required, a uniformly random standard Young tableau of square shape \square_N . A naive guess would be that one possible choice for the random variable $\tilde{\Psi}_N$ is again (a rescaled version of) the first entry of the permutation, i.e., $\pi_1^{(N)}$.

Uniformly random extremal Erdős–Szekeres permutations were investigated by Romik [Rom06] who proved, among other results, that the probability distribution of $\frac{1}{N^2} \pi_1^{(N)}$ converges to the point measure concentrated in $\frac{1}{2}$. For this reason it seems that the random variables $\pi_1^{(N)}$ do not carry any information which would be useful for our purposes, hence the approach from [RŚ15] is not applicable here directly, and the construction of the random variables $\tilde{\Psi}_N$ must follow different ideas.

Despite this fundamental difference, an astute reader may notice that our proof of Theorem 2.3 follows a path parallel to the one of [RS15, Theorem 5.1]. For example, the counterpart of our Proposition 6.5 (which can be viewed as a result about a certain random process of *removal* of boxes from a Young diagram) is [RS15, Theorem 4.4] (which concerns a certain random process of *addition* of boxes to a Young diagram).

3. PRELIMINARIES

3.1. Permutations, Young diagrams and Young tableaux, continued. We continue Section 1.3.1 where some basic definitions were introduced.

By \mathbb{N} we denote the set of positive integers and we denote $\mathbb{N}_0 := \mathbb{N} \cup \{0\}$. For any natural number n , we define the set $[n] := \{1, \dots, n\}$. From the following on (unlike in Section 1.2) we will view the symmetric group \mathfrak{S}_n as the group of permutations of the set $[n]$. We define *the length of a permutation* π to be the minimal number of factors necessary to write π as a product of (arbitrary, not necessarily adjacent!) transpositions, and denote it by $|\pi|$.

For any Young diagram λ , we denote *the number of standard Young tableaux* of shape λ by $f^\lambda = |\mathcal{T}_\lambda|$. If $T \in \mathcal{T}_\lambda$ and $0 \leq p \leq |\lambda|$ we consider the *restriction of T to its p least boxes* by removing the entries which are bigger than p , and denote the obtained tableau by $T|_{\leq p}$ (clearly, it is also a standard Young tableau).

For $C \geq 1$ we say that a Young diagram λ is *C -balanced* if λ has at most $C\sqrt{|\lambda|}$ rows and at most $C\sqrt{|\lambda|}$ columns.

For a tableau T and an integer p which appears exactly once in T (which will always be the case in our considerations) we define *the u -coordinate of the box with the entry p* as

$$u_p^T := x - y \quad \text{for } (x, y) = \text{pos}_p(T).$$

Note that in the literature, for instance in [CSST10], such a u -coordinate is called the *content*.

We will also consider skew tableaux obtained by removing some boxes from Young tableaux. Let $T \in \mathcal{T}_\lambda$ be a standard Young tableau. If T with the boxes with entries a_1, \dots, a_i removed is a skew tableau, we denote it by $T \setminus \{a_1, \dots, a_i\}$. Clearly, $T \setminus \{p+1, \dots, |\lambda|\} = T|_{\leq p}$ is also a standard Young tableau.

3.2. Representation theory. If G is a finite group and $\rho: G \rightarrow \text{End } V$ is its representation on a finite-dimensional complex linear space V , then by

$$\xi_V(g) := \text{Tr } \rho(g), \quad g \in G,$$

we denote its *character* (we write just ξ if it is clear which representation we consider). We also consider the *normalized character* $\chi_V : G \rightarrow \mathbb{C}$ given by

$$\chi_V := \frac{1}{\dim V} \cdot \xi_V = \frac{1}{\xi_V(\text{id})} \cdot \xi_V.$$

Additionally, for any element of the group algebra

$$f = \sum_{g \in G} f_g g \in \mathbb{C}G$$

we denote by $\chi_V(f)$ the *extension of the character by linearity* given by

$$\chi_V(f) := \sum_{g \in G} f_g \chi_V(g) \in \mathbb{C}.$$

On the vector space of functions $\mathcal{G} := \{f : G \rightarrow \mathbb{C}\}$ we consider the *standard scalar product* given by

$$\langle f, g \rangle := \frac{1}{|G|} \sum_{h \in G} f(h) \overline{g(h)}, \quad \text{for } f, g \in \mathcal{G},$$

where $\bar{}$ denotes the complex conjugation.

We will denote by \hat{G} the family of irreducible representations (*irreps* for short) of G . It is known that the system of irreducible characters $\{\xi_{V_x}\}_{x \in \hat{G}}$ is orthonormal. Therefore for the normalized irreducible characters the following holds:

$$\langle \chi_{V_1}, \chi_{V_2} \rangle = \begin{cases} \frac{1}{\dim V_1} & \text{if } \chi_{V_1} = \chi_{V_2}, \\ 0 & \text{otherwise.} \end{cases}$$

Let V be a finite-dimensional representation and let

$$V = \bigoplus_{x \in \hat{G}} m_x V_x$$

be its decomposition into irreducible components, where $m_x \in \mathbb{N}$ denotes the multiplicity of x . By a *random irreducible component* of V we will understand a random element of \hat{G} sampled according to the probability measure \mathcal{P}_V which is proportional to the total dimension of all copies of a given irrep in V :

$$(3.1) \quad \mathcal{P}_V(x) := \frac{m_x \dim V_x}{\dim V} = (\dim V_x)^2 \cdot \langle \chi_V, \chi_x \rangle \quad \text{for } x \in \hat{G}.$$

The *trivial representation* will be denoted by triv . If H is a subgroup of G then we denote by $\rho \downarrow_H^G$ the *restriction of a representation ρ to H* (if G is fixed we just write $\rho \downarrow_H$).

For $\lambda \in \mathbb{Y}_n$ we denote by $\rho_\lambda: \mathfrak{S}_n \rightarrow \text{End } V_\lambda$ the irreducible representation of the symmetric group \mathfrak{S}_n corresponding to the Young diagram λ and by χ_λ its normalized character.

3.3. Asymptotics of characters and the approximate factorization property. We will use two results concerning asymptotics of characters. The first one, due to Feráý and the second named author, gives an upper bound on the irreducible characters.

Fact 3.1 ([FŚ11, Theorem 1]). *There exists a constant $a > 0$ such that for any Young diagram λ and any permutation $\pi \in \mathfrak{S}_{|\lambda|}$*

$$(3.2) \quad |\chi_\lambda(\pi)| \leq \left[a \max \left(\frac{r(\lambda)}{|\lambda|}, \frac{c(\lambda)}{|\lambda|}, \frac{|\pi|}{|\lambda|} \right) \right]^{|\pi|}$$

where $r(\lambda)$ and $c(\lambda)$ stand, accordingly, for the number of rows and the number of columns of λ .

The second result, due to Biane (and its generalization due to the second-named author), shows that the character calculated on the product of two fixed permutations with disjoint supports approximately factorizes.

Fact 3.2 ([Bia98, Corollary 1.3], [Bia01, Section 0], [Śni06, Theorem 1]). *Let $C \geq 1$ and $m \in \mathbb{N}$. There exists a constant $K > 0$ such that for each C -balanced Young diagram λ and all permutations $\sigma, \tau \in \mathfrak{S}_{|\lambda|}$ with disjoint supports and satisfying $|\sigma|, |\tau| \leq m$ we have*

$$|\chi_\lambda(\sigma\tau) - \chi_\lambda(\sigma)\chi_\lambda(\tau)| \leq \frac{K}{\left(\sqrt{|\lambda|}\right)^{|\sigma|+|\tau|+2}}.$$

3.4. Jucys–Murphy elements. In the applications of Fact 3.1 and Fact 3.2 we will encounter the expressions in the left-hand-side of (3.4). The lemma below gives an upper bound for their values.

Its proof uses *Jucys–Murphy elements* which often appear in the modern approach to the representation theory of the symmetric groups (see [CSST10]) and are defined as the following elements of the symmetric group algebra $\mathbb{C}\mathfrak{S}_n$

$$(3.3) \quad J_k := \sum_{1 \leq i < k} (i, k) = (1, k) + \cdots + (k-1, k) \in \mathbb{C}\mathfrak{S}_n \quad \text{for } 1 \leq k \leq n.$$

The elements $J_1, \dots, J_n \in \mathbb{C}\mathfrak{S}_n$ form a commuting family in the symmetric group algebra. We will use them intensively in Section 6.

Lemma 3.3. *For any $c > 0$ and $n \in \mathbb{N}$*

$$(3.4) \quad \sum_{\pi \in \mathfrak{S}_n} c^{|\pi|} < \exp\left(\frac{n^2 c}{2}\right).$$

Proof. For any $c \in \mathbb{C}$ the following simple identity in the symmetric group algebra holds true

$$\sum_{\pi \in \mathfrak{S}_n} c^{|\pi|} \pi = (1 + cJ_1)(1 + cJ_2) \cdots (1 + cJ_n).$$

By applying the trivial representation to both sides of the above equality we get that for $c > 0$

$$\begin{aligned} \sum_{\pi \in \mathfrak{S}_n} c^{|\pi|} &= (1 + c)(1 + 2c) \cdots (1 + (n - 1)c) < \\ &e^c e^{2c} \cdots e^{(n-1)c} < \exp\left(\frac{n^2 c}{2}\right). \quad \square \end{aligned}$$

4. THE LONGITUDE AND SURFING

Our strategy towards the proof of Theorem 2.3 is to pass to the geographic coordinates of the point $X_t = X_t(T_N)$ from the scaled evacuation trajectory (2.5). Having the choice between the latitude and the longitude, we start with the more challenging problem of understanding how the longitude $\psi(X_t)$ changes over time t .

Instead of considering the longitude $\psi(X_t)$ directly, it will be more convenient to study the following random variable which we call *the theoretical longitude*:

$$(4.1) \quad \Psi_N^{\text{th}}(t) := F_{\nu_{1-t}}(u(X_t)),$$

where $u(X_t)$ denotes the u -coordinate of $X_t = X_t(T_N)$, and $F_{\nu_{1-t}}$ is the cumulative distribution function of the limit measure ν_{1-t} which was defined in Section 2.3. Notice that if in time t the box with the biggest number is positioned *exactly* on the circle of latitude $\alpha = 1 - t$, that is, $\alpha(X_t) = 1 - t$, then the theoretical longitude coincides with the longitude, i.e., $\Psi_N^{\text{th}}(t) = \psi(X_t)$. Heuristically one would expect that $\Psi_N^{\text{th}}(t) \approx \psi(X_t)$ for $N \rightarrow \infty$.

Roughly speaking, the following result states that (away from the polar regions which correspond to $t = 0$ and $t = 1$) the theoretical longitude of X_t does not change too much over time.

Theorem 4.1. *Assume that $0 < t_1 < t_2 < 1$. Then for each $\varepsilon > 0$*

$$\lim_{N \rightarrow \infty} \mathbb{P}_N \left\{ T_N \in \mathcal{T}_{\square_N} : |\Psi_N^{\text{th}}(t_2) - \Psi_N^{\text{th}}(t_1)| > \varepsilon \right\} = 0.$$

In other words, the difference $\Psi_N^{\text{th}}(t_2) - \Psi_N^{\text{th}}(t_1)$ converges in probability to 0 when $N \rightarrow \infty$, that is shortly,

$$\Psi_N^{\text{th}}(t_2) - \Psi_N^{\text{th}}(t_1) \xrightarrow[N \rightarrow \infty]{P} 0.$$

The proof is quite involved; Sections 4 to 7.2 are a preparation while the proof of Theorem 4.1 itself will be given in Sections 7.3 and 7.4. The remaining part of the current section is devoted to a rough sketch of the proof.

Clearly, Theorem 4.1 is equivalent to the conjunction of the following two statements for $\varepsilon > 0$:

$$(4.2) \quad \lim_{N \rightarrow \infty} \mathbb{P}_N \left\{ T_N \in \mathcal{T}_{\square_N} : \Psi_N^{\text{th}}(t_2) - \Psi_N^{\text{th}}(t_1) > \varepsilon \right\} = 0,$$

$$(4.3) \quad \lim_{N \rightarrow \infty} \mathbb{P}_N \left\{ T_N \in \mathcal{T}_{\square_N} : \Psi_N^{\text{th}}(t_2) - \Psi_N^{\text{th}}(t_1) < -\varepsilon \right\} = 0.$$

We start with the proof of the upper bound (4.2). Then we will use the symmetry of the problem in order to prove the lower bound (4.3).

4.1. The single surfer scenario. We would like to present the problem of the evacuation path in a different, more vivid light. We will speak about a *square pool of side N* (=the square Young diagram \square_N) filled with $N^2 - 1$ *particles of water* (=the Young tableau T_N with the largest entry removed), a passive *surfer* (=the box with the biggest entry N^2) and its trajectory (or behavior) when the pool is being drained (=iteratively applying jeu de taquin). Our goal in Theorem 2.3 is to show that, when the pool is big enough, the surfer has some typical paths along which he/she moves as the pool is being drained.

In our proof of Theorem 4.1 we start our analysis at time t_1 when jeu de taquin was already applied

$$(4.4) \quad m_1 := \lfloor t_1 N^2 \rfloor$$

times. Our starting point is therefore the standard tableau

$$(4.5) \quad T'_N := \partial^{*m_1}(T_N) \Big|_{\leq N^2 - m_1}$$

with $N^2 - m_1$ boxes (compare with (1.9)). We denote

$$(4.6) \quad w_1 = N^2 - m_1 - 1.$$

In this way the boxes with numbers $1, \dots, w_1$ correspond to the *water* and the box with the maximal number $w_1 + 1$ to the *surfer*. The position of the latter box will be called *the initial position of the surfer* and we will refer to the tableau T'_N as *the initial surfer configuration*. By removing the box with the surfer

$$(4.7) \quad W'_N := T'_N \setminus \{w_1 + 1\}$$

we get a standard Young tableau which encodes *the initial configuration of the water*.

As time goes by, at the time t_2 the jeu de taquin was already applied

$$m_2 := \lfloor t_2 N^2 \rfloor$$

times and we investigate the tableau

$$T''_N = \partial^{*m_2}(T_N) \big|_{\leq N^2 - m_2} = \partial^{*m_2 - m_1}(T'_N) \big|_{\leq N^2 - m_2}$$

with $w_2 + 1$ boxes, where

$$(4.8) \quad w_2 = N^2 - m_2 - 1.$$

The boxes with the numbers $1, \dots, w_2$ correspond to the remaining particles of water and the box with the maximal number $w_2 + 1$ corresponds to the surfer; the position of the latter box will be called *the final position of the surfer*.

Our aim is to relate the final position of the surfer at the time t_2 to its initial position at the time t_1 , preferably in the language of the theoretical longitude. As a point of reference we will introduce an additional *multi-surfer story* which happens in a parallel universe in which we pay attention to k surfers.

4.2. Pieri tableaux. We consider the partial order on the plane \mathbb{R}^2 defined by:

$$(x_1, y_1) \preceq (x_2, y_2) \iff (x_1 \leq x_2 \wedge y_1 \geq y_2).$$

Let k be a fixed natural number and M be a tableau in which the k largest entries are numbered by consecutive integers $l + 1, \dots, l + k$. We say that the tableau M is a *k-Pieri tableau* if these k largest boxes are placed in *the increasing order* with respect to \preceq (i.e., they are placed from north-west to south-east) or, equivalently, their u -coordinates are ordered increasingly, that is:

$$u_{l+1}^M < \dots < u_{l+k}^M.$$

If the value of the number k is clear from the context, we will shortly say that M is *Pieri*.

It is easy to check that if M has at least $k + 1$ boxes then M is a k -Pieri tableau if and only if $j(M)$ is a k -Pieri tableau.

For standard Young tableaux we will consider the following more general notion. For a (skew) standard Young tableau T with n boxes and positive integers w and k such that $w + k \leq n$ we say that T is a $(w + 1, w + k)$ -Pieri tableau if

$$(4.9) \quad u_{w+1}^T < \dots < u_{w+k}^T.$$

The set of $(w + 1, w + k)$ -Pieri standard tableaux of (skew) shape λ will be denoted by $\tilde{\mathcal{T}}_{\lambda}^{(w+1, w+k)}$.

4.3. The multisurfer scenario. For the multisurfer scenario let $k = k(N)$ be a sequence of positive integers such that

$$(4.10) \quad \lim_{N \rightarrow \infty} k = \infty \quad \text{and} \quad \lim_{N \rightarrow \infty} \frac{k^2}{N} = 0.$$

For a fixed value of N we consider the $N \times N$ square pool filled with $N^2 - k$ particles of water on which k surfers ($=k$ boxes with the biggest entries) are positioned in the increasing order. Formally speaking, by

$$\tilde{\mathcal{T}}_{\square_N} = \tilde{\mathcal{T}}_{\square_N}^{(N^2-k+1, N^2)}$$

we denote the set of standard Young tableaux of the square shape \square_N which are k -Pieri, and by $\tilde{\mathbb{P}}_N$ the uniform distribution on the set $\tilde{\mathcal{T}}_{\square_N}$. We assume that M_N is a random tableau sampled with the uniform probability distribution $\tilde{\mathbb{P}}_N$ on the set $\tilde{\mathcal{T}}_{\square_N}$. In this scenario, in order to refer to the k surfers, we will use the name *multisurfers*.

We start our analysis when jeu de taquin was already applied $m_1 + 1 - k$ times with m_1 given again by (4.4) (notice that $m_1 + 1 - k \geq 0$ for N big enough). Our starting point is therefore the tableau

$$(4.11) \quad M'_N := \partial^{*m_1+1-k}(M_N) \Big|_{\leq N^2-m_1-1+k}$$

with $N^2 - m_1 - 1 + k = w_1 + k$ boxes. We will refer to this tableau as *the initial multisurfer configuration*. In this way, just as in the single surfer scenario, the boxes with the numbers $1, \dots, w_1$ correspond to the *water* (in particular, there is the same number of water particles as in the single surfer scenario). On the other hand, the boxes with the numbers $w_1 + 1, \dots, w_1 + k$ correspond to the *multisurfers*. By removing the multisurfers

$$(4.12) \quad \widetilde{W}'_N := M'_N \setminus \{w_1 + 1, \dots, w_1 + k\}$$

we get a standard Young tableau which encodes the initial configuration of the water.

As time goes by, at the time t_2 the jeu de taquin was already applied $m_2 + 1 - k$ times and we investigate the tableau

$$(4.13) \quad M''_N = \partial^{*m_2+1-k}(M_N) \Big|_{\leq w_2+k} = \partial^{*m_2-m_1}(M'_N) \Big|_{\leq w_2+k}$$

which consists of $w_2 + k$ boxes which correspond to w_2 particles of water and k multisurfers; we will refer to this tableau as *the final multisurfer configuration*.

4.4. Sketch of the proof of the upper bound (4.2).

4.4.1. *The collective behavior of the multisurfers is not very random.* Since the number of the multisurfers is small in comparison to the number of the rows/columns, as a first-order approximation we may treat the set of positions of k multisurfers at any fixed time as a collection of k independent copies of the position of a single surfer. We can expect therefore that the law of large numbers is applicable and, as $k \rightarrow \infty$, *the multisurfer empirical measure* (which is a random measure which encodes the scaled down u -coordinates of the multisurfers) converges in probability to the probability distribution of the position of the single surfer. In other words: *the collective behavior of the multisurfers is much less random than the behaviour of the single surfer*. This phenomenon is beneficial and will allow us to use the multisurfers as a moving frame of reference for tracing the position of the single surfer over time.

The above naive first-order approximation clearly cannot be true if $k = k(N)$ grows too fast with the size N of the square. Nevertheless, in Theorem 6.2 we will show that if $k = k(N)$ grows at the right speed then a version of the law of large numbers indeed holds true. The proof of Theorem 6.2 is quite technically involved and the whole Section 6 is devoted to its proof.

4.4.2. *The multisurfers provide information about the surfer.* Let us fix some common initial configuration of the water for both the surfer and the multisurfers. In another first-order approximation let us assume for a moment that the density of the multisurfers is small enough that during the time interval $[t_1, t_2]$ all neighboring pairs of multisurfers are separated so that the multisurfers do not touch each other. If this is indeed the case and there are no interferences between the multisurfers then the time evolution of each multisurfer clearly coincides with the time evolution of the single surfer who would have the same initial position; by reversing the optics this means that we have a very direct information about some specific single surfer trajectories (namely, the ones which start from the positions of the multisurfers) in terms of the dynamics of the multisurfers, which we understand pretty well thanks to the aforementioned Theorem 6.2.

It is very convenient that *for a fixed initial configuration of the water, the trajectory of the single surfer depends in a monotonic way on the initial position of the surfer*. For this reason it is possible to get some partial information also about the single surfer trajectories starting from the points *between* the initial positions of two multisurfers. If the number $k = k(N)$ of

the multisurfers tends to infinity as $N \rightarrow \infty$ such neighboring multisurfers should not be too far (in comparison to the size N of the square) which is enough to prove Theorem 4.1.

4.4.3. The single surfer and the multisurfer scenario on the same water configuration. Above we used the idea of considering the single surfer scenario *and* the multisurfer scenario on the same configuration of water. This idea sounds self-contradictory because each of these two scenarios gives rise to a *different* probability distribution on the set of configurations of the water. In Section 5 we shall explain how to overcome this difficulty and to (asymptotically) couple the surfer and the multisurfers on a single probability space. The resulting object can be visualized as water on which in two parallel universes there is (i) a single surfer, and (ii) k multisurfers. The single surfer and the multisurfers are like ghosts to one another and do not interact. Furthermore, *as long as the multisurfers do not touch each other, the relative position (with respect to the partial order \prec on the plane) of the surfer and the ghosts of the multisurfers does not change over time: overtaking of the surfer by the multisurfers is not allowed.*

4.4.4. Overtaking is allowed in one direction only. The above discussion was based on a simplistic assumption that the multisurfers do not touch each other. Regretfully, in the real world this is not the case; multisurfers might influence each other and hence the multisurfer trajectories might differ from the single surfer trajectories on the same configuration of the water.

On the bright side, the assumption that the multisurfers are ordered as in the definition of the Pieri tableaux implies that the movement of each multisurfer depends only on (1) the configuration of the water, and (2) on these multisurfers which are to the north-west; the other multisurfers which are south-east have no influence on its dynamics. Furthermore, the impact of the multisurfers is unidirectional: the presence of the north-west multisurfer-neighbor can only push the multisurfer in the south-east direction. For the ‘coupling’ of the stories of the single surfer and the multisurfers on the common water this means that the ghosts of the multisurfers *are* allowed to overtake the surfer, but only in one direction. More precisely, the number of the multisurfers which are north-west to the single surfer can only decrease over time (see Lemma 7.1 for the formal description of the above heuristics).

4.4.5. The order in which the proof of the upper bound (4.2) will be conducted. The rigorous proof of (4.2) will be conducted in the following order. First in Section 5 we will develop the content of Section 4.4.3. Then in Section 6 we will deal with the collective behavior of the multisurfers described in Section 4.4.1. In Section 7.1 we will work out the dynamics

contained in Section 4.4.4. Finally, in the rest of Section 7 we will formally justify the heuristics from Section 4.4.2 and complete the proof.

5. SINGLE SURFER VERSUS THE MULTISURFER SCENARIO

In Sections 4.1 and 4.3 we considered two random tableaux: T'_N and M'_N defined on two different probability spaces (which correspond to the single surfer and the multisurfer scenario respectively). In order to proceed with the ideas sketched in Section 4.4.3 we need to define some random tableaux \mathbf{T}'_N and \mathbf{M}'_N on a *common* probability space with (almost) the same distributions as T'_N and M'_N and such that the corresponding configurations of water coincide. A solution to this problem is provided by Proposition 5.1 below which is also the main result of the current section. We will compare the distributions with respect to *the total variation distance*.

Suppose that X and Y are random variables (possibly defined on different probability spaces) taking values in some finite set S with probability distributions \mathbb{P}_X and \mathbb{P}_Y respectively. We define the *total variation distance* between the random variables X and Y [Dur10, Section 3.6.1] (or, alternatively, between the probability distributions \mathbb{P}_X and \mathbb{P}_Y) as

$$(5.1) \quad \delta(X, Y) = \delta(\mathbb{P}_X, \mathbb{P}_Y) := \frac{1}{2} \sum_{s \in S} |\mathbb{P}_X(s) - \mathbb{P}_Y(s)| = \max_{Z \subset S} |\mathbb{P}_X(Z) - \mathbb{P}_Y(Z)|.$$

Sometimes we will also denote this quantity by $\delta(X, \mathbb{P}_Y)$, etc.

Proposition 5.1. *For each $C \geq 1$ and $\Delta \in (0, 1)$ there exists a constant $d > 0$ with the following property.*

Let λ be a C -balanced Young diagram and let k, w, a be positive integers such that $w < (1 - \Delta) |\lambda|$ and $w \leq a \leq |\lambda| - k$.

Then there exists a pair of random tableaux \mathbf{T} and \mathbf{M} which are defined on the same probability space with the following properties:

- (a) \mathbf{T} is a uniformly random element of \mathcal{T}_λ ;
- (b) \mathbf{M} is a random element of $\tilde{\mathcal{T}}_\lambda^{(a+1, a+k)}$;
- (c) *the total variation distance between the distribution of \mathbf{M} and the uniform distribution on $\tilde{\mathcal{T}}_\lambda^{(a+1, a+k)}$ fulfills the bound*

$$(5.2) \quad \delta(\mathbf{M}, \mathbb{P}_{\tilde{\mathcal{T}}_\lambda^{(a+1, a+k)}}) < d \frac{k^2}{\sqrt{|\lambda| - w}};$$

- (d) $\mathbf{T}|_{\leq w} = \mathbf{M}|_{\leq w}$ holds true almost surely.

The proof is postponed to Section 5.3. In the next two subsections we prepare to it by proving general lemmas on the probabilities of some particular events in the multisurfers scenario (Section 5.1) and comparing the distributions of water beneath surfer(s) in both scenarios (Section 5.2). It turns out that these distributions are similar in terms of the total variation distance which asymptotically converges to 0, see Lemma 5.4.

5.1. Probability that a random tableau is Pieri.

Lemma 5.2. *Let λ/μ be a skew Young diagram with n boxes and let $1 \leq k \leq n$. Then the cardinality of the set*

$$(5.3) \quad \tilde{\mathcal{T}}_{\lambda/\mu}^{(w+1, w+k)} \quad \text{for } w \in \{0, \dots, n-k\}$$

does not depend on the choice of w .

Proof. There is a simple bijection between the set $\tilde{\mathcal{T}}_{\lambda/\mu}^{(w+1, w+k)}$ and the set of semistandard skew tableaux of shape λ/μ and of weight $(1^w, k, 1^{n-w-k})$ which is defined as follows. For a tableau $T \in \tilde{\mathcal{T}}_{\lambda/\mu}^{(w+1, w+k)}$ we replace each entry from the set $\{w+1, \dots, w+k\}$ by the same number $w+1$, and we replace each entry $i \in \{w+k+1, \dots, n\}$ by $i+1-k$. It follows therefore that the cardinality of (5.3) is equal to the coefficient

$$\left[x_1 \cdots x_w x_{w+1}^k x_{w+2} \cdots x_{n+1-k} \right] s_{\lambda/\mu}$$

in the expansion of the skew Schur function in the basis of monomials. Since the skew Schur function is a symmetric polynomial, the proof is completed. \square

Some notions defined for ordinary Young diagrams have their natural counterparts in the skew setup, given as follows. For $C \geq 1$ we say that a skew Young diagram λ/μ is C -balanced if λ/μ has at most $C\sqrt{|\lambda/\mu|}$ rows and at most $C\sqrt{|\lambda/\mu|}$ columns. Moreover we denote by $\mathbb{P}_{\lambda/\mu}$ the uniform measure on the set of standard Young tableaux of skew shape λ/μ .

We calculate now the probability of choosing a Pieri tableau from the set of standard Young tableaux of a specified skew shape.

Lemma 5.3. *For each $C \geq 1$ there exists a constant $c > 0$ with the following property. Let λ/μ be a C -balanced skew Young diagram with n boxes. Let k and w be integers such that $1 \leq k < \sqrt[4]{n}$ and $0 \leq w \leq n-k$. Then*

$$(5.4) \quad \left| k! \mathbb{P}_{\lambda/\mu} \left(\tilde{\mathcal{T}}_{\lambda/\mu}^{(w+1, w+k)} \right) - 1 \right| < c \frac{k^2}{\sqrt{n}}.$$

Proof. Let T be a uniformly random standard tableau of skew shape λ/μ . It is easy to check that T is $(w+1, w+k)$ -Pieri if and only if the rectified tableau $\text{rect } T$ is $(w+1, w+k)$ -Pieri (see Section 4.2 for the definition of Pieri tableaux). In the following we will describe the probability distribution of $\text{rect } T$.

Recall that the plactic skew Schur polynomial $S_{\lambda/\mu}$ is the formal sum of the elements in the plactic monoid which correspond to all semistandard tableaux of shape λ/μ . The relations in the plactic monoid [Ful97, Section 2, Corollary 1] allow us to identify a skew tableau with its rectification and to express the skew plactic Schur polynomial as a linear combination of (non-skew) plactic Schur polynomials [Ful97, Section 5.1, Corollary 4]:

$$(5.5) \quad \frac{S_{\lambda/\mu}}{f^{\lambda/\mu}} = \sum_{\nu} \frac{c_{\mu\nu}^{\lambda} f^{\nu}}{f^{\lambda/\mu}} \cdot \frac{S_{\nu}}{f^{\nu}},$$

where $c_{\mu\nu}^{\lambda}$ is the Littlewood–Richardson coefficient. If we restrict our attention only to the summands which correspond to (skew) *standard* tableaux, the left-hand side can be identified with the probability distribution of $\text{rect } T$. The right-hand side can be interpreted as a linear combination (over some Young diagrams ν) of the uniform measure on the set \mathcal{T}_{ν} .

In this way we proved that a random tableau with the same distribution as $\text{rect } T$ can be generated by the following two step procedure. Firstly, we select a random Young diagram ν with the probability distribution

$$\mathbb{P}(\nu) = \frac{c_{\mu\nu}^{\lambda} f^{\nu}}{f^{\lambda/\mu}}.$$

Secondly, we select a uniformly random standard tableau with the shape ν .

In particular, the probability that $\text{rect } T$ is a $(w+1, w+k)$ -Pieri tableau is a weighted arithmetic mean (over certain diagrams ν) of the probability that a uniformly random element of \mathcal{T}_{ν} is a $(w+1, w+k)$ -Pieri tableau. It follows that it is enough to prove a version of the inequality (5.4) in which the skew diagram λ/μ is replaced by any diagram ν which contributes to (5.5); we will do it in the following.

We start with an observation that in the process of rectification the number of rows and the number of columns of a tableau cannot increase. Since λ/μ is C -balanced, it follows that any Young diagram ν which contributes to (5.5) is also C -balanced.

By Lemma 5.2 it is enough to consider the case $w = 0$. Let T be a uniformly random standard tableau of shape ν and let $\xi = \text{sh } T|_{\leq k}$ be the positions of the first k boxes of T . The tableau T is $(1, k)$ -Pieri if and only if $\xi = (k)$ is the one-row diagram. The remaining difficulty is therefore to identify the probability distribution of ξ .

The link between the combinatorics of standard Young tableaux and the irreducible representations of the symmetric groups (in particular, the branching rule) implies that the probability distribution of ξ coincides with the measure $\mathcal{P}_{V_\nu \downarrow \mathfrak{S}_k}$ on the irreducible components of $V_\nu \downarrow \mathfrak{S}_k$ which was defined in (3.1). Equation (3.1) gives therefore an exact formula

$$(5.6) \quad k! \mathbb{P}\left(T \in \tilde{\mathcal{T}}_\nu^{(1,k)}\right) = k! \mathcal{P}_{V_\nu \downarrow \mathfrak{S}_k}(\text{triv}) = k! \left\langle \chi_\nu \downarrow \mathfrak{S}_k, \chi_{\text{triv}} \right\rangle = \sum_{\pi \in \mathfrak{S}_k} \chi_\nu(\pi) \overline{\chi_{\text{triv}}(\pi)} = 1 + \sum_{\substack{\pi \in \mathfrak{S}_k \\ \pi \neq \text{id}}} \chi_\nu(\pi).$$

In the following we will find an asymptotic bound for the second summand on the right-hand side.

By Fact 3.1 there exists a universal constant $a > 0$ (which depends only on C) such that for any $\pi \in \mathfrak{S}_k$

$$(5.7) \quad |\chi_\nu(\pi)| \leq \left(\frac{a}{\sqrt{n}}\right)^{|\pi|}.$$

It follows that the second summand on the right-hand side of (5.6) is bounded by

$$\left| \sum_{\substack{\pi \in \mathfrak{S}_k \\ \pi \neq \text{id}}} \chi_\nu(\pi) \right| \leq \sum_{\pi \in \mathfrak{S}_k} \left(\frac{a}{\sqrt{n}}\right)^{|\pi|} - 1 \leq e^{\frac{ak^2}{\sqrt{n}}} - 1 = O\left(\frac{k^2}{\sqrt{n}}\right),$$

where we used Lemma 3.3 and the assumption that $\frac{k^2}{\sqrt{n}} = O(1)$. \square

5.2. Comparison of distributions of water beneath surfer(s) in both scenarios. The following lemma shows that in the asymptotic setting the probability distributions of water beneath surfer(s) in the single surfer and the multisurfer scenarios are nearly equal.

Lemma 5.4. *For each $C \geq 1$ and $\Delta \in (0, 1)$ there exists a constant $d > 0$ with the following property.*

Let λ be a C -balanced Young diagram and k, w and a be positive integers such that $w < (1 - \Delta) |\lambda|$ and $w \leq a \leq |\lambda| - k$. Denote by T a uniformly random element of \mathcal{T}_λ and by M a uniformly random element of $\tilde{\mathcal{T}}_\lambda^{(a+1, a+k)}$. The total variation distance between the distributions of the restricted tableaux $T|_{\leq w}$ and $M|_{\leq w}$ fulfills the bound

$$(5.8) \quad \delta\left(T|_{\leq w}, M|_{\leq w}\right) < d \frac{k^2}{\sqrt{|\lambda| - w}}.$$

Proof. We start with an observation that the total variation distance is trivially bounded from above by 1. It follows that (provided $d \geq 1$) it is enough to consider the case when $k^4 \leq |\lambda| - w$.

Notice that the probability distribution $\mathbb{P}_{\tilde{\mathcal{T}}_\lambda^{(a+1, a+k)}}(\cdot)$ coincides with the conditional probability $\mathbb{P}_{\mathcal{T}_\lambda}(\cdot \mid \tilde{\mathcal{T}}_\lambda^{(a+1, a+k)})$. Therefore, for any $\mu \in \mathbb{Y}_w$ such that $\mu \subseteq \lambda$ and any $S \in \mathcal{T}_\mu$ we have, by the Bayes rule, that

$$\begin{aligned} \mathbb{P}_{\tilde{\mathcal{T}}_\lambda^{(a+1, a+k)}}(M|_{\leq w} = S) &= \\ &= \frac{\mathbb{P}_{\mathcal{T}_\lambda}(M \in \tilde{\mathcal{T}}_\lambda^{(a+1, a+k)} \mid M|_{\leq w} = S)}{\mathbb{P}_{\mathcal{T}_\lambda}(\tilde{\mathcal{T}}_\lambda^{(a+1, a+k)})} \cdot \mathbb{P}_{\mathcal{T}_\lambda}(M|_{\leq w} = S). \end{aligned}$$

By elementary algebra this equality can be rewritten as

$$\begin{aligned} (5.9) \quad & \mathbb{P}_{\tilde{\mathcal{T}}_\lambda^{(a+1, a+k)}}(M|_{\leq w} = S) - \mathbb{P}_{\mathcal{T}_\lambda}(M|_{\leq w} = S) = \\ &= \mathbb{P}_{\tilde{\mathcal{T}}_\lambda^{(a+1, a+k)}}(M|_{\leq w} = S) \left[1 - k! \mathbb{P}_{\mathcal{T}_\lambda}(\tilde{\mathcal{T}}_\lambda^{(a+1, a+k)}) \right] + \\ &+ \mathbb{P}_{\mathcal{T}_\lambda}(M|_{\leq w} = S) \left[k! \mathbb{P}_{\mathcal{T}_\lambda}(M \in \tilde{\mathcal{T}}_\lambda^{(a+1, a+k)} \mid M|_{\leq w} = S) - 1 \right]. \end{aligned}$$

Our strategy is to find an upper bound for the absolute value of the right-hand side.

The conditional probability in the second summand on the right-hand side, i.e.,

$$(5.10) \quad \mathbb{P}_{\mathcal{T}_\lambda}(M \in \tilde{\mathcal{T}}_\lambda^{(a+1, a+k)} \mid M|_{\leq w} = S),$$

is equal to the conditional probability that the restricted tableau $M|_{>w}$ is an $(a+1, a+k)$ -Pieri tableau. In order to calculate this conditional probability we notice that the conditional probability distribution of the restricted tableau $M|_{>w}$ (under the condition $M|_{\leq w} = S$) is the uniform measure on the set of tableaux of shape λ/μ such that their entries form the multiset $(w+1, \dots, n)$. In other words, the probability distribution of the random tableau $(M|_{>w}) - w$ (which is obtained by decreasing each entry of $M|_{>w}$ by w) is given by $\mathbb{P}_{\mathcal{T}_{\lambda/\mu}}$. In this way we proved that (5.10) is equal to

$$(5.11) \quad \mathbb{P}_{\mathcal{T}_{\lambda/\mu}}(\tilde{\mathcal{T}}_{\lambda/\mu}^{(a+1-w, a+k-w)}).$$

By comparing the number of rows and columns, as well as the number of boxes of the skew diagram λ/μ with their counterparts for λ it follows that λ/μ is C' -balanced with

$$C' = C \sqrt{\frac{|\lambda|}{|\lambda| - w}} < \frac{C}{\sqrt{\Delta}}.$$

A fortiori λ and λ/μ are C'' -balanced, where C'' is the right-hand side of the above inequality.

We apply Lemma 5.3 twice: for both expressions in the square brackets on the right-hand side of (5.9). It follows that there exists a universal constant $c > 0$ (which depends only on C'') such that

$$\begin{aligned} & \left| \mathbb{P}_{\tilde{\mathcal{T}}_\lambda^{(a+1, a+k)}}(M|_{\leq w} = S) - \mathbb{P}_{\mathcal{T}_\lambda}(M|_{\leq w} = S) \right| \leq \\ & \leq \mathbb{P}_{\tilde{\mathcal{T}}_\lambda^{(a+1, a+k)}}(M|_{\leq w} = S) \frac{ck^2}{\sqrt{|\lambda|}} + \mathbb{P}_{\mathcal{T}_\lambda}(M|_{\leq w} = S) \frac{ck^2}{\sqrt{|\lambda| - w}}. \end{aligned}$$

By summing over all choices of S we get (5.8) for $d := \max(1, 2c)$, as required. \square

5.3. Proof of Proposition 5.1.

Proof of Proposition 5.1. We will sample the random tableaux \mathbf{T} and \mathbf{M} by the following two-step procedure. Firstly, we sample \mathbf{T} with the uniform probability measure on \mathcal{T}_λ , that is $\mathbb{P}(\mathbf{T} = T) := \mathbb{P}_{\mathcal{T}_\lambda}(T)$ for any $T \in \mathcal{T}_\lambda$. After the tableau \mathbf{T} was selected, we sample the tableau \mathbf{M} with the conditional probability

$$\begin{aligned} \mathbb{P}(\cdot \mid \mathbf{T} = T) := \\ \mathbb{P}_{\tilde{\mathcal{T}}_\lambda^{(a+1, a+k)}}(\cdot \mid \{M \in \tilde{\mathcal{T}}_\lambda^{(a+1, a+k)} : M|_{\leq w} = \mathbf{T}|_{\leq w}\}). \end{aligned}$$

In this way the condition (d) is fulfilled trivially.

Therefore the probability distribution of \mathbf{M} is given by

$$\begin{aligned} (5.12) \quad \mathbb{P}(\mathbf{M} = M) = \\ \mathbb{P}_{\mathcal{T}_\lambda}\{T \in \mathcal{T}_\lambda : T|_{\leq w} = M|_{\leq w}\} \times \\ \mathbb{P}_{\tilde{\mathcal{T}}_\lambda^{(a+1, a+k)}}\left(M \mid \{T \in \tilde{\mathcal{T}}_\lambda^{(a+1, a+k)} : T|_{\leq w} = M|_{\leq w}\}\right). \end{aligned}$$

The probability measure $\mathbb{P}_{\tilde{\mathcal{T}}_\lambda^{(a+1,a+k)}}$ can be written in an analogous way as

$$(5.13) \quad \mathbb{P}_{\tilde{\mathcal{T}}_\lambda^{(a+1,a+k)}}(M) = \mathbb{P}_{\tilde{\mathcal{T}}_\lambda^{(a+1,a+k)}} \left\{ T \in \tilde{\mathcal{T}}_\lambda^{(a+1,a+k)} : T|_{\leq w} = M|_{\leq w} \right\} \times \mathbb{P}_{\tilde{\mathcal{T}}_\lambda^{(a+1,a+k)}} \left(M \mid \left\{ T \in \tilde{\mathcal{T}}_\lambda^{(a+1,a+k)} : T|_{\leq w} = M|_{\leq w} \right\} \right).$$

It follows that the process of sampling \mathbf{M} as well as the process of sampling the uniformly random element of $\tilde{\mathcal{T}}_\lambda^{(a+1,a+k)}$ can be viewed as a two-step procedure: we first sample the positions of the boxes $1, \dots, w$ and in the second step the remaining boxes. Notice that in both sampling procedures in the second step we sample the remaining boxes with the same conditional distribution. It follows that the total variation distance between the measures (5.12) and (5.13) is bounded from above by the total variation distance (5.8) from Lemma 5.4 which completes the proof. \square

6. THE DISTRIBUTION OF THE u -COORDINATES OF THE MULTISURFERS

Our main result in this section is Theorem 6.2 which shows that the multisurfer empirical measure (i.e., the distribution of the u -coordinates of the multisurfers) after draining a $(1 - \alpha)$ -fraction of the water converges to the limit measure ν_α (the limit distribution of the u -coordinate of the single surfer on the level curve g_α , cf. Section 2.3). Also Proposition 6.5 might be interesting from the viewpoint of algebraic combinatorics as it provides a direct link between the statistical properties of uniformly random (a, b) -Pieri tableaux of some fixed shape and the celebrated Jucys–Murphy elements.

The following assumption on the ‘amount of water’ and the number of multisurfers will be central in the forthcoming results (Theorem 6.2 and Propositions 7.2 and 6.3).

Assumption 6.1. *Let $c > 0$ be the constant in Lemma 5.3 obtained for $C = 1$ for which (5.4) holds. We assume that $k = k(N)$ and $w = w(N)$ are sequences of positive integers which fulfill*

$$\lim_{N \rightarrow \infty} k(N) = \infty \quad \text{and} \quad k < \sqrt{\frac{N}{2c}} \quad \text{and} \quad w + k < N^2.$$

6.1. Counting multisurfers gives the longitude. Let $w = w(N)$ and $k = k(N)$ be sequences of nonnegative integers such that $0 < w + k < N^2$. Let M_N be a uniformly random tableau from $\tilde{\mathcal{T}}_{\square_N}^{(w+1,w+k)}$. We use a shorthand notation $u_n := u_n^{M_N}$ for the u -coordinate of the box with the number n in the tableau M_N . For $u \in \mathbb{R}$ we define the random variable $G_N(u)$

to be the fraction of the multisurfers which have their scaled u -coordinate smaller than u , that is

$$(6.1) \quad G_N(u) := \frac{1}{k} \max \left\{ p \in \{1, \dots, k\} : \frac{1}{N} u_{w+p} \leq u \right\}.$$

Clearly, G_N is the cumulative distribution function of the random measure m_N on \mathbb{R}

$$m_N := \frac{1}{k} \sum_{1 \leq p \leq k} \delta_{N^{-1} u_{w+p}}$$

where δ_x denotes the *delta measure concentrated at x* .

Theorem 6.2. *Let $\alpha \in (0, 1)$. Let $w = w(N)$ and $k = k(N)$ fulfill Assumption 6.1 and*

$$\lim_{N \rightarrow \infty} \frac{w}{N^2} = \alpha.$$

Then for each $\varepsilon > 0$

$$\mathbb{P}_{\tilde{\mathcal{T}}_{\square_N}^{(w+1, w+k)}} \left\{ M_N : \sup_{u \in \mathbb{R}} |F_{\nu_\alpha}(x) - G_N(x)| > \varepsilon \right\} = O \left(\frac{1}{k} + \frac{k^2}{N} \right)$$

with the constant in the O -notation depending only on α and ε .

In particular, if $k(N) \rightarrow \infty$ and $k(N) = o(\sqrt{N})$, i.e., (4.10) is satisfied, then the random sequence of cumulative distribution functions G_N with respect to the supremum norm converges in probability to the cumulative distribution function F_{ν_α} when $N \rightarrow \infty$, that is shortly,

$$\sup_{x \in \mathbb{R}} |F_{\nu_\alpha}(x) - G_N(x)| \xrightarrow{P} 0.$$

In order to prove this result we will compare the (random) moments of the empirical measure m_N and the moments of the measure ν_α which gives the asymptotics of the u -coordinate of a single box, cf. Section 2.3. In Proposition 6.3 below we shall calculate the moments of the empirical measure m_N . In Section 6.8 we will complete the proof of Theorem 6.2.

6.2. Moments of the empirical measure G_N . For each $\beta \in \mathbb{N}$ we define the β -th moment of the random measure m_N as

$$M_\beta := M_\beta(w, k) := \int_{\mathbb{R}} z^\beta dm_N(z) = \frac{1}{k} N^{-\beta} \sum_{1 \leq p \leq k} u_{w+p}^\beta.$$

Notice that M_β is also a random variable. The following result expresses the first two moments of the random variable $M_\beta(w, k)$ (which is related to the problem of multisurfers) in terms of the first moment of the random variable $M_\beta(w, 1)$ (which is related to the much simpler problem of a single surfer). This proposition is crucial to the proof of Theorem 6.2.

Proposition 6.3. *Let $w = w(N)$ and $k = k(N)$ fulfill Assumption 6.1. For each $\beta \in \mathbb{N}$, we have*

$$(6.2) \quad \mathbb{E}_{\tilde{\mathbb{P}}_N} M_\beta(w, k) = \mathbb{E}_{\mathbb{P}_N} M_\beta(w, 1) + O\left(\frac{k^2}{N}\right);$$

$$(6.3) \quad \text{Var}_{\tilde{\mathbb{P}}_N} M_\beta(w, k) = O\left(\frac{1}{k} + \frac{k^2}{N}\right)$$

with the constants in the O -notation depending only on β .

Remark 6.4. The counterpart of the above proposition in the paper of Romik and the second named author is [RS15, Theorem 4.6]. There the error terms for the expected value and variance are much smaller, accordingly, $O\left(\frac{k}{N}\right)$ and $O\left(\frac{1}{k} + \frac{k}{N}\right)$. There are two reasons for which our error terms are much bigger, of the form, accordingly, $O\left(\frac{k^2}{N}\right)$ and $O\left(\frac{1}{k} + \frac{k^2}{N}\right)$.

- In the proof of Proposition 6.5 we will view the probability distribution of the multisurfs as a *conditional distribution* of the boxes with certain numbers in a uniformly random standard skew tableau with a specified shape *under the condition* that these boxes are suitably ordered (i.e., the tableau is Pieri). Unfortunately, the probability of the latter event depends heavily on the shape of the diagram and we do not have a very good control over the error term, see Lemma 5.3.

Using our terminology in their context, the placement of the multisurfs by Romik and the second named author can also be seen as a conditional process: one first adds k boxes to a given Young diagram λ by k independent steps of the Plancherel growth process, and then *conditions* that these boxes are suitably ordered. In this case, however, the conditioning does not create additional difficulties because the probability of the event that the newly created boxes are Pieri is equal to $\frac{1}{k!}$ and does not depend on the shape of λ .

- The error $O\left(\frac{k^2}{N}\right)$ also appears during the application of Proposition 6.9. Romik and the second named author make use of [RS15, Theorem 4.4] which is a counterpart of ours Proposition 6.5. They deal with the character of the left-regular representation which obviously is not troublesome and need not be estimated.

The proof of Proposition 6.3 is quite long. In Sections 6.3 to 6.5 we gather some tools helpful in proving Proposition 6.3. In particular, the goal of Section 6.3 is to provide a connection between the statistical properties

of the multisurfers and the representation theory (see Proposition 6.5). Section 6.4 gives background for calculating the character χ_{\square_N} of the cosets appearing in (6.4). Section 6.5 is devoted mostly to an analysis of the permutations arising from the powers of Jucys–Murphy elements. Eventually, in Section 6.6 we give the proof of (6.2) and in Section 6.7 the proof of (6.3) which completes the proof of Proposition 6.3.

6.3. Multisurfers and the representation theory. The following result, Proposition 6.5, provides a link between the statistical properties of the multisurfers and the representation theory of the symmetric groups.

Let w, k, n be positive integers such that $w+k \leq n$. With a small abuse of notation we denote by \mathfrak{S}_w the group of permutations of the set $\{1, \dots, w\}$ and by \mathfrak{S}_k the group of permutations of the set $\{w+1, \dots, w+k\}$. In this way \mathfrak{S}_w and \mathfrak{S}_k are commuting subgroups of $\mathfrak{S}_{w+k} \subset \mathfrak{S}_n$. We define the element of the symmetric group algebra

$$p_{\mathfrak{S}_k} = \frac{1}{k!} \sum_{\sigma \in \mathfrak{S}_k} \sigma \in \mathbb{C}\mathfrak{S}_n.$$

Recall from Section 3.4 that the Jucys–Murphy elements J_1, \dots, J_n form a commuting family in the symmetric group algebra $\mathbb{C}\mathfrak{S}_n$ and are given by

$$J_k := \sum_{1 \leq i < k} (i, k) = (1, k) + \dots + (k-1, k) \in \mathbb{C}\mathfrak{S}_n \quad \text{for } 1 \leq k \leq n.$$

Proposition 6.5. *Let w, k, n be positive integers such that $w+k \leq n$. Let $W(x_1, \dots, x_k)$ be a symmetric polynomial in k variables. Let $\lambda \in \mathbb{Y}_n$ be a Young diagram and T be a random element (sampled with the uniform distribution) of the set $\tilde{\mathcal{T}}_\lambda^{(w+1, w+k)}$ of $(w+1, w+k)$ -Pieri tableaux of shape λ . Then*

$$\begin{aligned} (6.4) \quad \mathbb{E} W(u_{w+1}^T, \dots, u_{w+k}^T) &= \frac{\chi_\lambda(W(J_{w+1}, \dots, J_{w+k}) \cdot p_{\mathfrak{S}_k})}{\chi_\lambda(p_{\mathfrak{S}_k})} \\ &= \frac{\chi_\lambda(W(J_{w+1}, \dots, J_{w+k}) \cdot p_{\mathfrak{S}_k})}{\mathbb{P}_{\mathcal{T}_\lambda}(\tilde{\mathcal{T}}_\lambda^{(w+1, w+k)})}. \end{aligned}$$

The proof is postponed until the end of the current section until we gather the necessary tools.

We start with the following fundamental property of Jucys–Murphy elements.

Fact 6.6 ([Juc74]). *Let $\lambda \in \mathbb{Y}_n$ be a Young diagram, and let u_1, \dots, u_n be the u -coordinates of its boxes (listed in an arbitrary order). Let $W(x_1, \dots, x_n)$ be a symmetric polynomial in n variables. Then:*

- $W(J_1, \dots, J_n) \in \mathbb{C}\mathfrak{S}_n$ belongs to the center of the group algebra.
- The operator $\rho_\lambda(W(J_1, \dots, J_n))$ is a multiple of the identity operator, so it can be identified with a complex number. The value of this number is equal to

$$(6.5) \quad \chi_\lambda(W(J_1, \dots, J_n)) = W(u_1, \dots, u_n).$$

Lemma 6.7. *Let $\mu \in \mathbb{Y}_{w+k}$ be a Young diagram and let $W(x_1, \dots, x_k)$ be a symmetric polynomial in k variables. Then the operator*

$$\rho_\mu(W(J_{w+1}, \dots, J_{w+k}))$$

acts on each irreducible component V_ν of the restriction $V_\mu \downarrow_{\mathfrak{S}_w}^{\mathfrak{S}_{w+k}}$ as a multiple of the identity operator and can be identified with the complex number

$$(6.6) \quad W(u_{w+1}^{\mu/\nu}, \dots, u_{w+k}^{\mu/\nu}).$$

Above, for a diagram ν with w boxes such that $\nu \subset \mu$ we denote by $u_{w+1}^{\mu/\nu}, \dots, u_{w+k}^{\mu/\nu}$ the u -coordinates of the boxes of the skew diagram μ/ν (listed in an arbitrary order).

Proof. We will show that the lemma holds in the particular case when W is the power-sum symmetric function, that is

$$W(x_1, \dots, x_k) := p_\beta(x_1, \dots, x_k) := \sum_{1 \leq i \leq k} x_i^\beta$$

for some $\beta \in \mathbb{N}_0$. Since the power-sum symmetric functions generate the algebra of the symmetric polynomials and the representation ρ_μ is an algebra homomorphism, in this way we will prove that the lemma holds true in general.

Clearly,

$$\begin{aligned} W(J_{w+1}, \dots, J_{w+k}) &= p_\beta(J_{w+1}, \dots, J_{w+k}) = \\ &= p_\beta(J_1, \dots, J_{w+k}) - p_\beta(J_1, \dots, J_w). \end{aligned}$$

By Fact 6.6, the operator $p_\beta(J_1, \dots, J_{w+k})$ acts on the component V_μ as multiplication by the factor

$$(6.7) \quad p_\beta(u_1^\mu, \dots, u_{w+k}^\mu) = \sum_{1 \leq i \leq w+k} (u_i^\mu)^\beta.$$

Again by Fact 6.6, for any $\nu \in \mathbb{Y}_w$, the operator $p_\beta(J_1, \dots, J_w)$ acts on the component V_ν as multiplication by the factor

$$(6.8) \quad p_\beta(u_1^\nu, \dots, u_w^\nu) = \sum_{1 \leq i \leq w} (u_i^\nu)^\beta.$$

Let $\nu \subset \mu$. The multiset of the u -coordinates of the boxes of μ is the union of (i) the multiset of the u -coordinates of the boxes of ν , and (ii) the multiset of the u -coordinates of the boxes of μ/ν . Therefore, by subtracting (6.8) from (6.7), we get that the operator $p_\beta(J_{w+1}, \dots, J_{w+k})$ acts on the component V_ν of the restriction $V_\mu \downarrow_{\mathfrak{S}_w}^{\mathfrak{S}_{w+k}}$ as multiplication by the scalar

$$p_\beta(u_{w+1}^{\mu/\nu}, \dots, u_{w+k}^{\mu/\nu}) = \sum_{1 \leq i \leq k} (u_{w+i}^{\mu/\nu})^\beta,$$

as required. \square

Proof of Proposition 6.5. Observe that any tableau $T \in \tilde{\mathcal{T}}_\lambda^{(w+1, w+k)}$ can be split into the following three parts: (i) a standard tableau P with entries from $\{1, \dots, w\}$; we denote its shape by ν , (ii) a skew tableau Q which is k -Pieri with entries in $\{w+1, \dots, w+k\}$; we denote its shape by μ/ν , and (iii) a skew tableau R with the entries $> w+k$ with shape λ/μ .

For fixed partitions μ and ν it is easy to count the number of tableaux P which contribute to (i) and the number of tableaux R which contribute to (iii): their cardinalities are by definition given by f^ν and $f^{\lambda/\mu}$ respectively.

The number of k -Pieri tableaux Q which contribute to (ii) is slightly more challenging: it is equal to 1 if μ/ν has at most one box in each column and is equal to zero otherwise. A combinatorial interpretation of the Littlewood–Richardson coefficient $c_{\nu, (k)}^\mu$ for a single-row partition (k) (or, nomen omen, the Pieri rule) implies that this coefficient coincides with the latter cardinality.

In this way we proved that the left-hand side of (6.4) is given by

$$(6.9) \quad \mathbb{E} W(u_{w+1}^T, \dots, u_{w+k}^T) = \frac{1}{|\tilde{\mathcal{T}}_\lambda^{(w+1, w+k)}|} \sum_{T \in \tilde{\mathcal{T}}_\lambda^{(w+1, w+k)}} W(u_{w+1}^T, \dots, u_{w+k}^T) = \frac{1}{|\tilde{\mathcal{T}}_\lambda^{(w+1, w+k)}|} \sum_{\substack{\mu \in \mathbb{Y}_{w+k} \\ \mu \subset \lambda}} \sum_{\substack{\nu \in \mathbb{Y}_w \\ \nu \subset \mu}} f^{\lambda/\mu} f^\nu c_{\nu, (k)}^\mu W(u_{w+1}^{\mu/\nu}, \dots, u_{w+k}^{\mu/\nu}).$$

We will now investigate the numerator on the right hand side of (6.4). Each multiplicity $f^{\lambda/\mu}$ in the decomposition of the restriction of V_λ into

irreducible components

$$V_\lambda \downarrow_{\mathfrak{S}_{w+k}}^{\mathfrak{S}_{N^2}} = \bigoplus_{\substack{\mu \in \mathbb{Y}_w \\ \mu \subset \lambda}} f^{\lambda/\mu} V_\mu$$

is equal to the number of skew standard Young tableaux of shape λ/μ . Since $W(J_{w+1}, \dots, J_{w+k}) \cdot p_{\mathfrak{S}_k} \in \mathbb{C}\mathfrak{S}_{w+k}$, we get that

$$\begin{aligned} (6.10) \quad C_\lambda &:= \chi_\lambda \left(W(J_{w+1}, \dots, J_{w+k}) \cdot p_{\mathfrak{S}_k} \right) \\ &= \frac{1}{\dim V_\lambda} \operatorname{Tr}_{V_\lambda} \rho_\lambda \left(W(J_{w+1}, \dots, J_{w+k}) \cdot p_{\mathfrak{S}_k} \right) = \\ &= \frac{1}{f^\lambda} \sum_{\substack{\mu \in \mathbb{Y}_{w+k} \\ \mu \subset \lambda}} f^{\lambda/\mu} \operatorname{Tr}_{V_\mu} \rho_\lambda \left(W(J_{w+1}, \dots, J_{w+k}) \cdot p_{\mathfrak{S}_k} \right). \end{aligned}$$

The multiplicities in the decomposition of the restricted representation into irreducible components

$$V_\mu \downarrow_{\mathfrak{S}_w \times \mathfrak{S}_k}^{\mathfrak{S}_{w+k}} = \bigoplus_{\substack{\nu \in \mathbb{Y}_w \\ \xi \in \mathbb{Y}_k}} c_{\nu, \xi}^\mu V_\nu \otimes V_\xi$$

are given by Littlewood–Richardson coefficients. Therefore, since $p_{\mathfrak{S}_k}$ is a projection to the trivial representation, its image is given by

$$(6.11) \quad p_{\mathfrak{S}_k}(V_\mu) = p_{\mathfrak{S}_k} \left(V_\mu \downarrow_{\mathfrak{S}_w \times \mathfrak{S}_k}^{\mathfrak{S}_{w+k}} \right) = \bigoplus_{\nu \in \mathbb{Y}_w} c_{\nu, (k)}^\mu V_\nu \otimes V_{(k)} = \bigoplus_{\nu \in \mathbb{Y}_w} c_{\nu, (k)}^\mu V_\nu.$$

By combining (6.10), (6.11), and Lemma 6.7 we get the following closed formula for the numerator on the right-hand side of (6.4)

$$(6.12) \quad C_\lambda = \frac{1}{f^\lambda} \sum_{\substack{\mu \in \mathbb{Y}_{w+k} \\ \mu \subset \lambda}} \sum_{\nu \in \mathbb{Y}_w} f^{\lambda/\mu} c_{\nu, (k)}^\mu f^\nu W(u_{w+1}^{\mu/\nu}, \dots, u_{w+k}^{\mu/\nu}).$$

On the other hand, by (6.12) evaluated for the constant polynomial $W \equiv 1$, we get the following formula for the denominator on the right-hand side of (6.4)

$$(6.13) \quad \chi_\lambda(p_{\mathfrak{S}_k}) = \frac{1}{f^\lambda} \sum_{\substack{\mu \in \mathbb{Y}_{w+k} \\ \mu \subset \lambda}} \sum_{\nu \in \mathbb{Y}_w} f^{\lambda/\mu} c_{\nu, (k)}^\mu f^\nu = \frac{1}{f^\lambda} \cdot \left| \tilde{\mathcal{T}}_\lambda^{(w+1, w+k)} \right|$$

where the last equality comes from (6.9) evaluated for $W \equiv 1$. Observe also that

$$(6.14) \quad \mathbb{P}_{\mathcal{T}_\lambda} \left(\tilde{\mathcal{T}}_\lambda^{(w+1, w+k)} \right) = \frac{f^\lambda}{\left| \tilde{\mathcal{T}}_\lambda^{(w+1, w+k)} \right|}.$$

Equations (6.9), (6.12), (6.13) and (6.14) complete the proof of (6.4). \square

6.4. Character on a coset. Let us call *small* the elements of the set $\{1, \dots, w\}$ and *big* the elements of the set $\{w+1, \dots, w+k\}$. As before, we view the symmetric group \mathfrak{S}_k as the subgroup of \mathfrak{S}_{w+k} which consists of the permutations which can permute only the big elements.

For a Young diagram $\lambda \in \mathbb{Y}_n$ and a permutation $\pi \in \mathfrak{S}_{w+k}$ we define *the value of the character χ_λ on a left coset $\pi\mathfrak{S}_k \in \mathfrak{S}_{w+k}/\mathfrak{S}_k$* as an appropriate sum over the coset, that is

$$\chi_\lambda(\pi\mathfrak{S}_k) := \sum_{\sigma \in \pi\mathfrak{S}_k} \chi_\lambda(\sigma).$$

This definition is motivated by Proposition 6.5 because expressions of a similar flavor (up to the factor $\frac{1}{k!}$) appear on the right-hand side of (6.4). Our goal in this section is to understand the asymptotics of such characters on cosets.

For a left coset $\pi\mathfrak{S}_k \in \mathfrak{S}_{w+k}/\mathfrak{S}_k$ we define its *length* as

$$(6.15) \quad \|\pi\mathfrak{S}_k\| := w - \#(\text{cycles of } \pi \text{ which consist of only small elements}).$$

It is easy to check that if $\pi_1\mathfrak{S}_k = \pi_2\mathfrak{S}_k$ then the cycles of π_1 which consist of only small elements coincide with the analogous cycles of π_2 ; it follows that the above definition does not depend on the choice of the representative π of the coset.

Remind that for a permutation π we denote by $|\pi|$ *the length of π* , i.e., the minimal number of transpositions required to write π as their product.

Lemma 6.8. *For each left coset $\pi\mathfrak{S}_k$*

$$(6.16) \quad \|\pi\mathfrak{S}_k\| = \min \{ |\sigma| : \sigma \in \pi\mathfrak{S}_k \}.$$

There exists a unique permutation $\pi_0 \in \pi\mathfrak{S}_k$ for which the minimum on the right-hand side is achieved; the permutation $\pi_0 = \pi_0(\pi\mathfrak{S}_k)$ with this property will be called minimal for the coset $\pi\mathfrak{S}_k$.

This minimal permutation has the following additional properties:

(a) *for each $\sigma \in \mathfrak{S}_k$,*

$$(6.17) \quad |\pi_0\sigma| = \|\pi\mathfrak{S}_k\| + |\sigma|.$$

(b) *If π is such that each of its cycles permutes at most one big element, then $\pi = \pi_0$ is the minimal element.*

Proof. We begin with the proof of the first assertion of the lemma. The permutation π can be written as a product of disjoint cycles $\pi = \pi_1 \cdots \pi_\ell \pi_{\ell+1} \cdots \pi_L$, where π_1, \dots, π_ℓ are the cycles which permute at least one big element, and $\pi_{\ell+1}, \dots, \pi_L$ permute only small elements.

Fix $i \in \{1, \dots, \ell\}$. Then π_i is a cycle of the form

$$\pi_i = (p_{1,1}, \dots, p_{1,r_1}, q_1, p_{2,1}, \dots, p_{2,r_2}, q_2, \dots, p_{n,1}, \dots, p_{n,r_n}, q_n),$$

for some $n \in \mathbb{N}$ and $r_1, \dots, r_n \in \mathbb{N}_0$, some big numbers q_1, \dots, q_n and some small numbers $p_{r,s}$. Define

$$\tau_i := (q_n, q_{n-1}, \dots, q_1) \in \mathfrak{S}_k$$

as the cycle permuting (in the reverse direction) the big elements of the cycle π_i . Clearly,

$$\pi_i \tau_i = (p_{1,1}, \dots, p_{1,r_1}, q_1) \cdots (p_{n,1}, \dots, p_{n,r_n}, q_n)$$

gives a product of disjoint cycles, each permuting exactly one big element.

Then

$$(6.18) \quad \pi_0 := (\pi_1 \tau_1) \cdots (\pi_\ell \tau_\ell) \pi_{\ell+1} \cdots \pi_L \in \pi \mathfrak{S}_k$$

provides a decomposition into disjoint cycles which has the property that each cycle permutes at most one big element. Hence for any $\sigma \in \mathfrak{S}_k$ which permutes only big elements, the decomposition into disjoint cycles of the product $\pi_0 \sigma \in \pi \mathfrak{S}_k$ is obtained by merging appropriate cycles of π_0 , it follows therefore that

$$(6.19) \quad |\pi_0 \sigma| = |\pi_0| + |\sigma|.$$

As a consequence, the minimum on the right-hand side of (6.16) is achieved on π_0 and it is the unique permutation with this property, as required.

We shall now show that the equality (6.16) holds true. It is enough to prove it in the special case when as the coset representative we take π_0 given by (6.18). In this special case (6.16) is equivalent to

$$(6.20) \quad \|\pi_0 \mathfrak{S}_k\| = |\pi_0|.$$

The explicit decomposition into disjoint cycles (6.18) implies that the left-hand side is equal to

$$w - (L - \ell).$$

On the other hand, (6.18) implies that π_0 has exactly $L - \ell$ cycles which permute only small elements and k additional cycles, one for each big element. It follows that the right-hand side of (6.20) is equal to

$$|\pi_0| = (w + k) - (L - \ell + k) = w - (L - \ell)$$

which concludes the proof of (6.16).

Property (a) is now a direct consequence of (6.19) and (6.20).

For the proof of property (b), if π is such that each of its cycles permutes at most one big element then our construction gives $\pi = \pi_0$ so π is the minimal representative of the coset. \square

The next proposition gives an insight to the irreducible characters corresponding to square diagrams evaluated on left cosets.

Proposition 6.9. *For each positive integer L there exists a constant C_L with the following property.*

Let positive integers w and k be arbitrary and let $\pi_0 \in \pi \mathfrak{S}_k$ be the minimal representative of a left coset $\pi \mathfrak{S}_k \in \mathfrak{S}_{w+k}/\mathfrak{S}_k$. If $\|\pi \mathfrak{S}_k\| \leq L$ and $N^2 \geq w + k$ and $N > k^2$ then

$$(6.21) \quad \left| \chi_{\square_N}(\pi \mathfrak{S}_k) - \chi_{\square_N}(\pi_0) \right| < \frac{C_L k^2}{N \|\pi \mathfrak{S}_k\| + 1},$$

$$(6.22) \quad \left| \chi_{\square_N}(\pi \mathfrak{S}_k) \right| < \frac{2C_L}{N \|\pi \mathfrak{S}_k\|}.$$

Proof. Let $d = d(L) \geq 1$ be a constant (which depends only on L) big enough so that it guarantees that

$$L + k \leq dN.$$

By Fact 3.1, Lemma 6.8(a) and Lemma 3.3 we have

$$\begin{aligned} \left| \chi_{\square_N}(\pi \mathfrak{S}_k) - \chi_{\square_N}(\pi_0) \right| &\leq \sum_{\substack{\sigma \in \mathfrak{S}_k \\ \sigma \neq \text{id}}} \left| \chi_{\square_N}(\pi_0 \sigma) \right| \leq \sum_{\substack{\sigma \in \mathfrak{S}_k \\ \sigma \neq \text{id}}} \left(\frac{ad}{N} \right)^{|\pi_0 \sigma|} \leq \\ &\left(\frac{ad}{N} \right)^{\|\pi \mathfrak{S}_k\|} \left[\exp \left(\frac{adk^2}{2N} \right) - 1 \right] = \\ &\frac{(ad)^{\|\pi \mathfrak{S}_k\|+1}}{2} \frac{k^2}{N \|\pi \mathfrak{S}_k\| + 1} \frac{\exp \left(\frac{adk^2}{2N} \right) - 1}{\frac{adk^2}{2N}}. \end{aligned}$$

Since $\frac{e^x - 1}{x}$ is a bounded function on the interval $(0, \frac{ad}{2}]$, we get (6.21) as required.

By (6.21) and Fact 3.1 we get

$$\left| \chi_{\square_N}(\pi \mathfrak{S}_k) \right| < \frac{C_L k^2}{N^{\|\pi \mathfrak{S}_k\|+1}} + \left(\frac{ad}{N} \right)^{|\pi_0|} = \frac{1}{N^{\|\pi \mathfrak{S}_k\|}} \left(C_L \frac{k^2}{N} + (ad)^{\|\pi \mathfrak{S}_k\|} \right).$$

It follows that we can increase the value of the constant C_L in such a way that both (6.21) and (6.22) are fulfilled. \square

6.5. Products of Jucys–Murphy elements.

6.5.1. Set partitions. For calculations of the moments (6.2) and (6.3) we will need to better understand the sum of products $\sum_{p=1}^k J_{w+p}^\beta$. We will use similar concepts and notions to the ones from [RŚ15, Section 4.9]. Notice that

$$(6.23) \quad J_{w+p}^\beta = \sum_{1 \leq j_1, \dots, j_\beta \leq w+p-1} (j_1, w+p) \cdots (j_\beta, w+p).$$

We denote the summands contributing to the right-hand side of (6.23) in the following way. For any p and a sequence $j = (j_1, \dots, j_\beta) \in [w+p-1]^\beta$ define

$$(6.24) \quad \sigma_{p,j} := (j_1, w+p) \cdots (j_\beta, w+p).$$

We also denote

$$\begin{aligned} Z_\Sigma(j) &:= \{r \in \{1, \dots, \beta\} : j_r \leq w\}; \\ Z_\Pi(j) &:= \{r \in \{1, \dots, \beta\} : j_r > w\}. \end{aligned}$$

The sets $Z_\Sigma(j)$ and $Z_\Pi(j)$ indicate which elements of the sequence j are, respectively, *small* and *big*. Notice that $Z_\Sigma \cup Z_\Pi = \{1, \dots, \beta\}$ and, since $Z_\Sigma(j)$ and $Z_\Pi(j)$ are disjoint,

$$|Z_\Sigma(j)| + |Z_\Pi(j)| = \beta.$$

We consider the equivalence relation \sim on $Z_\Sigma(j)$ (respectively, on $Z_\Pi(j)$) given by

$$m \sim n \iff j_m = j_n.$$

We denote by $\Sigma(j)$ and $\Pi(j)$ the sets of the equivalence classes of the relation \sim on, respectively, $Z_\Sigma(j)$ and $Z_\Pi(j)$. Then the numbers of the equivalence classes

$$\begin{aligned} |\Sigma(j)| &= |\{j_1, \dots, j_\beta\} \cap \{1, \dots, w\}|, \\ |\Pi(j)| &= |\{j_1, \dots, j_\beta\} \cap \{w+1, \dots, w+k\}| \end{aligned}$$

indicate how many different small / big elements appear in the sequence j .

We say that A is a set *a set-partition* of X , and denote it by $A \in \text{SPar}(X)$, if A is a collection of disjoint non-empty subsets of X such that $\bigcup A = X$.

We call (A, B) a pair of complementary set-partitions of X if $A \cup B$ is a set-partition of X such that

$$\left(\bigcup A\right) \cap \left(\bigcup B\right) = \emptyset.$$

This terminology may be a bit misleading since neither A nor B need to be a set-partition of X . Note also that we allow the situations when $A = \emptyset$ or $B = \emptyset$. For example, consider a sequence $j \in [w + p - 1]^\beta$, then the pair $(\Sigma(j), \Pi(j))$ is a pair of complementary set-partitions of $[\beta]$.

For a pair (Σ, Π) of complementary set-partitions of $[\beta]$ we will say that the sequence $j \in [w + p - 1]^\beta$ is of type (Σ, Π) if $\Sigma = \Sigma(j)$ and $\Pi = \Pi(j)$. If this is the case, we will use a shorthand notation $j \in (\Sigma, \Pi)$.

Lemma 6.10. *Let $p_1, p_2 \in \{1, \dots, k\}$ and $s \in [w + p_1 - 1]^\beta$, and $t \in [w + p_2 - 1]^\beta$. Suppose that s and t are of the same type. Denote $\sigma_1 := \sigma_{p_1, s}$ and $\sigma_2 := \sigma_{p_2, t}$. Then*

- (a) *There exists a permutation $g \in \mathfrak{S}_w \times \mathfrak{S}_k$ such that $g(w + p_1) = w + p_2$ and $g(s_m) = t_m$ for $m \in \{1, \dots, \beta\}$;*
- (b) *Permutations σ_1 and σ_2 are conjugate by g , that is $\sigma_1 = g^{-1}\sigma_2g$;*
- (c) $\|\sigma_1\mathfrak{S}_k\| = \|\sigma_2\mathfrak{S}_k\|$.

Proof. Denote

$$\begin{aligned} A_{\leq w} &:= [w] \setminus \{s_m : m = 1, \dots, \beta\}; \\ B_{\leq w} &:= [w] \setminus \{t_m : m = 1, \dots, \beta\}. \end{aligned}$$

Since $\Sigma(s) = \Sigma(t)$, we have $|A_{\leq w}| = |B_{\leq w}|$, so there exists a bijection $\delta_1 : A_{\leq w} \rightarrow B_{\leq w}$. For the same reason, there exists a bijection $\delta_2 : A_{>w} \rightarrow B_{>w}$ between analogously defined sets

$$\begin{aligned} A_{>w} &:= \{w + 1, \dots, w + k\} \setminus (\{s_m : m = 1, \dots, \beta\} \cup \{w + p_1\}); \\ B_{>w} &:= \{w + 1, \dots, w + k\} \setminus (\{t_m : m = 1, \dots, \beta\} \cup \{w + p_2\}). \end{aligned}$$

Then $g : \mathfrak{S}_{w+k} \rightarrow \mathfrak{S}_{w+k}$ given by

$$g(x) := \begin{cases} w + p_2 & \text{if } x = w + p_1, \\ t_m & \text{if } x = s_m \text{ for some } m \in \{1, \dots, \beta\}, \\ \delta_1(x) & \text{if } x \in A_{\leq w}, \\ \delta_2(x) & \text{if } x \in A_{>w}. \end{cases}$$

clearly fulfills the properties required in (a) and it is easy to check that (b) indeed holds true.

In order to prove (c) it is enough to notice that (b) implies that σ_1 and σ_2 have the same number of cycles permuting only small elements. \square

6.5.2. *Inequalities concerning the character of J_{w+p}^β .* In the proof of Proposition 6.3 we will deal with the numbers of the form $O(N^x)$ where the exponent is given by the right-hand-side of (6.25). Our next aim is to show that these exponents are always nonpositive and only in some special cases are equal to 0.

Lemma 6.11. *Let $x_1, x_2, \dots \in \{1, \dots, w+k\}$ and $y_1, y_2, \dots \in \{w+1, \dots, w+k\}$ be infinite sequences. Define a function $f : \mathbb{N}_0 \rightarrow \mathbb{Z}$ by*

$$(6.25) \quad f(\ell) := 2\#(\{x_1, \dots, x_\ell\} \cap \{1, \dots, w\}) + \\ \#(\{x_1, \dots, x_\ell\} \cap \{w+1, \dots, w+k\}) - \\ \|(x_1, y_1) \cdots (x_\ell, y_\ell) \mathfrak{S}_k\| - \ell.$$

Then $f \leq 0$ and f is weakly decreasing.

Moreover, suppose that $\ell \in \mathbb{N}$ is such that $x_{\ell+1} \in \{x_1, \dots, x_\ell\}$ and $x_{\ell+1}$ and $y_{\ell+1}$ belong to different cycles in the cycle decomposition of the product $(x_1, y_1) \cdots (x_\ell, y_\ell)$. Then $f(\ell+1) < f(\ell)$ and, in particular, $f(n) < 0$ for all $n \geq \ell+1$.

Proof. Let ℓ be a non-negative integer; we will show that $f(\ell+1) \leq f(\ell)$.

Consider first the case $x_{\ell+1} > w$. Then

$$(x_1, y_1) \cdots (x_{\ell+1}, y_{\ell+1}) \mathfrak{S}_k = (x_1, y_1) \cdots (x_\ell, y_\ell) \mathfrak{S}_k$$

so

$$(6.26) \quad f(\ell+1) = \begin{cases} f(\ell) - 1 & \text{if } x_{\ell+1} \in \{x_i : i \leq \ell\}, \\ f(\ell) & \text{otherwise,} \end{cases}$$

thus $f(\ell+1) \leq f(\ell)$, as required.

Assume now that $x_{\ell+1} \leq w$. Our strategy is to compare the cycle decomposition of the products

$$(6.27) \quad (x_1, y_1) \cdots (x_\ell, y_\ell) \quad \text{and} \quad (x_1, y_1) \cdots (x_{\ell+1}, y_{\ell+1})$$

and to deduce in this way (via the definition (6.15)) the relationship between the coset lengths

$$\|(x_1, y_1) \cdots (x_{\ell+1}, y_{\ell+1}) \mathfrak{S}_k\| \quad \text{and} \quad \|(x_1, y_1) \cdots (x_\ell, y_\ell) \mathfrak{S}_k\|.$$

Consider the following two cases.

- Suppose $x_{\ell+1} \notin \{x_i : i \leq \ell\}$. Then the cycle decomposition of the permutation on the right-hand side of (6.27) arises from its counterpart on the left-hand side by merging the fixpoint $x_{\ell+1}$ with the cycle which contains $y_{\ell+1}$. It follows that

$$\|(x_1, y_1) \cdots (x_{\ell+1}, y_{\ell+1}) \mathfrak{S}_k\| = \|(x_1, y_1) \cdots (x_\ell, y_\ell) \mathfrak{S}_k\| + 1$$

hence $f(\ell + 1) = f(\ell)$, as required.

- Suppose $x_{\ell+1} \in \{x_i : i \leq \ell\}$. The cycle decomposition of the right-hand side of (6.27) is obtained from its counterpart on the left-hand side either by merging two cycles or by splitting one cycle into two cycles. Each of these two operations can change the number of cycles which permute only small elements by at most 1. It follows that

$$\|(x_1, y_1) \cdots (x_{\ell+1}, y_{\ell+1}) \mathfrak{S}_k\| \geq \|(x_1, y_1) \cdots (x_\ell, y_\ell) \mathfrak{S}_k\| - 1$$

so $f(\ell + 1) \leq f(\ell)$, as required.

This completes the proof that f is weakly decreasing.

Since $f(0) = 0$ it follows that $f \leq 0$ and the proof of the first part of the lemma is complete.

We will prove the second part of the lemma by revisiting the above proof.

If $x_{\ell+1} > w$ then by (6.26), $f(\ell) = f(\ell - 1) - 1$, as required.

On the other hand, when $x_{\ell+1} \leq w$ the cycle decomposition of the right-hand side of (6.27) is obtained from its counterpart on the left-hand side by merging two cycles: the one containing $x_{\ell+1}$ with the one containing $y_{\ell+1}$. Therefore the number of cycles which consist of only small elements at the right-hand side of (6.27) is bounded from above by its counterpart for the left-hand side of (6.27). Hence

$$\|(x_1, y_1) \cdots (x_{\ell+1}, y_{\ell+1}) \mathfrak{S}_k\| \geq \|(x_1, y_1) \cdots (x_\ell, y_\ell) \mathfrak{S}_k\|$$

and so $f(\ell + 1) \leq f(\ell) - 1$, as required. \square

Corollary 6.12. *Let $x_1, \dots, x_\ell \in \{1, \dots, w + k\}$ and $y_1, \dots, y_\ell \in \{w + 1, \dots, w + k\}$. Denote*

$$\begin{aligned} |\Sigma| &:= \#(\{x_1, \dots, x_\ell\} \cap \{1, \dots, w\}); \\ |\Pi| &:= \#(\{x_1, \dots, x_\ell\} \cap \{w + 1, \dots, w + k\}); \\ \|\sigma S_k\| &:= \|(x_1, y_1) \cdots (x_\ell, y_\ell) S_k\|. \end{aligned}$$

Then for $N \geq 1$

$$N^{2|\Sigma|} k^{|\Pi|} N^{-\|\sigma S_k\| - \ell} \leq \left(\frac{k}{N}\right)^{|\Pi|}.$$

6.6. The mean value of M_β – the proof of (6.2).

Proof of (6.2). Our goal is to calculate the expected value of the moment $M_\beta(w, k)$ (recall Section 6.2). By Proposition 6.5,

$$(6.28) \quad \mathbb{E}_{\tilde{\mathbb{P}}_N} M_\beta(w, k) = \frac{1}{\mathbb{P}_N\left(\tilde{\mathcal{T}}_{\square_N}^{(w+1, w+k)}\right)} \cdot \frac{1}{k} N^{-\beta} \chi_{\square_N}(\mathcal{J} p_{\mathfrak{S}_k}) =$$

$$= \frac{1}{k! \mathbb{P}_N\left(\tilde{\mathcal{T}}_{\square_N}^{(w+1, w+k)}\right)} \cdot \frac{1}{k} N^{-\beta} \chi_{\square_N}(\mathcal{J} \mathfrak{S}_k)$$

where (recall the definition (6.24) of $\sigma_{p,j}$)

$$\mathcal{J} := \sum_{p=1}^k J_{w+p}^\beta = \sum_{p=1}^k \sum_{j \in [w+p-1]^\beta} \sigma_{p,j} \in \mathbb{C} \mathfrak{S}_{w+k}.$$

Since \square_N is C -balanced with $C = 1$, by Lemma 5.3 the denominator on the right-hand side of (6.28) fulfills

$$k! \mathbb{P}_N\left(\tilde{\mathcal{T}}_{\square_N}^{(w+1, w+k)}\right) = 1 + O\left(\frac{k^2}{N}\right)$$

with the constant in the O -notation equal to c from Lemma 5.3. By Assumption 6.1 the right hand side is separated from 0 and therefore

$$(6.29) \quad \frac{1}{k! \mathbb{P}_N\left(\tilde{\mathcal{T}}_{\square_N}^{(w+1, w+k)}\right)} = 1 + O\left(\frac{k^2}{N}\right).$$

Equation (6.32) from Proposition 6.13 below provides the necessary asymptotics of the numerator and completes the proof of (6.2). \square

We consider an analogue of \mathcal{J} in which each summand is replaced by the minimal element of the appropriate coset

$$\mathcal{J}_0 := \pi_0(\mathcal{J}) = \sum_{p=1}^k \sum_{j \in [w+p-1]^\beta} \pi_0(\sigma_{p,j}) \in \mathbb{C} \mathfrak{S}_{w+k}.$$

The following proposition provides the missing element of the above proof of (6.2).

Proposition 6.13. *Let $\beta \in \mathbb{N}$ be fixed. Let $k, N \in \mathbb{N}$ be such that $N^2 > w + k$ and $k^2 < N$. Then*

$$(6.30) \quad \chi_{\square_N}(\mathcal{J}_0) = kN^\beta \left[\mathbb{E}_{\mathbb{P}_N} M_\beta(w, 1) + O\left(\frac{k}{N}\right) \right];$$

$$(6.31) \quad \chi_{\square_N}(\mathcal{J}\mathfrak{S}_k) = \chi_{\square_N}(\mathcal{J}_0) + O\left(kN^\beta \frac{k^2}{N}\right);$$

$$(6.32) \quad \chi_{\square_N}(\mathcal{J}\mathfrak{S}_k) = kN^\beta \left[\mathbb{E}_{\mathbb{P}_N} M_\beta(w, 1) + O\left(\frac{k^2}{N}\right) \right]$$

with the constants in the O -notation depending only on β .

The remaining part of this section is devoted to its proof.

6.6.1. *Decomposition of $\chi_{\square_N}(\mathcal{J}_0)$.* Denote

$$A := \sum_{p=1}^k \sum_{j \in [w]^\beta} \chi_{\square_N}(\pi_0(\sigma_{p,j}));$$

and for a pair of complementary set-partitions (Σ, Π) of $[\beta]$ let us also denote

$$(6.33) \quad B^{(\Sigma, \Pi)} := \sum_{p=1}^k \sum_{j \in (\Sigma, \Pi)} \chi_{\square_N}(\pi_0(\sigma_{p,j})).$$

With these notations

$$(6.34) \quad \chi_{\square_N}(\mathcal{J}_0) = A + \sum_{\substack{(\Sigma, \Pi) \\ \Pi \neq \emptyset}} B^{(\Sigma, \Pi)}.$$

Notice that the number of summands is finite, depends only on β and does not depend on N or k . Therefore, it is enough to find the asymptotics for each individual summand on the right-hand side.

6.6.2. *Asymptotics of A .* By Lemma 6.8(b), $\pi_0(\sigma_{p,j}) = \sigma_{p,j}$ for all $j \in [w]^\beta$. Since the character is constant on each conjugacy class, the contribution of the summands in A to the character is the same for each value of p and

$$A = \sum_{p=1}^k \chi_{\square_N} \left(\sum_{j \in [w]^\beta} \sigma_{p,j} \right) = k \cdot \chi_{\square_N} \left(J_{w+1}^\beta \right).$$

We apply Proposition 6.5 for $k = 1$; in this special case $p_{\mathfrak{S}_1} = \text{id}$ and $\chi_{\square_N}(p_{\mathfrak{S}_1}) = 1$, thus

$$(6.35) \quad A = k \mathbb{E}_{\mathbb{P}_N} u_{w+1}^\beta = k N^\beta \mathbb{E}_{\mathbb{P}_N} M_\beta(w, 1).$$

6.6.3. *Asymptotics of $B^{(\Sigma, \Pi)}$.* Let $j \in [w + p - 1]^\beta$. By Lemma 6.8 the coset length

$$\|\sigma_{p,j} \mathfrak{S}_k\| \leq \|\sigma_{p,j}\| \leq \beta$$

is uniformly bounded from above by the number of factors in (6.24). By Fact 3.1 and Lemma 6.8 it follows that there exists a universal constant C_β such that

$$\left| \chi_{\square_N} \left(\pi_0(\sigma_{p,j}) \right) \right| \leq C_\beta N^{-\|\sigma_{p,j} \mathfrak{S}_k\|}$$

holds true for each $j \in [w + p - 1]^\beta$.

Let us fix a pair (Σ, Π) of complementary set-partitions of $[\beta]$. The number of the summands on the right-hand side of (6.33) is equal to the following sum of falling factorials

$$\sum_{p=1}^k (w)_{|\Sigma|} \cdot (p)_{|\Pi|} \leq N^{2|\Sigma|} k^{|\Pi|+1}.$$

By combining these observations with Corollary 6.12 we conclude that

$$(6.36) \quad \left| B^{(\Sigma, \Pi)} \right| \leq C_\beta N^{-\|\sigma_{p,j} \mathfrak{S}_k\|} \cdot N^{2|\Sigma|} k^{|\Pi|+1} \leq C_\beta k N^\beta \left(\frac{k}{N} \right)^{|\Pi|}.$$

The last two arguments imply also that for any $p \in \{1, \dots, k\}$

$$(6.37) \quad \sum_{j \in (\Sigma, \Pi)} \frac{k^2}{N^{\|\sigma_{p,j} \mathfrak{S}_k\|+1}} \leq \frac{k^2}{N} N^\beta \left(\frac{k}{N} \right)^{|\Pi|}.$$

6.6.4. *Proof of Proposition 6.13.*

Proof of Proposition 6.13. The asymptotics of the summands which contribute to the right-hand side of (6.34) is provided by the equality (6.35) and the estimate (6.36) (for pairs (Σ, Π) of complementary set-partitions of $[\beta]$ with $\Pi \neq \emptyset$). In this way the proof of (6.30) is complete.

By Proposition 6.9 there exists $H_\beta > 0$ such that

$$(6.38) \quad \left| \chi_{\square_N}(\mathcal{J} \mathfrak{S}_k) - \chi_{\square_N}(\mathcal{J}_0) \right| \leq H_\beta \sum_{p=1}^k \sum_{j \in [w+p-1]^\beta} \frac{k^2}{N^{\|\sigma_{p,j} \mathfrak{S}_k\|+1}}.$$

The summands on the right-hand side can be grouped according to the type (Σ, Π) of the sequence j . For a fixed value of β there are only finitely many possible types, and the total contribution of the sequences j of a specific

type (Σ, Π) is bounded from above by (6.37) which completes the proof of (6.31).

Equation (6.32) is a direct consequence of (6.30) and (6.31). \square

6.7. The variance of M_β – the proof of (6.3). We will mimic the concepts from Section 6.6, however, the calculations will be more involved.

Proof of (6.3). We first calculate the second moment of M_β . By Proposition 6.5 and then (6.29)

$$(6.39) \quad \mathbb{E}_{\tilde{\mathbb{P}}_N} M_\beta(w, k)^2 = \frac{1}{k! \mathbb{P}_N(\tilde{\mathcal{T}}_{\square_N}^{(w+1, w+k)})} \cdot \frac{1}{k^2} N^{-2\beta} \chi_{\square_N}(\mathcal{J}^2 \mathfrak{S}_k) \\ = \left(1 + O\left(\frac{k^2}{N}\right) \right) \frac{1}{k^2} N^{-2\beta} \chi_{\square_N}(\mathcal{J}^2 \mathfrak{S}_k)$$

where (recall the definition (6.24) of $\sigma_{p,j}$)

$$\mathcal{J}^2 := \left(\sum_{p=1}^k J_{w+p}^\beta \right)^2 = \sum_{p_1, p_2=1}^k \sum_{\substack{s \in [w+p_1-1]^\beta \\ t \in [w+p_2-1]^\beta}} \sigma_{p_1, s} \sigma_{p_2, t} \in \mathbb{C} \mathfrak{S}_{w+k}.$$

Equation (6.42) from Proposition 6.14 below provides the necessary asymptotics of the numerator in (6.39) and gives us

$$\mathbb{E}_{\tilde{\mathbb{P}}_N} M_\beta(w, k)^2 = \frac{1}{k} \mathbb{E}_{\mathbb{P}_N} M_{2\beta}(w, 1) + \left(1 - \frac{1}{k} \right) \left(\mathbb{E}_{\mathbb{P}_N} M_\beta(w, 1) \right)^2 + O\left(\frac{k^2}{N}\right)$$

with the constant in the O -notation depending only on β . By (6.2) we finally get

$$\text{Var}_{\tilde{\mathbb{P}}_N} M_\beta(w, k) = \mathbb{E}_{\tilde{\mathbb{P}}_N} M_\beta(w, k)^2 - \left(\mathbb{E}_{\tilde{\mathbb{P}}_N} M_\beta(w, k) \right)^2 = \\ \frac{1}{k} \left[\mathbb{E}_{\mathbb{P}_N} M_{2\beta}(w, 1) - \left(\mathbb{E}_{\mathbb{P}_N} M_\beta(w, 1) \right)^2 \right] + O\left(\frac{k^2}{N}\right) = O\left(\frac{1}{k} + \frac{k^2}{N}\right)$$

with the constant in the O -notation depending only on β . This completes the proof of (6.3) (and Proposition 6.3). \square

We consider an analogue of \mathcal{J}^2 in which each summand is replaced by the minimal element of the appropriate coset

$$\mathcal{J}_*^2 := \pi_0(\mathcal{J}^2) = \sum_{p_1, p_2=1}^k \sum_{\substack{s \in [w+p_1-1]^\beta \\ t \in [w+p_2-1]^\beta}} \pi_0(\sigma_{p_1, s} \sigma_{p_2, t}) \in \mathbb{C} \mathfrak{S}_{w+k}.$$

The following proposition provides the missing component of the above proof of (6.3).

Proposition 6.14. *Let $\beta \in \mathbb{N}$ and $k, N \in \mathbb{N}$ be such that $N^2 \geq w + k$ and $k^2 < N$. Then*

$$(6.40) \quad \chi_{\square_N}(\mathcal{J}_*^2) = k^2 N^{2\beta} \left[\frac{1}{k} \mathbb{E}_{\mathbb{P}_N} M_{2\beta}(w, 1) + \left(1 - \frac{1}{k}\right) (\mathbb{E}_{\mathbb{P}_N} M_{\beta}(w, 1))^2 + O\left(\frac{k}{N}\right) \right];$$

$$(6.41) \quad \chi_{\square_N}(\mathcal{J}^2 \mathfrak{S}_k) = \chi_{\square_N}(\mathcal{J}_*^2) + O\left(k^2 N^{2\beta} \frac{k^2}{N}\right);$$

$$(6.42) \quad \chi_{\square_N}(\mathcal{J}^2 \mathfrak{S}_k) = k^2 N^{2\beta} \left[\frac{1}{k} \mathbb{E}_{\mathbb{P}_N} M_{2\beta}(w, 1) + \left(1 - \frac{1}{k}\right) (\mathbb{E}_{\mathbb{P}_N} M_{\beta}(w, 1))^2 + O\left(\frac{k^2}{N}\right) \right]$$

with the constants in the O -notation depending only on β .

The remaining part of this section is devoted to its proof.

6.7.1. *Decomposition of $\chi_{\square_N}(\mathcal{J}_*^2)$.* For any $p_1, p_2 \in \{1, \dots, k\}$ denote

$$P_{p_1, p_2}(\beta) := [w + p_1 - 1]^\beta \times [w + p_2 - 1]^\beta$$

and let

$$A := \sum_{p=1}^k \sum_{s, t \in [w]^\beta} \chi_{\square_N} \left(\pi_0(\sigma_{p, s} \sigma_{p, t}) \right);$$

Let us define *the concatenation of sequences* $a = (a_1, \dots, a_x)$ and $b = (b_1, \dots, b_y)$ as the sequence $a \sqcup b := (a_1, \dots, a_x, b_1, \dots, b_y)$. For any pair of complementary set-partitions (Σ, Π) of the set $[2\beta]$ let us denote

$$(6.43) \quad B^{(\Sigma, \Pi)} := \sum_{p_1, p_2=1}^k \sum_{\substack{(s, t) \in P_{p_1, p_2}(\beta), \\ s \sqcup t \in (\Sigma, \Pi)}} \chi_{\square_N} \left(\pi_0(\sigma_{p_1, s} \sigma_{p_2, t}) \right)$$

and if Σ is a set-partition of $[2\beta]$ denote

$$(6.44) \quad C^\Sigma := \sum_{\substack{p_1, p_2 \in \{1, \dots, k\}, \\ p_1 \neq p_2}} \sum_{\substack{s, t \in [w]^\beta, \\ s \sqcup t \in (\Sigma, \emptyset)}} \chi_{\square_N} \left(\pi_0(\sigma_{p_1, s} \sigma_{p_2, t}) \right).$$

With these notations

$$(6.45) \quad \chi_{\square_N}(\mathcal{J}_*^2) = A + \sum_{\substack{(\Sigma, \Pi) \\ \Pi \neq \emptyset}} B^{(\Sigma, \Pi)} + \sum_{\Sigma} C^{\Sigma}.$$

Notice that the number of summands on the right hand side of (6.45) is finite, depends only on β and does not depend on N or k . Therefore, it is enough to find the asymptotics for each individual summand on the right-hand side.

6.7.2. *Asymptotics of A .* We proceed in the same way as in Section 6.6.2 to get an exact formula

$$(6.46) \quad A = kN^{2\beta} \mathbb{E}_{\mathbb{P}_N} M_{2\beta}(w, 1).$$

6.7.3. *Asymptotics of $B^{(\Sigma, \Pi)}$.* We follow the lines from Section 6.6.3.

Let us fix some pair (Σ, Π) of complementary set-partitions of $[2\beta]$. By Fact 3.1 and Lemma 6.8 there exists $C_\beta > 0$ such that each summand corresponding to $(s, t) \in P_{p_1, p_2}(\beta)$ such that $s \sqcup t \in (\Sigma, \Pi)$ fulfills the asymptotic bound

$$\left| \chi_{\square_N} \left(\pi_0 \left(\sigma_{p_1, s} \sigma_{p_2, t} \right) \right) \right| \leq C_\beta N^{-\|\sigma_{p_1, s} \sigma_{p_2, t} \mathfrak{S}_k\|}.$$

On the other hand, the number of the summands on the right-hand side of (6.43) is bounded from above by

$$\sum_{p_1, p_2=1}^k w_{|\Sigma|} \cdot \max\{p_1, p_2\}_{|\Pi|} \leq N^{2|\Sigma|} k^{|\Pi|+2}.$$

By combining these observations with Corollary 6.12 used for the concatenated sequence $s \sqcup t$ we conclude that

$$(6.47) \quad \left| B^{(\Sigma, \Pi)} \right| \leq C_\beta k^2 N^{2\beta} \left(\frac{k}{N} \right)^{|\Pi|}.$$

The last two arguments imply also that

$$(6.48) \quad \sum_{p_1, p_2=1}^k \sum_{\substack{(s, t) \in P_{p_1, p_2}(\beta), \\ s \sqcup t \in (\Sigma, \Pi)}} \frac{k^2}{N^{\|\sigma_{p_1, s} \sigma_{p_2, t} \mathfrak{S}_k\|+1}} \leq \frac{k^2}{N} \cdot k^2 N^{2\beta} \left(\frac{k}{N} \right)^{|\Pi|}.$$

These estimations show that if a pair (Σ, Π) of complementary set-partitions of $[2\beta]$ is such that $\Pi \neq \emptyset$ then the contribution of $B^{(\Sigma, \Pi)}$ to (6.45) is of relatively small order.

6.7.4. *Asymptotics of C^Σ . Connected set-partitions of $[2\beta]$.* We will need to be much more subtle in calculating (and estimating) the summand C^Σ . We will treat the summand C^Σ in two different ways depending on the structure of Σ .

Let Σ be a set-partition of $[2\beta]$. We say that Σ is *connected* if there exists a block $\pi \in \Sigma$ which contains simultaneously some element of the set $\{1, \dots, \beta\}$ and some element of the set $\{\beta + 1, \dots, 2\beta\}$, that is formally, $\pi \cap [\beta] \neq \emptyset$ and $\pi \cap \{\beta + 1, \dots, 2\beta\} \neq \emptyset$. Each such a block $\pi \in \Sigma$ will be called a *link*. If Σ does not have any links then we say that Σ is *disconnected*.

6.7.5. *Asymptotics of C^Σ for connected Σ .* Let us fix a connected set-partition Σ of $[2\beta]$. We set

$$n_\Sigma := \min \{i \in \{\beta + 1, \dots, 2\beta\} : \exists \pi \in \Sigma \ (i \in \pi \text{ and } \pi \text{ is a link in } \Sigma)\}.$$

In other words, n_Σ indicates the least number $i > \beta$ belonging to some link π of Σ .

Notice that for distinct p_1, p_2 and a pair of sequences (s, t) such that $s \sqcup t \in (\Sigma, \emptyset)$ the assumptions of the second part of Lemma 6.11 are fulfilled for the sequences $(x_i) = s \sqcup t$ and $(y_i) = (p_1, \dots, p_1, p_2, \dots, p_2)$, and $\ell := \beta + n_\Sigma - 1$. Therefore an inequality

$$2|\Sigma| - \|\sigma_{p_1, s} \sigma_{p_2, t} \mathfrak{S}_k\| - 2\beta \leq -1$$

holds for any (s, t) such that $s \sqcup t \in (\Sigma, \emptyset)$ with Σ connected.

We now follow the lines in Section 6.7.3 to get the upper bound

$$(6.49) \quad |C^\Sigma| \leq C_\beta (k^2 - k) N^{2\beta-1}$$

which holds for each connected set-partition Σ of the set $[2\beta]$. This shows that the contribution of C^Σ with connected Σ to (6.45) is of relatively small order.

6.7.6. *Asymptotics of C^Σ for disconnected Σ .* We will show that

$$(6.50) \quad \sum_{\substack{\Sigma: \\ \Sigma \text{ is disconnected}}} C^\Sigma = (k^2 - k) N^{2\beta} \left((\mathbb{E}_{\mathbb{P}_N} M_\beta(w, 1))^2 + O(N^{-2}) \right)$$

with the constant in the O -notation depending only on β .

Recall that the C^Σ , defined in (6.44), is the sum of characters χ_{\square_N} evaluated on the minimal permutations $\pi_0(\sigma_{p_1, s} \sigma_{p_2, t})$. When Σ is disconnected and $p_1 \neq p_2$, in the permutation $\sigma_{p_1, s} \sigma_{p_2, t}$ each cycle permutes at most one big element, so by Lemma 6.8(b) $\sigma_{p_1, s} \sigma_{p_2, t}$ is the minimal permutation.

Hence whenever Σ is disconnected

$$C^\Sigma = \sum_{\substack{p_1, p_2 \in \{1, \dots, k\}, \\ p_1 \neq p_2}} \sum_{\substack{s, t \in [w]^\beta, \\ s \sqcup t \in (\Sigma, \emptyset)}} \chi_{\square_N}(\sigma_{p_1, s} \sigma_{p_2, t}).$$

For any set partition Σ of $[2\beta]$ let us define

$$\tilde{C}^\Sigma := \sum_{\substack{p_1, p_2 \in \{1, \dots, k\}, \\ p_1 \neq p_2}} \sum_{\substack{s, t \in [w]^\beta, \\ s \sqcup t \in (\Sigma, \emptyset)}} \chi_{\square_N}(\sigma_{p_1, s}) \chi_{\square_N}(\sigma_{p_2, t}).$$

Then by Proposition 6.5 applied twice for $k = 1$

(6.51)

$$\begin{aligned} \sum_{\Sigma} \tilde{C}^\Sigma &= \sum_{\substack{p_1, p_2 \in \{1, \dots, k\}, \\ p_1 \neq p_2}} \left(\sum_{s \in [w]^\beta} \chi_{\square_N}(\sigma_{p_1, s}) \right) \left(\sum_{t \in [w]^\beta} \chi_{\square_N}(\sigma_{p_2, t}) \right) = \\ &= (k^2 - k) N^{2\beta} (\mathbb{E}_{\mathbb{P}_N} M_\beta(w, 1))^2. \end{aligned}$$

Our aim is to show that (6.51) is a good approximation for the left-hand-side of (6.50).

By Fact 3.2 there exists a constant $K_\beta > 0$ which depends only on β (in particular it does not depend on N or k) such that for any distinct p_1, p_2 and a pair of sequences (s, t) such that $s \sqcup t \in (\Sigma, \emptyset)$ with Σ disconnected

$$\left| \chi_{\square_N}(\sigma_{p_1, s} \sigma_{p_2, t}) - \chi_{\square_N}(\sigma_{p_1, s}) \chi_{\square_N}(\sigma_{p_2, t}) \right| \leq K_\beta \left(N^{-|\sigma_{p_1, s}| - |\sigma_{p_2, t}| - 2} \right).$$

Let us denote for any set-partition Σ of $[2\beta]$

$$R^\Sigma := \sum_{\substack{p_1, p_2 \in \{1, \dots, k\}, \\ p_1 \neq p_2}} \sum_{\substack{s, t \in [w]^\beta, \\ s \sqcup t \in (\Sigma, \emptyset)}} N^{-|\sigma_{p_1, s}| - |\sigma_{p_2, t}| - 2}.$$

With the introduced notation the following inequality holds

(6.52)

$$\left| \sum_{\Sigma} \tilde{C}^\Sigma - \sum_{\substack{\Sigma: \\ \Sigma \text{ is disconnected}}} C^\Sigma \right| \leq \sum_{\substack{\Sigma: \\ \Sigma \text{ is disconnected}}} K_\beta R^\Sigma + \sum_{\substack{\Sigma: \\ \Sigma \text{ is connected}}} |\tilde{C}^\Sigma|.$$

We now investigate the asymptotics of the sums on the right-hand-side of (6.52).

6.7.7. *Asymptotics of the right-hand-side of (6.52).* Observe that if Σ is connected and (s, t) is a pair of sequence such that $s \sqcup t \in (\Sigma, \emptyset)$ then

$$|\Sigma| = |\Sigma(s \sqcup t)| \leq |\Sigma(s)| + |\Sigma(t)| - 1.$$

We follow the lines from Section 6.6.3 to get the upper bound

$$(6.53) \quad \left| \tilde{C}^\Sigma \right| \leq C_\beta^2 (k^2 - k) N^{2\beta-2}$$

for any connected Σ with universal constant $C_\beta > 0$ depending only on β .

On the other hand, by Lemma 6.8(b) and (6.37) for any set-partition Σ of $[2\beta]$

$$(6.54) \quad R^\Sigma \leq (k^2 - k) \left[\sum_{s \in [w]^\beta} N^{-|\sigma_{p_1, s}|-1} \right]^2 \leq (k^2 - k) N^{2\beta-2}.$$

Inserting approximations (6.53) for connected Σ and (6.54) for disconnected Σ into (6.52) and taking into account (6.51) proves (6.50).

6.7.8. *Asymptotics of the sum $\sum_{\Sigma} C^\Sigma$.* By (6.49) and (6.50) we get

$$(6.55) \quad \sum_{\Sigma} C^\Sigma = (k^2 - k) N^{2\beta} \left((\mathbb{E}_{\mathbb{P}_N} M_\beta(w, 1))^2 + O(N^{-1}) \right).$$

6.7.9. *Finishing the proof of Proposition 6.14.*

Proof of Proposition 6.14. Inserting the equality (6.46) and approximations (6.47) (for complementary set-partitions (Σ, Π) with $\Pi \neq \emptyset$) and (6.55) into (6.45) we conclude that (6.40) holds true.

By Proposition 6.9 there exists $C_\beta > 0$ such that

$$(6.56) \quad \left| \chi_{\square_N}(\mathcal{J}^2 \mathfrak{S}_k) - \chi_{\square_N}(\mathcal{J}_*^2) \right| \leq C_\beta \sum_{p_1, p_2=1}^k \sum_{(s, t) \in P_{p_1, p_2}(\beta)} \frac{k^2}{N^{\|\sigma_{p_1, s} \sigma_{p_2, t} \mathfrak{S}_k\|+1}}.$$

The summands on the right-hand side can be grouped according to the types (Σ, Π) of the sequences $s \sqcup t$. By (6.48) the right-hand side of (6.56) estimates by $\frac{k^2}{N} k^2 N^{2\beta}$ which ends the proof of (6.41).

Equation (6.42) is a direct consequence of (6.40) and (6.41). \square

This finishes the proof of Proposition 6.3

6.8. Proof of Theorem 6.2. The proof is based on [RŚ15, Section 4.10]. We start with a general fact.

Lemma 6.15. *Let $\varepsilon > 0$ and μ be a compactly supported probability measure on \mathbb{R} . Let $x \in \mathbb{R}$ be a continuity point of the cumulative distribution function F_μ of μ . Then there exist $\delta > 0$ and an integer $A > 0$ with the following property:*

if m is a probability measure on \mathbb{R} such that its moments (up to order A) are δ -close to the moments of μ then

$$|F_\mu(x) - F_m(x)| \leq \varepsilon$$

where F_m is the cumulative distribution function of m .

Proof. If this would not be the case, there would exist a sequence of probability measures which converges to μ in moments, but would not converge to μ in the weak topology of probability measures. This is not possible, since μ is compactly supported and therefore uniquely determined by its moments [Dur10, Section 3.3.5]. \square

We now prove Theorem 6.2.

Proof of Theorem 6.2. We mimic the proof of [RŚ15, Theorem 4.1]. Pittel and Romik [PR07, Theorem 2] found explicitly the limit distribution ν_α which describes the u -coordinate of the (scaled) position of the box with the entry $\lfloor \alpha N^2 \rfloor$ in a uniformly random tableau $T_N \in \mathcal{T}_{\square_N}$ as the semicircle distribution (2.4) (recall Section 2.3). In our setting this result describes the u -coordinate of the surfer after draining $1 - \alpha$ fraction of water. Since ‘the amount of remaining water w ’ is such that $\frac{w}{N^2} \rightarrow \alpha$, the β -th moment γ_β of the distribution ν_α equals

$$\gamma_\beta := \int x^\beta d\nu_\alpha(x) = \lim_{N \rightarrow \infty} \mathbb{E}_{\mathbb{P}_N} M_\beta(w, 1).$$

By Proposition 6.3 we get using Chebyshev’s inequality that for any $\varepsilon > 0$ and $\beta \in \mathbb{N}$

$$\mathbb{P}_{\tilde{\mathcal{T}}_{\square_N}^{(w+1, w+k)}} \left(|M_\beta(w, k) - \gamma_\beta| > \varepsilon \right) = O \left(\frac{1}{k} + \frac{k^2}{N} \right).$$

The cumulative distribution function F_{ν_α} of the semicircle measure ν_α is continuous and therefore any $x \in \mathbb{R}$ is its continuity point. Let $x \in \mathbb{R}$ and let A and δ be the constants given by Lemma 6.15. Then by the union

bound

$$(6.57) \quad \mathbb{P}_{\tilde{\mathcal{T}}_{\square_N}^{(w+1, w+k)}} \left\{ |F_{\nu_\alpha}(x) - G_N(x)| > \varepsilon \right\} \leq \sum_{\beta=1}^A \mathbb{P}_{\tilde{\mathcal{T}}_{\square_N}^{(w+1, w+k)}} \left(|M_\beta(w, k) - \gamma_\beta| > \delta \right) = O \left(\frac{1}{k} + \frac{k^2}{N} \right)$$

with the constant in the O -notation depending only on ε .

For the proof of Theorem 6.2 we need to obtain the uniform version of (6.57) in which the event on the left hand side is taken with supremum over $u \in \mathbb{R}$. This can be easily done by choosing a finite set $X \subseteq \mathbb{R}$ with the property that its image F_{ν_α} is an ϵ -net for the interval $[0, 1]$; such a set exists because F_{ν_α} is continuous. The pointwise result (6.57) implies that the following estimate for the supremum over the finite set X holds true:

$$(6.58) \quad \mathbb{P}_{\tilde{\mathcal{T}}_{\square_N}^{(w+1, w+k)}} \left\{ M_N : \sup_{x \in X} |F_{\nu_\alpha}(x) - G_N(x)| > \varepsilon \right\} = O \left(\frac{1}{k} + \frac{k^2}{N} \right).$$

Let $x_1 < \dots < x_\ell$ be the elements of X . The assumption about the set X implies that

$$(6.59) \quad F_{\nu_\alpha}(x_1) < \epsilon, \quad F_{\nu_\alpha}(x_{i+1}) < F_{\nu_\alpha}(x_i) + 2\epsilon, \quad F_{\nu_\alpha}(x_\ell) > 1 - \epsilon.$$

The elements of X divide the real line into $\ell + 1$ intervals:

$$(-\infty, x_1], [x_1, x_2], \dots, [x_{\ell-1}, x_\ell], [x_\ell, \infty).$$

By considering each interval separately, using monotonicity of the cumulative distribution function F_{ν_α} and the monotonicity of G_N , as well as (6.59) it follows that

$$\sup_{x \in \mathbb{R}} |F_{\nu_\alpha}(x) - G_N(x)| < 2\epsilon + \sup_{x \in X} |F_{\nu_\alpha}(x) - G_N(x)|.$$

In this way (6.58) completes the proof. \square

7. PROOF OF THEOREM 4.1

The current section is devoted to the proof of Theorem 4.1.

7.1. Overtaking only in one direction. We start with a precise statement of the heuristic ideas from Section 4.4.4.

Lemma 7.1. *Fix $k, n \in \mathbb{N}$. Let tableaux $T \in \mathcal{T}_\mu$ of shape μ with $n+1$ boxes and $M \in \tilde{\mathcal{T}}_\nu^{(n+1, n+k)}$ of shape ν with $n+k$ boxes be such that*

$$T|_{\leq n} = M|_{\leq n}.$$

If $1 \leq p \leq k$ is such that

$$\text{pos}_T(n+1) \preceq \text{pos}_M(n+p) \preceq \cdots \preceq \text{pos}_M(n+k)$$

then jeu de taquin preserves the latter relations, that is

$$\text{pos}_{j(T)}(n+1) \preceq \text{pos}_{j(M)}(n+p) \preceq \cdots \preceq \text{pos}_{j(M)}(n+k).$$

Proof. Clearly, $j(T)|_{\leq n} = j(M)|_{\leq n}$. Notice also that the boxes in jeu de taquin paths for tableaux T and M match at least to the boxes $\leq n$. As mentioned in Section 4.2, $j(M)$ is a k -Pieri tableau, so

$$\text{pos}_{j(M)}(n+p) \preceq \cdots \preceq \text{pos}_{j(M)}(n+k)$$

and therefore it remains to prove that

$$(7.1) \quad \text{pos}_{j(T)}(n+1) \preceq \text{pos}_{j(M)}(n+p).$$

We consider the following two cases:

1. The box $n+1$ in T slid during jeu de taquin, i.e., $\text{pos}_T(n+1) \neq \text{pos}_{j(T)}(n+1)$. Consider two subcases:
 - 1a) The box $n+1$ in T slid to the left; in this case it does not matter how (and if) the box $n+p$ in M slid and (7.1) holds.
 - 1b) The box $n+1$ in T slid to the bottom. Then we use the assumption that M is k -Pieri to show that if $\text{pos}_M(n+p) = \text{pos}_T(n+1)$ then $n+p$ in M also slid to the bottom and (7.1) holds. On the other hand if $\text{pos}_T(n+1) \prec \text{pos}_M(n+p)$ then the box $n+p$ in M must be strictly to the right of $n+1$ in T and it does not matter if it slides or not, so (7.1) also holds.
2. The box $n+1$ in T did not slide, i.e., $\text{pos}_T(n+1) = \text{pos}_{j(T)}(n+1)$. In this case, the JDT path in T ends on some box $\leq n$ which is strictly left-top or strictly right-bottom to the $\text{pos}_T(n+1)$. Hence, if $\text{pos}_T(n+1) = \text{pos}_M(n+p)$ then the box $n+p$ in M does not slide. Otherwise, (by the initial relation) it must be strictly to the right (and weakly to the bottom) of $\text{pos}_T(n+1)$ and it does not matter if it slides or not. All in all, (7.1) holds. \square

7.2. Relative position of the surfer. We recommend the reader to recall the notions in Section 4 and heuristics for the proof of Theorem 4.1 in Section 4.4.

Let $0 < t_1 < t_2 < 1$ and denote

$$w := \lceil (1 - t_1)N^2 \rceil - 1.$$

Let k be a positive integer such that $w + k \leq N^2$. By Proposition 5.1 used for $C = 1$, $\Delta = t_1$, $a = w$ and $\lambda = \square_N$ there exists a pair of random tableaux \mathbf{T} , \mathbf{M} defined on the same probability space with the following properties:

- (A1) \mathbf{T} is a uniformly random element of \mathcal{T}_{\square_N} ;
 (A2) \mathbf{M} is a random element of $\tilde{\mathcal{T}}_{\square_N}^{(w+1, w+k)}$ sampled according to the distribution which fulfills the following total variation distance bound

$$\delta \left(\mathbf{M}, \mathbb{P}_{\tilde{\mathcal{T}}_{\square_N}^{(w+1, w+k)}} \right) \leq d \frac{k^2}{\sqrt{N^2 - w}}$$

for some universal constant $d > 0$ which depends only on t_1 ;

- (A3) $\mathbf{T}|_{\leq w} = \mathbf{M}|_{\leq w}$ holds true almost surely.

Since the dual promotion ∂^* is a bijection, by (A1) the tableau $\mathbf{T}|_{\leq w+1}$ has the same distribution as the initial configuration of the single surfer T'_N (see (4.5)) and by (A2) the tableau $\mathbf{M}|_{\leq w+k}$ has approximately the same distribution (up to the total variation distance in (A2)) as the initial configuration of the multisurfers M'_N (see (4.11)). Moreover, by (A3) the initial configurations of water are the same for both stories. Therefore we will refer to the box $w+1$ in \mathbf{T} as the *surfer* and to the boxes $w+1, \dots, w+k$ in \mathbf{M} as the *multisurfers*.

Recall that the definition (6.1) of the random variable $G_N(u)$ depends implicitly on the choice of the tableau M_N . For an integer $0 \leq q \leq w$ we denote by $G_N^q(u)$ this random variable obtained by substituting M_N with $j^q(\mathbf{M})$. We underline here that M_N and $j^q(\mathbf{M})$ need not have the same distribution. We also define \tilde{G}_N^q to be the fraction of the multisurfers which are to the left of the surfer, more precisely

(7.2)

$$\tilde{G}_N^q := G_N^q \left(\frac{1}{N} u_{w+1}^{j^q(\mathbf{T})} \right) = \frac{1}{k} \max \left\{ p \in \{1, \dots, k\} : u_{w+p}^{j^q(\mathbf{M})} \leq u_{w+1}^{j^q(\mathbf{T})} \right\}.$$

The following proposition gives a relation between \tilde{G}_N^q and the theoretical longitude of the surfer on the common probability space of the surfer and multisurfers defined in the beginning of this section.

Proposition 7.2. *Let $s \geq 0$ and $t > 0$ be such that $s + t < 1$. Let $w(N) = \lceil (1-t)N^2 \rceil - 1$ for $N \in \mathbb{N}$ and let $k = k(N)$ fulfill Assumption 6.1. Let $q = q(N)$ be a sequence of non-negative integers such that*

$$0 \leq q(N) \leq \lfloor (1-t)N^2 \rfloor \quad \text{and} \quad \lim_{N \rightarrow \infty} \frac{q}{N^2} = s.$$

Then for any $\varepsilon > 0$

$$\mathbb{P} \left((\mathbf{T}, \mathbf{M}) : \left| \tilde{G}_N^q - F_{\nu_{1-t-s}} \left(\frac{1}{N} u_{w+1}^{j^q(\mathbf{T})} \right) \right| > \varepsilon \right) = O \left(\frac{1}{k} + \frac{k^2}{N} \right)$$

and the constant in the O -notation depends only on $s, t+s$ and ε .

Proof. By the discussion below Equation (7.2)

$$\begin{aligned} \mathbb{P} \left((\mathbf{T}, \mathbf{M}) : \left| \tilde{G}_N^q - F_{\nu_{1-t-s}} \left(\frac{1}{N} u_{w+1}^{j^q(\mathbf{T})} \right) \right| > \varepsilon \right) = \\ \mathbb{P} \left((\mathbf{T}, \mathbf{M}) : \left| G_N^q \left(\frac{1}{N} u_{w+1}^{j^q(\mathbf{T})} \right) - F_{\nu_{1-t-s}} \left(\frac{1}{N} u_{w+1}^{j^q(\mathbf{T})} \right) \right| > \varepsilon \right). \end{aligned}$$

The latter is bounded from above by

$$(7.3) \quad \mathbb{P} \left((\mathbf{T}, \mathbf{M}) : \sup_{x \in \mathbb{R}} \left| G_N^q(x) - F_{\nu_{1-t-s}}(x) \right| > \varepsilon \right).$$

The random event in (7.3) is expressed purely in terms of the random tableau $j^q(\mathbf{M})$ and does not involve the random tableau \mathbf{T} . For this reason the probability in (7.3), due to the condition (A2) on page 64 and the bijectivity of the dual promotion ∂^* , is equal to

$$\mathbb{P}_{\tilde{\mathcal{T}}_{\square_N}^{(w-q+1, w-q+k)}} \left(M_N : \sup_{x \in \mathbb{R}} \left| G_N(x) - F_{\nu_{1-t-s}}(x) \right| > \varepsilon \right) + O\left(\frac{k^2}{N}\right)$$

with the constant in the O -notation depending only on t . Since $\lim_{N \rightarrow \infty} \frac{w-q}{N^2} = 1 - t - s > 0$ we can apply Theorem 6.2 which completes the proof. \square

7.3. Proof of the upper bound (4.2) in Theorem 4.1. Let $k = k(N)$ be such that $k(N) \rightarrow \infty$ and $k(N) = o(\sqrt{N})$, i.e., (4.10) is satisfied. We will use the results from Section 7.2 to prove the upper bound (4.2). Let $q := \lfloor t_2 N^2 \rfloor - \lfloor t_1 N^2 \rfloor$. Recall that $w = \lceil (1 - t_1) N^2 \rceil - 1$ (cf. Section 7.2).

By (A1) from Section 7.2 we can translate the probability on the left-hand-side of (4.2) into the setting of \mathbf{T} in the following way

$$\begin{aligned} \mathbb{P}_N \left(T \in \mathcal{T}_{\square_N} : \Psi_N^{\text{th}}(t_2) - \Psi_N^{\text{th}}(t_1) > \varepsilon \right) = \\ \mathbb{P} \left((\mathbf{T}, \mathbf{M}) : F_{\nu_{1-t_2}} \left(\frac{1}{N} u_{w+1}^{j^q(\mathbf{T})} \right) - F_{\nu_{1-t_1}} \left(\frac{1}{N} u_{w+1}^{\mathbf{T}} \right) > \varepsilon \right); \end{aligned}$$

note that the event on the right-hand side *does not* involve the tableau \mathbf{M} . The latter probability can be estimated from above via the union bound by the sum of probabilities of the following three events:

- the fraction of the multisurfers in the final position (i.e., in time t_2) which are to the left of the surfer is ‘unusually small’, that is

$$A := \left\{ (\mathbf{T}, \mathbf{M}) : F_{\nu_{1-t_2}} \left(\frac{1}{N} u_{w+1}^{j^q(\mathbf{T})} \right) - \tilde{G}_N^q > \frac{\varepsilon}{2} \right\};$$

- the number of the multisurfers which are to the left of the surfer increases over time, more precisely

$$B := \left\{ (\mathbf{T}, \mathbf{M}) : \tilde{G}_N^q - \tilde{G}_N^0 > 0 \right\};$$

- the fraction of the multisurfers in the initial position (i.e, in time t_1) which are to the left of the surfer is ‘unusually big’, that is

$$C := \left\{ (\mathbf{T}, \mathbf{M}) : \tilde{G}_N^0 - F_{\nu_{1-t_1}} \left(\frac{1}{N} u_{w+1}^{\mathbf{T}} \right) > \frac{\varepsilon}{2} \right\}.$$

By Proposition 7.2 the probabilities of the events A and C are of order $O\left(\frac{1}{k} + \frac{k^2}{N}\right)$. By Lemma 7.1 the event $B = \emptyset$ is impossible. The choice of the sequence k as in the beginning of this subsection implies that the upper bound (4.2) holds.

7.4. Proof of the lower bound (4.3) in Theorem 4.1. For any Young diagram λ and tableau $T \in \mathcal{T}_\lambda$ we will denote by λ^{tr} and T^{tr} , respectively, the diagram and the tableau obtained by a *transposition* of the diagram λ and the tableau T .

The transposition of tableaux gives a natural bijection between the sets \mathcal{T}_λ and $\mathcal{T}_{\lambda^{\text{tr}}}$ of standard tableaux, respectively, of shape λ and its transpose λ^{tr} . Moreover, under the transposition the u -coordinate of the given box in a standard tableau T changes its sign, namely for any $n \in \{1, \dots, |T|\}$

$$(7.4) \quad u_n^T = -u_n^{T^{\text{tr}}}.$$

In particular, the u -coordinate of the surfer $u(X_t)$ changes its sign under the transposition, i.e., $u(X_t) = -u(X_t^{\text{tr}})$ where X_t^{tr} denotes the position of the surfer in the transposed tableau T^{tr} .

Recall that for any $\alpha \in (0, 1)$ by ν_α we denote the limit measure found by Pittel and Romik on the circle of latitude α , see Section 2.3. The push-forward of the measure ν_α under the involution $\mathbb{R} \ni z \mapsto -z$ is a measure $\tilde{\nu}_\alpha$ which fulfills the following equality

$$(7.5) \quad \tilde{\nu}_\alpha((-\infty, u]) = \nu_\alpha([-u, \infty)) \quad \text{for all } u \in \mathbb{R}.$$

Notice that by (7.4) the measure $\tilde{\nu}_\alpha$ is the limit measure on the circle of latitude α for the transposed sequence of Young diagrams (\square_N^{tr}) .

Let us denote the position of the surfer in the transposed tableau by X_t^* , cf. (2.5), and the theoretical longitude of the surfer in the transposed tableau by η , i.e.,

$$\eta(t) := F_{\tilde{\nu}_{1-t}}(u(X_t^*)) \quad \text{for } t \in [0, 1].$$

Observe that by (7.5) and the continuity of $F_{\nu_{1-t}}$

$$(7.6) \quad \eta(t) = 1 - F_{\nu_{1-t}}(-u(X_t^*)).$$

Equation (4.2) applied to the transposed tableaux gives

$$\lim_{N \rightarrow \infty} \mathbb{P}_N \left\{ T \in \mathcal{T}_{\square_N^{\text{tr}}} : \eta(t_2) - \eta(t_1) > \varepsilon \right\} = 0.$$

On the other hand by (7.6) and then (7.4) we get

$$\begin{aligned} \eta(t_2) - \eta(t_1) &= [1 - F_{\nu_1-t_2}(-u(X_{t_2}^*))] - [1 - F_{\nu_1-t_1}(-u(X_{t_1}^*))] = \\ &= F_{\nu_1-t_1}(u((X_{t_1}^*)^{\text{tr}})) - F_{\nu_1-t_2}(u((X_{t_2}^*)^{\text{tr}})). \end{aligned}$$

Since $(X_t^*)^{\text{tr}}$ reflects the position of the surfer in the original (not-transposed) tableau we have

$$\eta(t_2) - \eta(t_1) = \Psi_N^{\text{th}}(t_1) - \Psi_N^{\text{th}}(t_2).$$

Since we consider the uniform distribution on the set of tableaux, this ends the proof of the lower bound (4.3) and completes the proof of Theorem 4.1.

8. PROOF OF THEOREM 2.3

8.1. Plan for the proof of Theorem 2.3. We will make the following steps in the proof of Theorem 2.3:

(S1) Pick a candidate for the random variable $\Psi_N : \mathcal{T}_{\square_N} \rightarrow [0, 1]$.

(S2) Prove a *pointwise version of Theorem 2.3*: with the help of Lemma 8.1 and Theorem 4.1 we will show that the chosen candidate gives a good approximation of surfer's position for an arbitrary $t \in (0, 1)$, i.e.,

$$(8.1) \quad \forall_{t \in (0,1)} \lim_{N \rightarrow \infty} \mathbb{P}_N \left(T_N \in \mathcal{T}_{\square_N} : |X_t(T_N) - P_{1-t, \Psi_N(T_N)}| > \varepsilon \right) = 0.$$

The proof will be given in Section 8.5.

(S3) Prove the *full (i.e., the original) version of Theorem 2.3*, i.e.,

$$\lim_{N \rightarrow \infty} \mathbb{P}_N \left(T_N \in \mathcal{T}_{\square_N} : \sup_{t \in [0,1]} |X_t(T_N) - P_{1-t, \Psi_N(T_N)}| > \varepsilon \right) = 0.$$

We will start with a finite ε -net of the family of level curves $\{h_\alpha : \alpha \in [0, 1]\}$ parameterized by $0 = \alpha_0 < \alpha_1 < \dots < \alpha_p < \alpha_{p+1} = 1$. By the previous point, (8.1) holds uniformly for $t \in \{\alpha_0, \dots, \alpha_{p+1}\}$ in a finite set. Then for the intermediate moments of time $\alpha_i < t < \alpha_{i+1}$ we will use the monotonicity of the sliding path and in this way justify that (8.1) holds *uniformly* over $t \in (0, 1)$. This proof will be given in Section 8.6.

In the very end, in Section 8.7, we will show that the probability distribution of the random variable Ψ_N converges to the uniform distribution on the unit interval $[0, 1]$.

8.2. Auxiliary notation. In the proof we will switch between the position of the surfer in the XY and the UV coordinate systems as well as in the geographic coordinates. For any $t \in (0, 1)$ let us introduce the notation for the true and the theoretical u - and v -coordinate; namely we define the following functions $\mathcal{T}_{\square_N} \rightarrow \mathbb{R}$ by

$$\begin{aligned} u_t &:= u(X_t), & \text{and} & & u_t^{\text{th}} &:= \left(F_{\nu_{1-t}}\right)^{-1}(\Psi_N^{\text{th}}(t)), \\ v_t &:= v(X_t) & & & v_t^{\text{th}} &:= h_{1-t}(u_t^{\text{th}}) \end{aligned}$$

(recall that $\Psi_N^{\text{th}}(t) = F_{\nu_{1-t}}(u_t)$, cf. (4.1), and see Section 2.2 for the definition of h_t). Denote additionally for any $t \in [0, 1]$

$$(x_t, y_t) := X_t \quad \text{and} \quad (x_t^{\text{th}}, y_t^{\text{th}}) := \left(\frac{v_t^{\text{th}} - u_t^{\text{th}}}{2}, \frac{u_t^{\text{th}} + v_t^{\text{th}}}{2} \right).$$

8.3. The surfer's position can be asymptotically recovered from the theoretical longitude. We start with the result which shows that, in principle, it is possible to recover the true position of the surfer X_t in the time $t \in (0, 1)$ from its theoretical longitude $\Psi_N^{\text{th}}(t)$.

Lemma 8.1. *Let $0 < t < 1$. For any $\varepsilon > 0$*

$$(8.2) \quad \lim_{N \rightarrow \infty} \mathbb{P}_N \left(T_N \in \mathcal{T}_{\square_N} : u_t(T_N) \neq u_t^{\text{th}}(T_N) \right) = 0$$

and

$$(8.3) \quad \lim_{N \rightarrow \infty} \mathbb{P}_N \left(T_N \in \mathcal{T}_{\square_N} : |v_t(T_N) - v_t^{\text{th}}(T_N)| > \varepsilon \right) = 0.$$

Proof. Let $0 < t < 1$ and $\varepsilon > 0$. We start with the proof of (8.2). Recall that the position of the surfer X_t corresponds to the position of the box with the number $\lceil (1-t)N^2 \rceil$ in the tableau $(\partial^*)^{\lfloor tN^2 \rfloor}(T_N)$, cf. (2.5), and so by [PR07, Theorem 2] the random variable u_t converges in distribution to the measure ν_{1-t} which has no atoms and has a compact connected support

$$\text{supp}(\nu_{1-t}) = \left[-2\sqrt{t(1-t)}, 2\sqrt{t(1-t)} \right].$$

Observe that since ν_{1-t} has no atoms, whenever $u_t \in \text{supp}(\nu_{1-t})$ then by the definition

$$(8.4) \quad u_t^{\text{th}} = F_{\nu_{1-t}}^{-1}(\Psi_N^{\text{th}}(t)) = u_t.$$

On the other hand

$$(8.5) \quad \mathbb{P}_N(T_N \in \mathcal{T}_{\square_N} : u_t(T_N) \notin \text{supp}(\nu_{1-t})) \xrightarrow{N \rightarrow \infty} 0.$$

Indeed, for any $\varepsilon > 0$ consider the function $f_\varepsilon : \mathbb{R} \rightarrow \mathbb{R}$ given by

$$f_\varepsilon(x) := 1 - \min \left\{ 1, \frac{1}{\varepsilon} \text{dist} \left(x, \mathbb{R} \setminus \text{supp}(\nu_{1-t}) \right) \right\}, \quad x \in \mathbb{R},$$

where $\text{dist}(x, A) := \inf\{d(x, y) : y \in A\}$ is the Hausdorff distance of the point x from a set A . Clearly f_ε is continuous and bounded.

The distribution of the random variable u_t is a pushforward of the measure \mathbb{P}_N under the mapping $T_N \mapsto u_t(T_N)$. Therefore by the convergence in distribution of the random variable u_t to the distribution given by the measure ν_{1-t} we get for any $\varepsilon > 0$

$$(8.6) \quad \mathbb{P}_N(T_N \in \mathcal{T}_{\square_N} : u_t(T_N) \notin \text{supp}(\nu_{1-t})) \leq \int_{\mathcal{T}_{\square_N}} f_\varepsilon(u_t) d\mathbb{P}_N \xrightarrow{N \rightarrow \infty} \int_{\mathbb{R}} f_\varepsilon d\nu_{1-t}.$$

Clearly, f_ε converges pointwise as $\varepsilon \rightarrow 0$ to the indicator function $\mathbb{1}_{\overline{\mathbb{R} \setminus \text{supp}(\nu_{1-t})}}$, therefore by the Lebesgue dominated convergence theorem

$$\lim_{\varepsilon \rightarrow 0} \int_{\mathbb{R}} f_\varepsilon d\nu_{1-t} = \nu_{1-t} \left(\overline{\mathbb{R} \setminus \text{supp}(\nu_{1-t})} \right) = \nu_{1-t} \left(\partial(\text{supp}(\nu_{1-t})) \right) = 0.$$

This together with (8.6) implies (8.5).

A conjunction of (8.4) and (8.5) proves (8.2).

Equation (8.3) follows from the result of Biane [Bia98, Theorem 1.5.1]. We will shortly describe it here, but the more developed discussion and precise statements formulated using our notation are placed in Section 10.

The boundary of a Young diagram λ seen in the (u, v) -coordinate system can be viewed as a non-negative 1-Lipschitz function ω_λ , see Figure 14. The function ω_λ is initially defined on the interval I given by the range of the u -coordinates of λ , but it can be extended to a function defined on the real line \mathbb{R} by gluing $\omega_\lambda|_I$ with the modulus function $x \mapsto |x|$. This extended function $\omega_\lambda : \mathbb{R} \rightarrow \mathbb{R}_+$ is called *the profile of λ* , cf. Section 10.1.

The restriction $T|_{\leq \lceil (1-t)N^2 \rceil}$ of the random tableau T has a (random) shape

$$\lambda_{1-t} := \text{sh } T|_{\leq \lceil (1-t)N^2 \rceil}$$

whose (random) profile $\omega_{\lambda_{1-t}}$ is such that the following equality in terms of the u - and v -coordinates of the surfer (in time t) holds true:

$$v_t(T_N) = \omega_{\lambda_{1-t}}(u_t(T_N)).$$

On the other hand if $u_t(T_N) = u_t^{\text{th}}(T_N)$ then

$$v_t^{\text{th}}(T_N) = h_{1-t}(u_t^{\text{th}}(T_N)) = h_{1-t}(u_t(T_N)).$$

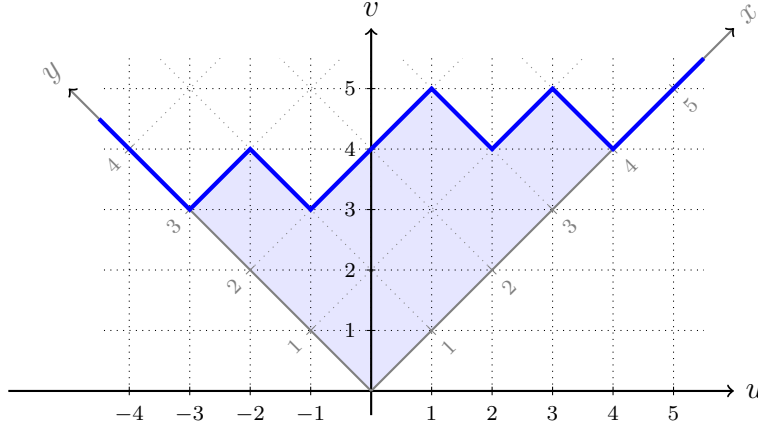


Figure 14. A Young diagram $\lambda = (4, 3, 1)$ shown in the Russian convention. The blue solid line represents its profile ω_λ . The (u, v) -coordinate system corresponding to the Russian convention and the XY - coordinate system corresponding to the French convention are shown.

We proved in (8.2) that the set of tableaux $T_N \in \mathcal{T}_{\square_N}$ for which $u_t(T_N) = u_t^{\text{th}}(T_N)$ has asymptotically full probability. Therefore with asymptotically full probability the following inequality holds

$$(8.7) \quad \left| v_t(T_N) - v_t^{\text{th}}(T_N) \right| \leq \sup_{x \in \mathbb{R}} |\omega_{\lambda_{1-t}}(x) - h_{1-t}(x)|.$$

By the aforementioned result [Bia98, Theorem 1.5.1] (see Proposition 10.1 for the precise general statement) the right-hand-side of (8.7) converges in probability to 0. This completes the proof of (8.3) and Lemma 8.1. \square

8.4. A candidate for the random variable $\Psi_N(T_N)$, development of (S1). Pick any $t_0 \in (0, 1)$ and define for $T_N \in \mathcal{T}_{\square_N}$

$$\Psi_N(T_N) := \Psi_N^{\text{th}}(t_0)(T_N).$$

We will show that the random variable Ψ_N has the desired properties from Theorem 2.3.

For any $t \in [0, 1]$ we define the *approximated u - and v -coordinate* of the surfer as

$$\begin{aligned} u_t^\Psi &:= \left(F_{\nu_{1-t}} \right)^{-1}(\Psi_N), \\ v_t^\Psi &:= h_{1-t}(u_t^\Psi). \end{aligned}$$

These definitions were chosen in such a way that that the *approximated position of the surfer* in the XY coordinate system

$$(x_t^\Psi, y_t^\Psi) := \left(\frac{v_t^\Psi - u_t^\Psi}{2}, \frac{u_t^\Psi + v_t^\Psi}{2} \right) = P_{1-t, \Psi_N(T_N)}$$

is the point which appears in the statement of Theorem 2.3 and Eq. (8.1).

With this notation the expression in the modulus in the event in (8.1) takes the form

$$|X_t(T_N) - P_{1-t, \Psi_N(T_N)}| = \frac{1}{\sqrt{2}} \left| (u_t, v_t) - (u_t^\Psi, v_t^\Psi) \right|.$$

8.5. The proof of (S2) – the pointwise version of Theorem 2.3. Let $\varepsilon > 0$ and $t \in (0, 1)$. By the triangle inequality,

$$(8.8) \quad |u_t(T_N) - u_t^\Psi(T_N)| \leq |u_t(T_N) - u_t^{\text{th}}(T_N)| + |u_t^{\text{th}}(T_N) - u_t^\Psi(T_N)|$$

and

$$(8.9) \quad |v_t(T_N) - v_t^{\text{th}}(T_N)| \leq |v_t(T_N) - v_t^{\text{th}}(T_N)| + |v_t^{\text{th}}(T_N) - v_t^\Psi(T_N)|.$$

By Lemma 8.1, in each of the above two inequalities the first summand on the right-hand side converges in probability to 0, that is,

$$|u_t(T_N) - u_t^{\text{th}}(T_N)| \xrightarrow{P} 0 \quad \text{and} \quad |v_t(T_N) - v_t^{\text{th}}(T_N)| \xrightarrow{P} 0.$$

The second summands on the right hand side of (8.8) and (8.9) are the distances between the values of uniformly continuous functions, respectively, $\psi \mapsto u_t^\psi$ and the composition $\psi \mapsto h_{1-t}(u_t^\psi)$ evaluated at the arguments

$$\Psi_N^{\text{th}}(t) \quad \text{and} \quad \Psi_N^{\text{th}}(t_0) = \Psi_N.$$

By Theorem 4.1 with $t_1 = \min(t, t_0)$ and $t_2 = \max(t, t_0)$ the distance between these two arguments converges in probability to 0, i.e.,

$$\Psi_N^{\text{th}}(t) - \Psi_N \xrightarrow{P} 0.$$

Therefore we get

$$|u_t^{\text{th}}(T_N) - u_t^\Psi(T_N)| \xrightarrow{P} 0 \quad \text{and} \quad |v_t^{\text{th}}(T_N) - v_t^\Psi(T_N)| \xrightarrow{P} 0.$$

As the result

$$|u_t(T_N) - u_t^\Psi(T_N)| \xrightarrow{P} 0 \quad \text{and} \quad |v_t(T_N) - v_t^\Psi(T_N)| \xrightarrow{P} 0$$

which completes the proof (8.1) which is the pointwise version of Theorem 2.3.

8.6. The proof of (S3) – the full version of Theorem 2.3.

8.6.1. *Uniform continuity of the geographic coordinate system.* We start with showing that the geographic coordinate system on the square (recall Section 2.4) is uniformly continuous.

Lemma 8.2. *The function*

$$[0, 1] \times [0, 1] \ni (\alpha, \psi) \mapsto P_{\alpha, \psi} = (x_{\alpha}^{\psi}, y_{\alpha}^{\psi})$$

is uniformly continuous.

Proof. Since the mapping $(x_{\alpha}^{\psi}, y_{\alpha}^{\psi}) \mapsto \frac{1}{\sqrt{2}} (u_{\alpha}^{\psi}, v_{\alpha}^{\psi})$ is an isometry (as a rotation in \mathbb{R}^2) it is enough to show that each coordinate of the function

$$[0, 1] \times [0, 1] \ni (\alpha, \psi) \mapsto (u_{\alpha}^{\psi}, v_{\alpha}^{\psi}) = (u_{\alpha}^{\psi}, h_{1-\alpha}(u_{\alpha}^{\psi}))$$

is uniformly continuous.

Recall that the limit distribution ν_{α} has density (2.4). It is easy to show that for any $\alpha \in (0, 1)$ the cumulative distribution function $F_{\nu_{\alpha}}$ of ν_{α} fulfills the equation

$$F_{\nu_{\alpha}}(u) = F_{\text{SC}}\left(\frac{u}{2\sqrt{\alpha(1-\alpha)}}\right) \quad \text{for all } |u| \leq 2\sqrt{\alpha(1-\alpha)}$$

where F_{SC} denotes the cumulative distribution function of the standard semi-circle distribution with the density (1.3). This implies that for any $\psi \in [0, 1]$ and $\alpha \in (0, 1)$ we get

$$\psi = F_{\nu_{1-\alpha}}(u_{\alpha}^{\psi}) = F_{\text{SC}}\left(\frac{u_{\alpha}^{\psi}}{2\sqrt{\alpha(1-\alpha)}}\right),$$

which after applying F_{SC}^{-1} gives

$$(8.10) \quad u_{\alpha}^{\psi} = 2\sqrt{\alpha(1-\alpha)} \cdot F_{\text{SC}}^{-1}(\psi).$$

Moreover, by the definition $P_{0, \psi} = (0, 0) \in \mathbb{R}^2$ and $P_{1, \psi} = (1, 1) \in \mathbb{R}^2$ (cf. Section 2.4), hence (8.10) holds for all $\psi \in [0, 1]$ and $\alpha \in [0, 1]$.

Therefore the mapping $(\alpha, \psi) \mapsto u_{\alpha}^{\psi}$ is uniformly continuous since $\psi \mapsto F_{\text{SC}}^{-1}(\psi)$ is uniformly continuous. Indeed, F_{SC}^{-1} is the inverse function of F_{SC} which is injective on $[-2\sqrt{\alpha(1-\alpha)}, 2\sqrt{\alpha(1-\alpha)}]$, continuous and has compact domain and range.

The function $(\alpha, u) \mapsto h_{\alpha}(u)$ is uniformly continuous on the domain

$$\diamond := \left\{ (\alpha, u) : \alpha \in [0, 1] \text{ and } |u| \leq 2\sqrt{\alpha(1-\alpha)} \right\}$$

(as a continuous mapping on the compact set \diamond). Hence the function $(\alpha, \psi) \mapsto v_\alpha^\psi$ is uniformly continuous as the composition of two uniformly continuous functions:

$$\diamond \ni (\alpha, u) \mapsto h_\alpha(u) \quad \text{and} \quad (\alpha, \psi) \mapsto (1 - \alpha, u_\alpha^\psi) \in \diamond. \quad \square$$

8.6.2. *The proof of (S3) – the full version of Theorem 2.3.* Let $\varepsilon > 0$. By Lemma 8.2 the function

$$[0, 1] \times [0, 1] \ni (\alpha, \psi) \mapsto P_{\alpha, \psi}$$

is uniformly continuous, so there exists $\delta > 0$ such that

$$(8.11) \quad \forall_{s, t \in [0, 1]} |s - t| < \delta \implies \forall_{\psi \in [0, 1]} |P_{s, \psi} - P_{t, \psi}| < \varepsilon.$$

Let us take a finite δ -net $0 = \alpha_1 < \dots < \alpha_n = 1$ of the interval $[0, 1]$. By the pointwise version (S2) of Theorem 2.3, which we proved in Section 8.5,

$$(8.12) \quad |X_{\alpha_i}(T_N) - P_{1-\alpha_i, \Psi_N(T_N)}| \xrightarrow{P} 0 \quad \text{for } i \in \{1, \dots, n\}$$

(the latter holds for $i = 1$ and $i = n$ by the definition of $P_{\alpha, \psi}$, cf. Section 2.4). Therefore there exists a subset $\mathcal{T}_N^* \subseteq \mathcal{T}_{\square_N}$ of asymptotically full measure which consists of tableaux T_N with the property that for each $i \in \{1, \dots, n\}$

$$(8.13) \quad |x_{\alpha_i}(T_N) - x_{\alpha_i}^\Psi(T_N)| < \varepsilon \quad \text{and} \quad |y_{\alpha_i}(T_N) - y_{\alpha_i}^\Psi(T_N)| < \varepsilon.$$

By the monotonicity of the sliding path for any $i \in \{1, \dots, n-1\}$ and $t \in [\alpha_i, \alpha_{i+1}]$

$$(8.14) \quad x_{\alpha_{i+1}} \leq x_t \leq x_{\alpha_i} \quad \text{and} \quad y_{\alpha_{i+1}} \leq y_t \leq y_{\alpha_i}.$$

By (8.13) and (8.14) for any $T_N \in \mathcal{T}_N^*$ and any $i \in \{1, \dots, n-1\}$ and $t \in [\alpha_i, \alpha_{i+1}]$ the following system of inequalities is satisfied:

$$\begin{cases} -\varepsilon + (x_{\alpha_{i+1}}^\Psi - x_t^\Psi) \leq x_t - x_t^\Psi \leq (x_{\alpha_i}^\Psi - x_t^\Psi) + \varepsilon; \\ -\varepsilon + (y_{\alpha_{i+1}}^\Psi - y_t^\Psi) \leq y_t - y_t^\Psi \leq (y_{\alpha_i}^\Psi - y_t^\Psi) + \varepsilon. \end{cases}$$

Since for any $t \in [0, 1]$

$$X_t = (x_t, y_t) \quad \text{and} \quad P_{1-t, \Psi_N(T_N)} = (x_t^\Psi, y_t^\Psi)$$

and by (8.11) for any $i \in \{1, \dots, n-1\}$ and $t \in [\alpha_i, \alpha_{i+1}]$

$$\max \left\{ |x_{\alpha_i}^\Psi - x_t^\Psi|, |x_{\alpha_{i+1}}^\Psi - x_t^\Psi|, |y_{\alpha_i}^\Psi - y_t^\Psi|, |y_{\alpha_{i+1}}^\Psi - y_t^\Psi| \right\} < \varepsilon$$

we infer that for $T_N \in \mathcal{T}_N^*$

$$\sup_{t \in [0, 1]} |X_t(T_N) - P_{1-t, \Psi_N(T_N)}| < 2\varepsilon.$$

This completes the proof of (S3) since \mathcal{T}_N^* has asymptotically full probability.

8.7. Limit distribution of the random variable Ψ_N . We will show the second component of Theorem 2.3, namely that the random variable Ψ_N converges in distribution to the uniform distribution on the unit interval $[0, 1]$.

Let G_N denote the cumulative distribution function of the random variable $\Psi_N : \mathcal{T}_{\square_N} \rightarrow [0, 1]$. For any $z \in [0, 1]$ we have (recall (4.1))

$$(8.15) \quad G_N(z) = \mathbb{P}_N \left(T_N : F_{\nu_{1-t_0}}(u_{t_0}(T_N)) \leq z \right) = \\ \mathbb{P}_N \left(T_N \in \mathcal{T}_{\square_N} : u_{t_0}(T_N) \leq \left(F_{\nu_{1-t_0}} \right)^{-1}(z) \right).$$

By [PR07, Theorem 2], the distribution of the random variable u_{t_0} converges weakly (as $N \rightarrow \infty$) to the measure ν_{1-t_0} which has no atoms, so the right-hand side of (8.15) converges to

$$F_{\nu_{1-t_0}} \left(F_{\nu_{1-t_0}}^{-1}(z) \right) = z$$

which is the cumulative distribution function of the uniform measure $U(0, 1)$. This completes the proof of the second component of Theorem 2.3, and hence the proof of Theorem 2.3.

9. THE CORRESPONDENCE BETWEEN EVACUATION AND SLIDING PATHS

The results which we consider in this section hold for general, not necessarily square tableaux. For a tableau $T \in \mathcal{T}_\lambda$ with $n = |\lambda|$ boxes we denote by

$$\text{revevac}(T) = \left(\text{pos}_n(j^{n-1}(T)), \dots, \text{pos}_n(j^1(T)), \text{pos}_n(T) \right)$$

the evacuation path (1.8) written in the reverse order.

The following result shows an intimate relationship between the sliding paths and the evacuation paths and, in particular, implies equivalence of Theorems 2.3 and 2.4 (see Section 9.2 for the proof).

Proposition 9.1. *Let λ be a fixed Young diagram and let $T \in \mathcal{T}_\lambda$ be a random standard Young tableau sampled according to the uniform measure on \mathcal{T}_λ . Then the probability distributions of the lazy sliding path $\mathbf{q}(T)$ and the evacuation path $\text{revevac}(T)$ coincide.*

Proof. We will construct a certain bijection $\varepsilon^* : \mathcal{T}_\lambda \rightarrow \mathcal{T}_\lambda$ on the set of tableaux of shape λ . Clearly, the random tableaux T and $\varepsilon^*(T)$ have the same distribution. An application of Proposition 9.3 below completes the proof. \square

In the remaining part of this section we will present the details of the map ε^* and we will prove that Proposition 9.3 indeed holds true.

9.1. Dual evacuation. The dual evacuation has a beautiful algorithmic description in terms of the manipulations of the boxes of T , cf. [PW11, Definition 2.10], however we will not make use of it. For our purposes it is more convenient to define the dual evacuation ε^* implicitly by Robinson–Schensted–Knuth correspondence as follows. For a permutation $\sigma = (\sigma_1, \dots, \sigma_n) \in \mathfrak{S}_n$ we denote

$$\sigma^\# := (n + 1 - \sigma_n, \dots, n + 1 - \sigma_1) \in \mathfrak{S}_n.$$

If σ corresponds to a pair (P, Q) under RSK, then $\sigma^\#$ corresponds to $(\varepsilon^*(P), \varepsilon^*(Q))$ under RSK, see [Sta99, A1.2.10].

We will use the following fact (see [Sag01, Proposition 3.9.3] for the proof).

Fact 9.2 ([Sch63]). *For any $\sigma \in \mathfrak{S}_n$, the following identity holds up to renumbering of the boxes on the left-hand side, so that the resulting tableau becomes standard*

$$(9.1) \quad (j \circ Q)(\sigma) = (Q \circ s)(\sigma) \quad \text{for } \sigma = (\sigma_1, \dots, \sigma_n) \in \mathfrak{S}_n$$

where $s(\sigma) = s(\sigma_1, \sigma_2, \dots, \sigma_n) := (\sigma_2, \dots, \sigma_n)$ is a shift.

Proposition 9.3.

$$\mathbf{q}(T) = \text{revevac}(\varepsilon^*(T)).$$

Proof. For any tableaux R, S we will use a shorthand notation

$$R/S = \text{sh } R / \text{sh } S$$

for the skew diagram obtained by subtracting their shapes. In all examples below this skew diagram $R/S = \{\square\}$ consists of a single box; we will write shortly $\square = R/S$.

Let $T = Q(\sigma)$ be a recording tableau of some permutation σ ; with these notations $\varepsilon^*(T) = Q(\sigma^\#)$.

By (9.1), the lazy sliding path fulfills for $i \in [n]$

$$(9.2) \quad \mathbf{q}_i(T) = Q(\sigma_1, \dots, \sigma_i) / j(Q(\sigma_1, \dots, \sigma_i)) = Q(\sigma_1, \sigma_2, \dots, \sigma_i) / Q(\sigma_2, \dots, \sigma_i).$$

On the other hand, by (9.1), applying jeu de taquin $n - i$ times to $\varepsilon^*(T) = Q(\sigma^\#)$, leads to the tableau (up to renumbering boxes on the left-hand side so that the tableau becomes standard)

$$j^{n-i}(\varepsilon^*(T)) = Q(n + 1 - \sigma_i, \dots, n + 1 - \sigma_2, n + 1 - \sigma_1).$$

The position of the box with the maximal entry in a recording tableau can be found by comparing this tableau to the recording tableau of a truncated sequence; it follows that

$$(9.3) \quad \text{pos}_n j^{n-i}(\varepsilon^*(T)) = Q(n+1-\sigma_i, \dots, n+1-\sigma_2, n+1-\sigma_1) / Q(n+1-\sigma_i, \dots, n+1-\sigma_2).$$

By the result of Schensted [Sch61, Lemma 7] and Greene theorem [Gre74, Theorem 3.1] the shapes of the tableaux which contribute to the right-hand sides of (9.2) and (9.3) are equal which concludes the proof. \square

9.2. Proof of Theorem 2.4.

Proof of Theorem 2.4. Let $N \in \mathbb{N}$. Let $\Psi_N: \mathcal{T}_{\square_N} \rightarrow [0, 1]$ be the random variable which is given by Theorem 2.3. We define the random variable $\tilde{\Psi}_N: \mathcal{T}_{\square_N} \rightarrow [0, 1]$ by

$$\tilde{\Psi}_N(T_N) := \Psi_N(\varepsilon^*(T_N)).$$

Since ε^* is a bijection,

$$\begin{aligned} \mathbb{P}_N \left\{ T_N \in \mathcal{T}_{\square_N} : \sup_{t \in [0,1]} |X_t(T_N) - P_{1-t, \Psi_N(T_N)}| > \varepsilon \right\} &= \\ \mathbb{P}_N \left\{ T_N \in \mathcal{T}_{\square_N} : \sup_{t \in [0,1]} |X_t(\varepsilon^*(T_N)) - P_{1-t, \Psi_N(\varepsilon^*(T_N))}| > \varepsilon \right\} &= \\ \mathbb{P}_N \left\{ T_N \in \mathcal{T}_{\square_N} : \sup_{t \in [0,1]} \left| \frac{1}{N} \mathbf{q}_{\lceil (1-t)N^2 \rceil}(T_N) - P_{1-t, \tilde{\Psi}_N(T_N)} \right| > \varepsilon \right\} &= \\ \mathbb{P}_N \left\{ T_N \in \mathcal{T}_{\square_N} : \sup_{t \in (0,1]} \left| \frac{1}{N} \mathbf{q}_{\lceil tN^2 \rceil}(T_N) - P_{t, \Psi_N(T_N)} \right| > \varepsilon \right\}, \end{aligned}$$

where the second equality is a consequence of Proposition 9.3. By Theorem 2.3 the left-hand side converges to 0 in the limit $N \rightarrow \infty$; on the other hand the right-hand side is the probability which appears in Theorem 2.4. \square

10. GENERALIZATIONS OF THE MAIN RESULTS FOR NON-SQUARE TABLEAUX

10.1. Continuous diagrams. We call a function $\omega: \mathbb{R} \rightarrow \mathbb{R}$ a *continuous diagram* [Ker93a; Ker98] if

- ω is a 1-Lipschitz function, i.e.,

$$|\omega(u_1) - \omega(u_2)| \leq |u_1 - u_2| \quad \text{for all } u_1, u_2 \in \mathbb{R};$$

- $\omega(u) = |u|$ for sufficiently large $|u|$.

We will denote the set of continuous diagrams by \mathcal{CY} ; we endow this set with the L^∞ -metric. (Our definition is more specific than the one of Kerov [Ker93a] who allows to additionally translate our *centered* continuous diagrams along the real line.)

Any (usual) Young diagram λ seen in the (u, v) -coordinate system is a 1-Lipschitz function defined on some interval (given by the range of the u -coordinates of λ) and has slopes equal to ± 1 . It can be extended outside its initial domain by a modulus function $x \mapsto |x|$. In this way we obtain a continuous diagram ω_λ to which we will refer as *the profile of λ* , see Figure 14.

Let $s > 0$. For a continuous diagram ω we define *the scaling of ω by s* as the following continuous diagram denoted by $s\omega$

$$s\omega: \mathbb{R} \ni u \mapsto s \cdot \omega(s^{-1}u).$$

Let (λ_N) be a sequence of Young diagrams with the property that the sequence of the corresponding rescaled profiles

$$\left(\frac{1}{\sqrt{|\lambda_N|}} \omega_{\lambda_N} \right)$$

converges to a continuous diagram Λ in the L^∞ -metric, that is,

$$\sup_{u \in \mathbb{R}} \left| \frac{1}{\sqrt{|\lambda_N|}} \omega_{\lambda_N} \left(\sqrt{|\lambda_N|} u \right) - \Lambda(u) \right| \xrightarrow{N \rightarrow \infty} 0.$$

We will call Λ *the limit shape* for the sequence of Young diagrams (λ_N) and denote such convergence by $\frac{1}{\sqrt{|\lambda_N|}} \lambda_N \rightarrow \Lambda$.

10.2. The asymptotic setup. Let $C \geq 1$ be a fixed constant. For each integer $N \geq 1$ let λ_N be a C -balanced Young diagram. We assume that

$$\lim_{N \rightarrow \infty} |\lambda_N| = \infty$$

and that there exists a limit shape $\Lambda \in \mathcal{CY}$ for the sequence (λ_N) , i.e., that $\frac{1}{\sqrt{|\lambda_N|}} \lambda_N \rightarrow \Lambda$.

Our goal in Section 10 is to find counterparts of Theorems 2.3 and 2.4 in which the sequence (\square_N) of square diagrams is replaced by the sequence (λ_N) of C -balanced Young diagrams.

10.3. The limit curves. The result of Pittel and Romik concerning the existence of the level curves [PR07, Theorem 1(i)], cf. Section 2.2, is a special case of a more general phenomenon. Using the results of Biane [Bia98, Theorem 1.2 and Theorem 1.5.1] one can show that under the assumptions from Section 10.2 there exists a family of level curves for a uniformly random Young tableau of the shape λ_N (in the limit as $N \rightarrow \infty$). The following proposition describes precisely this result.

Proposition 10.1. *Let (λ_N) be a sequence of C -balanced Young diagrams such that $|\lambda_N| \rightarrow \infty$ and $\frac{1}{\sqrt{|\lambda_N|}}\lambda_N \rightarrow \Lambda$ for some continuous diagram $\Lambda \in \mathcal{CY}$ (i.e., (λ_N) fulfills the assumptions in Section 10.2). For any $\alpha \in [0, 1]$ there exists a continuous diagram $\Lambda_\alpha \in \mathcal{CY}$ such that*

$$\frac{1}{\sqrt{|\lambda_N|}} \text{sh}\left(T_N|_{\leq \lfloor \alpha \cdot |\lambda_N| \rfloor}\right) \xrightarrow{P} \Lambda_\alpha$$

where T_N is a uniformly random element of \mathcal{T}_{λ_N} .

We will say that Λ_α is the α -level curve for the sequence (λ_N) or, shortly, the α -level curve for the diagram Λ . Note that Λ_0 is the empty diagram and $\Lambda_1 = \Lambda$.

For example, in the case when $\lambda_N = \square_N$ is a square Young diagram, the α -level curve for (λ_N) is the curve h_α , cf. Section 2.2.

Remark 10.2. Biane proved his results [Bia98, Theorem 1.2 and Theorem 1.5.1] with the tools of the free probability theory [MS17], but Proposition 10.1 can be also showed using the beam models [Sun18] or by solving a gradient variational problem [KP21].

10.4. The limit measures on the level curves. The second result of Pittel and Romik which gives explicitly the limit measure on the α -level curve for the square diagram [PR07, Theorem 2], cf. Section 2.3, is a special case of another general result. It turns out that to every continuous diagram we can associate two natural measures – the *transition measure* and the *cotransition measure* – which have very natural interpretations in the case of the usual Young diagrams.

10.4.1. Transition measure of a continuous diagram. To any continuous diagram $\omega \in \mathcal{CY}$, one can associate a probability measure μ_ω , called the *transition measure of ω* [Ker93b; Bia98], as the unique compactly supported measure on \mathbb{R} such that its Cauchy transform

$$G_{\mu_\omega}(z) := \int_{\mathbb{R}} \frac{1}{z - x} d\mu_\omega(x)$$

is given by the equation

$$G_{\mu_\omega}(z) = \frac{1}{z} \exp \int_{\mathbb{R}} \frac{1}{x - z} \sigma'(x) dx = \frac{1}{z} \exp \int_{\mathbb{R}} \frac{1}{(x - z)^2} \sigma(x) dx$$

where $\sigma(u) := (\omega(u) - |u|)/2$.

The motivations for this notion are related to random walks on the set of Young diagrams: the atoms of the transition measure μ_{ω_λ} of a usual Young diagram λ correspond to the Markov's transition probabilities in the Plancherel growth process starting in λ [Ker93b, Section 3.2].

The mapping which to a continuous diagram ω assigns the transition measure μ_ω is a *homeomorphism* [Ker93b, Section 2.3]. Moreover, a continuous diagram is uniquely determined by its transition measure.

10.4.2. *Cotransition measure of a continuous diagram.* For a continuous diagram $\omega \in \mathcal{CY}$ we define its *area* as the area of the region between the profile and the x - and the y -axis:

$$A(\omega) = \int_{\mathbb{R}} (\omega(x) - |x|) dx.$$

The *cotransition measure* ν_ω of ω is defined as the unique probability measure with the Cauchy transform G_{ν_ω} given by the following equation [Rom04, Equation (8)]:

$$(10.1) \quad \frac{A(\omega)}{2} G_{\nu_\omega}(x) = x - \frac{1}{G_{\mu_\omega}(x)}.$$

By convention, the cotransition measure of the empty diagram $\nu_{\omega_\emptyset} = \delta_0$ is defined to be the measure concentrated in 0.

The cotransition measure ν_{ω_λ} of a usual Young diagram λ is the distribution of the u -coordinate of the box with the maximal entry $|\lambda|$ in a uniformly random standard tableau of shape λ , cf. [Rom04, page 628 and the comment below Eq. (6)]. In particular, the measure ν_α introduced in Section 2.3 to which we referred as *the limit measure* is the cotransition measure corresponding to the continuous diagram h_α (more precisely, to the proper extension of the function h_α given by (2.2) by $x \mapsto |x|$ and $x \mapsto 2 - |x|$).

Be advised that diagrams of different shape may have the same cotransition measure. For example, the square Young diagram \square_N has the same cotransition measure $\nu_{\omega_{\square_N}} = \delta_0$ concentrated at the point $u = 0$, no matter which size of the square $N \in \mathbb{N}$ we choose. However, if we restrict our considerations to the set of (centered) continuous diagrams of fixed positive area, then any diagram is uniquely determined by its cotransition measure and this correspondence is a homeomorphism, [Rom04, Theorem 6].

10.4.3. *The limit measures on the level curves of continuous diagram.* We will refer to the cotransition measure ν_{Λ_α} corresponding to the α -level curve Λ_α for a continuous diagram Λ as *the limit (or cotransition) measure* on the level curve Λ_α .

The cumulative distribution function of the limit measure ν_{Λ_α} will be denoted by F_{Λ_α} , i.e.,

$$F_{\Lambda_\alpha}(u) := \nu_{\Lambda_\alpha}((-\infty, u]) \text{ for each } u \in \mathbb{R}.$$

The density of the limit measure ν_{Λ_α} will be denoted by f_{Λ_α} , whenever this density exists.

10.5. The geographic coordinate system. We will endow a continuous diagram Λ with the system of geographic coordinates, cf. Section 2.4. For this purpose we view the shape Λ as the following compact subset of the (x, y) -Cartesian plane

$$\Lambda^{\text{Cart}} := \overline{\{(x, y) \in \mathbb{R}^2 : |x - y| < x + y < \Lambda(x - y)\}} = \overline{\{(x, y) \in [0, \infty)^2 : x + y < \Lambda(x - y)\}}.$$

(Recall that $u = x - y$ and $v = x + y$ are the (u, v) coordinates, cf. Section 2.2.)

For any $\alpha \in [0, 1]$ we define *the quantile function* for the limit measure ν_{Λ_α} by the formula

$$(10.2) \quad Q_{\Lambda_\alpha}(\psi) := \inf\{u \in \text{supp}(\nu_{\Lambda_\alpha}) : F_{\Lambda_\alpha}(u) \geq \psi\} \quad \text{for } \psi \in [0, 1]$$

where $\text{supp}(\mu)$ denotes *the support* of the measure μ . In particular, $Q_{\Lambda_0} \equiv 0$.

For given $\alpha \in [0, 1]$ and $\psi \in [0, 1]$ there is exactly one point $p = (x, y) \in \Lambda^{\text{Cart}}$ such that

- p lies on the level curve Λ_α seen in the XY -coordinates system, i.e.,

$$x + y = \Lambda_\alpha(x - y);$$

- the u -coordinate of p is given by the quantile function:

$$u(p) = x - y = Q_{\Lambda_\alpha}(\psi).$$

We will denote this point by $P_{\alpha, \psi} := (x_\alpha^\psi, y_\alpha^\psi) \in \Lambda^{\text{Cart}}$. In particular, by the definition of $\nu_{\Lambda_0} = \delta_0$ we have $P_{0, \psi} = (0, 0) \in \mathbb{R}^2$ for any $\psi \in [0, 1]$. Additionally we denote by

$$u_\alpha^\psi := x_\alpha^\psi - y_\alpha^\psi \quad \text{and} \quad v_\alpha^\psi := x_\alpha^\psi + y_\alpha^\psi$$

the u - and v -coordinate of the point $P_{\alpha, \psi}$.

We will refer to the mapping $[0, 1]^2 \ni (\alpha, \psi) \mapsto P_{\alpha, \psi} \in \Lambda^{\text{Cart}}$ as to *the geographic coordinates system*.

Remark 10.3. There may be some problem with defining the counterparts of the longitude and the latitude (the geographic coordinates) of the point $p \in \Lambda^{\text{Cart}}$ like we did in Section 2.4. We defined *the latitude* as *the unique* $\alpha \in [0, 1]$ for which p lies on the level curve h_α (more precisely, on the restriction of the level curve h_α to the support of the corresponding cotransition measure ν_α). We are not sure if such uniqueness holds in a general case when Λ is an arbitrary continuous diagram. To make things worse, the definition of *the longitude* depends on the limit measure $\nu_{\Lambda_{\alpha(p)}}$ corresponding to the $\alpha(p)$ -level curve (circle of latitude with the latitude $\alpha(p)$, cf. Sections 2.2 and 2.4). In the worst scenario, not only we shall pick some

latitude $\alpha(p)$, but also the limit measure $\nu_{\Lambda_\alpha(p)}$ may have atoms. In particular, an attempt of using these direct counterparts of the definitions from Section 2.4 in the more general context may lead to the situation in which several points have the same geographic coordinates or some geographic coordinates (α, ψ) are not used. The case of the L -shape diagram, see Figure 10, is an example of the first problem.

Problem 10.4. *Let Λ be a continuous diagram. Show that for any point*

$$p \in \Lambda^{\text{UV}} := \overline{\{(u, v) : u \in \mathbb{R} \text{ and } |u| < v < \Lambda(u)\}}$$

there is a unique $\alpha \in [0, 1]$ with the property that

$$p \in \{(u, \Lambda_\alpha(u)) : u \in \text{supp}(\nu_{\Lambda_\alpha})\}.$$

In other words, show that for any point $p \in \Lambda^{\text{UV}}$ there exists a unique level curve Λ_α (for some $\alpha \in [0, 1]$) which restricted to the support of the corresponding cotransition measure ν_{Λ_α} contains p .

10.6. Extension of the main results.

Theorem 10.5. *Let (λ_N) fulfill the assumptions in Section 10.2) and assume that*

- (\star) *the geographic coordinates system is continuous, i.e., the map $[0, 1]^2 \ni (\alpha, \psi) \mapsto P_{\alpha, \psi}$, is continuous.*

Then the analogues of Theorems 2.3 and 2.4 hold true, i.e., if T_N is a uniformly random element of \mathcal{T}_{λ_N} then:

- *there exists a family of random variables $\Psi_N : \mathcal{T}_{\lambda_N} \rightarrow [0, 1]$ indexed by $N \in \mathbb{N}$ such that*

$$(10.3) \quad \sup_{t \in [0, 1]} |X_t(T_N) - P_{1-t, \Psi_N(T_N)}| \xrightarrow{P} 0,$$

- *there exists a family of random variables $\tilde{\Psi}_N : \mathcal{T}_{\lambda_N} \rightarrow [0, 1]$ indexed by $N \in \mathbb{N}$ such that*

$$\sup_{t \in [0, 1]} \left| \frac{1}{N} \mathbf{q}_{\lceil t \lambda_N \rceil}(T_N) - P_{t, \tilde{\Psi}_N(T_N)} \right| \xrightarrow{P} 0.$$

The probability distribution of the random variable Ψ_N (respectively, $\tilde{\Psi}_N$) converges, as $N \rightarrow \infty$, to the uniform distribution on the unit interval $[0, 1]$.

Proof. The proof of Theorem 2.3 is applicable in this more general case – one shall replace all occurrences of the \square_N by λ_N and change the references to the limit measures. We enumerate the properties of square Young diagrams which played the crucial role in the proof of Theorem 2.3.

- \square_N is a 1-balanced Young diagram (we used this property in Proposition 5.1 and Theorem 6.2);
- the cotransition measure ν_α corresponding to the level curve h_α has no atoms and has a connected support (we used this property in Theorem 4.1 and Proposition 5.1);
- the distribution of u_α – the u -coordinate of the surfer in time α – converges to the cotransition measure $\nu_{1-\alpha}$ (we used this property in Lemma 8.1);
- the uniform continuity of the geographic coordinates system, i.e., the uniform continuity of the mapping $(\alpha, \psi) \mapsto P_{\alpha, \psi}$, cf. Lemma 8.2.

Notice that the counterparts of all these properties are present in our new setting. In particular, the distribution of the u -coordinate of the surfer converges to the proper limit measure since the correspondence between the (centered) continuous diagrams of fixed positive area and the cotransition measures is a homeomorphism, cf. Section 10.4.2. Moreover, the assumption (\star) on the continuity of the geographic coordinates system assures that for any $\alpha \in [0, 1]$ the support of the limit measure ν_{Λ_α} is connected. \square

10.7. Example: random rectangular tableaux. For any real numbers $a, b > 0$ let $\square_{a \times b}$ denote the rectangle with the left bottom corner positioned in $(0, 0) \in \mathbb{R}^2$ and with sides a and b (on X and Y axis, respectively, when seen in the (x, y) -coordinates system).

Let (M_i) and (N_i) be two sequences of positive integers which fulfill the conditions from Section 1.1.3, i.e., $M_i \rightarrow \infty$ and $N_i \rightarrow \infty$, and there is some (shape parameter) $\theta > 0$ such that

$$\lim_{i \rightarrow \infty} \frac{M_i}{N_i} = \theta.$$

We define for $i \in \mathbb{N}$

$$\lambda_i := \square_{M_i \times N_i}$$

to be the rectangular Young diagram which has M_i rows and N_i columns.

The following theorem generalizes Theorem 2.4 (which is a special case for $M_i = N_i = i$).

Corollary 10.6. *For $i \in \mathbb{N}$ let T_i be a uniformly random tableau of the shape $\square_{M_i \times N_i}$. Then the rescaled lazy sliding path $\frac{1}{\sqrt{M_i N_i}} \mathbf{q}(T_i)$ with respect to the supremum norm converges in probability to the random function*

$$(10.4) \quad t \mapsto \Xi_S(t) = 2\sqrt{t(1-t)} S + \frac{\theta - 1}{\sqrt{\theta}} t$$

where S denotes the random variable with the standard semicircular distribution, cf. (1.3).

Proof. We will check that the assumptions of Theorem 10.5 are fulfilled and find the explicit formula for the geographic coordinates system.

Clearly, the sequence $\left(\frac{1}{\sqrt{M_i N_i}} \square_{M_i \times N_i}\right)$ converge to the limit shape $\Lambda = \square_{\sqrt{\theta} \times 1/\sqrt{\theta}}$. We apply Lemma 10.7 below with $a := 1/\sqrt{\theta}$ and $b := \sqrt{\theta}$ to see that

- the geographic coordinates system on $\square_{\sqrt{\theta} \times 1/\sqrt{\theta}}$ is continuous,
- for any $\psi \in [0, 1]$ and $\alpha \in [0, 1]$ the ψ -th quantile u_ψ of the cotransition measure ν_{Λ_α} is given by

$$u_\psi = 2\sqrt{\alpha(1-\alpha)}F_{\text{SC}}^{-1}(\psi) + \frac{\theta-1}{\sqrt{\theta}}\alpha$$

where F_{SC} denotes the cumulative distribution function of the standard semicircle distribution, cf. (1.3).

Notice that if U is a random variable with the uniform $U(0, 1)$ distribution then $F_{\text{SC}}^{-1}(U)$ has the standard semicircle distribution.

By Theorem 10.5 (its second and third part) the (rescaled) lazy sliding path $\frac{1}{\sqrt{M_i N_i}} \mathbf{q}(T_i)$ with respect to the supremum norm converges in probability to the random function (10.4). \square

Lemma 10.7. *Let $a, b > 0$ and $\Lambda := \omega_{\square_{a \times b}}$ be the profile of $\square_{a \times b}$. Then for any $\alpha \in (0, 1)$ the cotransition measure ν_{Λ_α} corresponding to the α -level curve Λ_α has the density*

$$(10.5) \quad f_{\nu_{\Lambda_\alpha}}(x) = \frac{1}{2\sqrt{ab \cdot \alpha(1-\alpha)}} f_{\text{SC}}\left(\frac{x + \alpha(a-b)}{2\sqrt{ab \cdot \alpha(1-\alpha)}}\right)$$

where f_{SC} is the density of the standard semicircular distribution, cf. (1.3).

Proof. The following calculations use (10.1) and some relations between the R -transform and the Cauchy transform of the appropriate transition measures, see [MS17, Section 3] for the theory.

The Cauchy transform of the transition measure μ_Λ of the rectangular diagram is given by [Rom04, Equation (2)]

$$(10.6) \quad G(z) := G_{\mu_\Lambda}(z) = \frac{z - (b-a)}{(z+a)(z-b)}.$$

It is an analytic function and in some neighborhood of ∞ it is invertible [MS17, Section 3, Theorem 17(i)]. Moreover, there exists a neighborhood $U \subset \mathbb{C}$ of 0 for which $G|_{G^{-1}(U)}$ is invertible [MS17, Section 3, Theorem 17(ii)] and we can calculate the R -transform of the measure μ_Λ with the formula [MS17, Section 3, Theorem 17(iii)]

$$R(z) := R_{\mu_\Lambda}(z) = G^{-1}(z) - \frac{1}{z} \quad \text{for } z \in U \setminus \{0\}.$$

Substituting in the latter z with $G(z')$ (for some $z' \in G^{-1}(U \setminus \{0\})$) we get the relation

$$(10.7) \quad z = R(G(z)) + \frac{1}{G(z)} \quad \text{for } z \in G^{-1}(U \setminus \{0\}).$$

We use this equality in order to substitute each occurrence of the variable z on the right-hand side of (10.6); by clearing of the denominator we obtain

$$(10.8) \quad R(G) + \frac{1}{G} - (b - a) = G \cdot \left(R(G) + \frac{1}{G} + a \right) \left(R(G) + \frac{1}{G} - b \right),$$

where we used the shorthand notation $G = G(z)$. By the choice of U as the neighborhood of 0 we get that (10.8) is fulfilled with G replaced by any complex number $z \in U \setminus \{0\}$, i.e., the R -transform fulfills the following quadratic equation for any $z \in U \setminus \{0\}$

$$(10.9) \quad R(z) + \frac{1}{z} - (b - a) = z \cdot \left(R(z) + \frac{1}{z} + a \right) \left(R(z) + \frac{1}{z} - b \right).$$

Now, we will calculate the Cauchy transform of the transition measure μ_{Λ_α} on the level curve Λ_α . Denote by R_α and G_α , respectively, the R -transform and the G -transform of μ_{Λ_α} . The R -transforms of the transition measures μ_Λ and μ_{Λ_α} are related by the following correspondence [Bia98, Theorem 1.2]

$$R_\alpha(z) := R_{\mu_{\Lambda_\alpha}}(z) = R(\alpha \cdot z) \quad \text{for } z \in U \setminus \{0\}.$$

Let us put $\alpha \cdot z$ instead of z in (10.9) (this substitution is legal since the neighborhood U can be taken to be a convex set). Equation (10.9) implies therefore that $R_\alpha(z)$ is a solution to the following quadratic equation

$$(10.10) \quad R_\alpha(z) + \frac{1}{\alpha z} - (b - a) = \alpha z \left(R_\alpha(z) + \frac{1}{\alpha z} + a \right) \left(R_\alpha(z) + \frac{1}{\alpha z} - b \right)$$

for any $z \in U \setminus \{0\}$.

In (10.10) we substitute each occurrence of the variable z by $G_\alpha(z)$; this substitution is valid as long as $|z|$ is big enough so that $G_\alpha(z) \in U \setminus \{0\}$. Let us denote additionally $H_\alpha = \frac{1}{G_\alpha}$; then we use the relation (10.7) and substitute each occurrence of $R_\alpha(G_\alpha(z))$ by $z - H_\alpha(z)$. Then (10.10) takes

the form

$$(10.11) \quad H_\alpha(z) \left(z - (b - a) + \left(\frac{1}{\alpha} - 1 \right) H_\alpha(z) \right) = \\ \alpha \left(z + a + \left(\frac{1}{\alpha} - 1 \right) H_\alpha(z) \right) \left(z - b + \left(\frac{1}{\alpha} - 1 \right) H_\alpha(z) \right)$$

which holds if $|z|$ is big enough. For any z big enough, the latter is a quadratic equation in $H_\alpha(z)$ which has two solutions given by explicit (but complicated, so we omit writing them here) formulas. These solutions come from two branches of the complex square root. The function H_α must be analytic in some neighborhood of ∞ and therefore can be given by only one (family) of these solutions. Moreover, H_α must have a proper asymptotics, more precisely [MS17, Section 3.1, Lemma 3]

$$\lim_{y \rightarrow \infty} \frac{H_\alpha(iy)}{y} = i,$$

which allows us to choose the proper solution.

The formula for H_α gives also an explicit formula for the Cauchy transform of the cotransition measure ν_{Λ_α} on the level curve Λ_α as (cf. (10.1))

$$G_{\nu_{\Lambda_\alpha}}(z) = \frac{1}{\alpha ab} (z - H_\alpha(z)).$$

The function $G_{\nu_{\Lambda_\alpha}}$ is analytic (since H_α is analytic); we will use its analytic continuation to the upper halfplane \mathbb{C}^+ .

With this (complicated) formula for $G_{\nu_{\Lambda_\alpha}}$ we can now recover the density of the cotransition measure ν_{Λ_α} using the Stieltjes inversion formula [MS17, Section 3, Theorem 6]. One can easily show that this density is the properly rescaled and translated standard semicircle distribution, cf. (1.3). \square

10.8. What if the geographic coordinates system is not uniformly continuous? The situation when the geographic coordinates system $(\alpha, \psi) \mapsto P_{\alpha, \psi} \in \Lambda^{\text{Cart}}$ (recall Section 10.5) is not uniformly continuous is not rare. One among many examples is the limit shape Λ which is the L -shape, cf. Figure 10. In this case there are some α -level curves (for α big enough) for which the corresponding cotransition measure is supported on two disjoint intervals. This forces the function $\psi \mapsto P_{\alpha, \psi}$ to have a discontinuity related to the hole between the intervals. Therefore in such situation Theorem 10.5 does not apply since the assumption (\star) is not fulfilled.

Problem 10.8. Find a counterpart of the assumption (\star) for which the conclusion of Theorem 10.5 holds true.

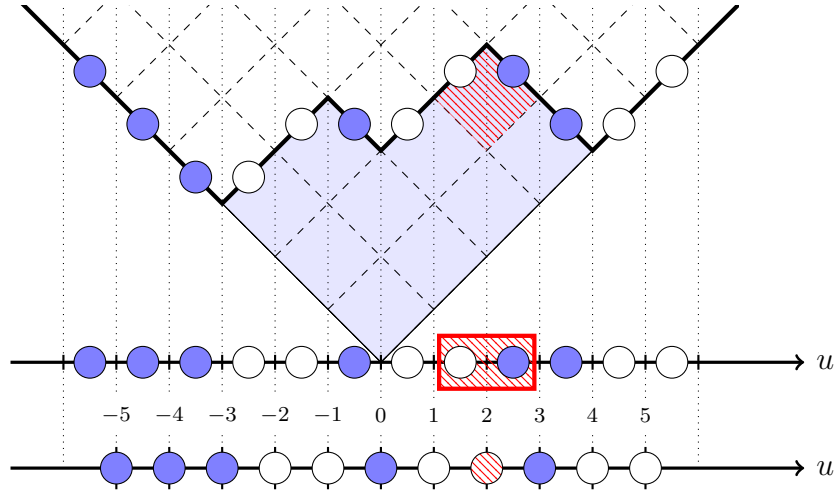


Figure 15. Above: the Young diagram $(4, 4, 2)$ and its marked inner corner in the second row. In the middle: the corresponding configuration of particles on the shifted lattice \mathbb{Z}' via Rost's mapping. The marked inner corner corresponds to the pair of nodes in the rectangle. Below: the corresponding configuration of particles (including the second class particle) on the lattice \mathbb{Z} .

11. THE CORRESPONDENCE BETWEEN YOUNG TABLEAUX AND PARTICLE SYSTEMS. PROOF OF THEOREM 1.1

We will first describe a bijection which links a recording tableau with a unique history of a particular Totally Asymmetric Simple Exclusion Process, recall Section 1.1. We will base on the articles of Rost [Ros81], as well as Romik and the second named author [RŚ15, Section 7]. Then, in Section 11.3 we will prove Theorem 1.1.

11.1. The correspondence between a Young diagram with a distinguished corner and a configuration of particles – Rost's mapping. Let λ be a non-empty Young diagram and \square be one of its inner corners, i.e., \square is a cell of λ such that the shape $\lambda \setminus \square$ is still a Young diagram, see Figure 15. Following [RŚ15, Section 7.1], we will present the two-step algorithm in which to the pair (λ, \square) we assign a configuration of holes and particles with exactly one second class particle. To our best knowledge the foundations for this mapping were first laid in [Ros81, Remark 1], and therefore we will call it *Rost's mapping*.

In the first step of the Rost's mapping, given a Young diagram λ we draw its profile ω_λ in the Russian coordinates system (see Figure 14 and

Section 10.1 for the definition of the profile). To the profile ω_λ there corresponds a unique configuration of holes and (first class) particles on $\mathbb{Z}' := \mathbb{Z} + \frac{1}{2}$ which appears in the following way. For each $m \in \mathbb{Z}$ exactly one of the following two cases holds true:

- in the case when the slope of the profile ω_λ on the interval $[m, m+1]$ is equal to -1 then we put a (first class) particle at the site $m + \frac{1}{2}$ of the lattice $\mathbb{Z}' := \mathbb{Z} + \frac{1}{2}$;
- in the case when the slope of the profile ω_λ on the interval $[m, m+1]$ is equal to $+1$ then we put a hole at the site $m + \frac{1}{2}$ (in other words, the site $m + \frac{1}{2}$ is vacant).

The distinguished inner corner \square corresponds in the above particle system to a *hole-particle pair*. We outline this hole-particle pair with a red rectangle, see the top and the middle part of Figure 15.

In the second step of Rost's mapping we define a particle configuration on \mathbb{Z} . We start with merging the hole-particle pair outlined in the red rectangle into the single particle which we will call *the second class particle*. We put it in the middle of the initial interval containing the hole-particle pair. Then we translate all holes and particles which are placed to the left of the second class particle by $+\frac{1}{2}$ and we translate all holes and particles which are placed to the right of the second class particle by $-\frac{1}{2}$. These steps are illustrated in the middle and bottom part of Figure 15. In this way we end up with the configuration of particles on \mathbb{Z} with a single second class particle.

11.2. The correspondence between the standard tableaux and the histories of TASEP. Recall that for a standard tableau T and a positive integer $p \leq |T|$ we define the restricted tableau $T|_{\leq p}$ to be the tableau which consists of only these boxes of T which have entries $\leq p$.

For a standard tableau T with $n \geq 1$ boxes and any $p \in \{1, \dots, n\}$ let us define

$$\begin{aligned}\lambda^{(p)} &:= \lambda^{(p)}(T) := \text{sh}(T|_{\leq p}), \\ \square^{(p)} &:= \square^{(p)}(T) := \mathbf{q}_p(T),\end{aligned}$$

that is, $(\lambda^{(p)}, \square^{(p)})$ is the pair which consists of the Young diagram $\lambda^{(p)}(T)$ which is the shape of the restricted tableau $T|_{\leq p}$ and the last box along the sliding path in T which contains a number $\leq p$, cf. Section 2.6.

Let T be a standard tableau with $n \geq 1$ boxes. For any $t \in \{1, \dots, n\}$ let us consider the system of particles $P_t := P_t(T)$ which corresponds to the pair $(\lambda^{(t)}, \square^{(t)})$ via Rost's mapping defined in Section 11.1. Notice that the initial configuration P_1 is such that the second class particle is located at the site $u = 0$, all negative nodes are occupied by the first class particles and

all positive nodes are occupied by holes. Such configuration is called *the Dirac sea*. Observe that for any $t \in \{1, \dots, n-1\}$ the neighboring states P_t and P_{t+1} differ by one of the three transitions described in Section 1.1.1 (cf. Figure 2, see [RŚ15, Sections 7.2 and 7.3] for a step-by-step proof). Therefore the family $(P_t)_{t \in \{1, \dots, n\}}$ is a history of the particle system starting from the Dirac sea.

Given the above observation, it is easy to see that the mapping which to the standard tableau T with n boxes associates the history $(P_t(T))_{t \in \{1, \dots, n\}}$ of the particle system is a *bijection* between the set of standard tableaux with n boxes and the possible n -step histories of particle systems starting from the Dirac sea. Moreover, for a tableau T and any $t \in \{1, \dots, |T|\}$ the u -coordinate of the box $\mathbf{q}_t(T)$ in the lazy sliding path is the position of the second class particle in time t in the corresponding TASEP, see [RŚ15, Proposition 7.1].

11.3. Proof of Theorem 1.1.

Proof of Theorem 1.1. Let us denote by $\mathcal{T}_{M \times N}$ the set of standard tableaux of $M \times N$ rectangular shape (where M is a number of rows and N is a number of columns).

In the following we discard the particles and holes which do not occupy the nodes (1.1). In this way the correspondence defined in Section 11.2 gives a bijection between $\mathcal{T}_{M_i \times N_i}$ and the set of histories of the particle system considered in Section 1.1.1. In this correspondence for any $t \in \{1, \dots, M_i N_i\}$ the position of the second class particle in time t in the TASEP corresponds to the u -coordinate of the box $\mathbf{q}_t(T)$ in the lazy sliding path. In the special case $M_i = N_i = i$ when $M_i \times N_i = \square_i$ an application of Theorem 2.4 completes the proof. In the general case we apply Corollary 10.6 instead. \square

ACKNOWLEDGMENTS

Research is supported by *Narodowe Centrum Nauki*, grant number 2017/26/A/ST1/00189. We thank Dan Romik and Serban Belinschi for valuable discussions.

REFERENCES

- [AHRV07] O. Angel, A. E. Holroyd, D. Romik, and B. Virág. “Random sorting networks”. In: *Adv. Math.* 215.2 (2007), pp. 839–868. DOI: 10.1016/j.aim.2007.05.019.
- [BF87] A. Benassi and J.-P. Fouque. “Hydrodynamical limit for the asymmetric simple exclusion process”. In: *Ann. Probab.* 15.2 (1987), pp. 546–560. DOI: 10.1214/aop/1176992158.

- [Bia01] P. Biane. “Approximate factorization and concentration for characters of symmetric groups”. In: *Internat. Math. Res. Notices* 4 (2001), pp. 179–192. DOI: 10.1155/S1073792801000113.
- [Bia98] P. Biane. “Representations of symmetric groups and free probability”. In: *Adv. Math.* 138.1 (1998), pp. 126–181. DOI: 10.1006/aima.1998.1745
- [Bur48] J. M. Burgers. “A mathematical model illustrating the theory of turbulence”. In: *Advances in Applied Mechanics*. edited by Richard von Mises and Theodore von Kármán, Academic Press, Inc., New York, 1948, pp. 171–199.
- [CSST10] T. Ceccherini-Silberstein, F. Scarabotti, and F. Tolli. *Representation theory of the symmetric groups*. Vol. 121. Cambridge Studies in Advanced Mathematics. The Okounkov-Vershik approach, character formulas, and partition algebras. Cambridge: Cambridge University Press, 2010, pp. xvi+412.
- [Dur10] R. Durrett. *Probability: theory and examples*. Fourth. Cambridge Series in Statistical and Probabilistic Mathematics. Cambridge: Cambridge University Press, 2010, pp. x+428.
- [DV20] D. Dauvergne and B. Virág. “Circular support in random sorting networks”. In: *Trans. Amer. Math. Soc.* 373.3 (2020), pp. 1529–1553. DOI: 10.1090/tran/7819.
- [Fer92] P. A. Ferrari. “Shock fluctuations in asymmetric simple exclusion”. In: *Probab. Theory Related Fields* 91.1 (1992), pp. 81–101. DOI: 10.1007/BF01194491.
- [FF94] P. A. Ferrari and L. R. G. Fontes. “Current fluctuations for the asymmetric simple exclusion process”. In: *Ann. Probab.* 22.2 (1994), pp. 820–832. DOI: 10.1214/aop/1176988731.
- [FK95] P. A. Ferrari and C. Kipnis. “Second class particles in the rarefaction fan”. In: *Ann. Inst. H. Poincaré Probab. Statist.* 31.1 (1995), pp. 143–154. URL: http://www.numdam.org/item?id=AIHPB_1995_
- [FŚ11] V. Féray and P. Śniady. “Asymptotics of characters of symmetric groups related to Stanley character formula”. In: *Ann. of Math.* (2) 173.2 (2011), pp. 887–906. DOI: 10.4007/annals.2011.173.2.6.
- [Ful97] W. Fulton. *Young tableaux*. Vol. 35. London Mathematical Society Student Texts. With applications to representation theory and geometry. Cambridge University Press, Cambridge, 1997, pp. x+260.
- [Gre74] C. Greene. “An extension of Schensted’s theorem”. In: *Advances in Math.* 14 (1974), pp. 254–265. DOI: 10.1016/0001-8708(74)90031-0.
- [Juc74] A.-A. A. Jucys. “Symmetric polynomials and the center of the symmetric group ring”. In: *Rep. Mathematical Phys.* 5.1 (1974), pp. 107–112.

- [Ker93a] S. Kerov. “The asymptotics of interlacing sequences and the growth of continual Young diagrams”. In: vol. 205. Nauka, St. Petersburg, 1993, pp. 21–29, DOI: 10.1007/BF02362775.
- [Ker93b] S. V. Kerov. “Transition probabilities of continual Young diagrams and the Markov moment problem”. In: *Funktsional. Anal. i Prilozhen.* 27.2 (1993), pp. 32–49, 96. DOI: 10.1007/BF01085981.
- [Ker98] S. Kerov. “Interlacing measures”. In: *Kirillov’s seminar on representation theory*. Vol. 181. Amer. Math. Soc. Transl. Ser. 2. Amer. Math. Soc., Providence, RI, 1998, pp. 35–83. DOI: 10.1090/trans2/181/02.
- [KP21] R. Kenyon and I. Prause. *Gradient variational problems in \mathbb{R}^2* . 2021. arXiv: 2006.01219 [math.AP].
- [Lig99] T. M. Liggett. *Stochastic interacting systems: contact, voter and exclusion processes*. Vol. 324. Grundlehren der Mathematischen Wissenschaften [Fundamental Principles of Mathematical Sciences]. Springer-Verlag, Berlin, 1999, pp. xii+332. DOI: 10.1007/978-3-662-03990-8.
- [MG05] T. Mountford and H. Guiol. “The motion of a second class particle for the TASEP starting from a decreasing shock profile”. In: *Ann. Appl. Probab.* 15.2 (2005), pp. 1227–1259. DOI: 10.1214/105051605000000151.
- [MS17] J. A. Mingo and R. Speicher. *Free probability and random matrices*. Vol. 35. Fields Institute Monographs. Springer, New York; Fields Institute for Research in Mathematical Sciences, Toronto, ON, 2017, pp. xiv+336. DOI: 10.1007/978-1-4939-6942-5.
- [MS20] Ł. Maślanka and P. Śniady. “Limit shapes of evacuation and jeu de taquin paths in random square tableaux”. In: *Sém. Lothar. Combin.* 84B (2020), Art. 8, 12. URL: <https://www.mat.univie.ac.at/~slc/>
- [PR07] B. Pittel and D. Romik. “Limit shapes for random square Young tableaux”. In: *Adv. in Appl. Math.* 38.2 (2007), pp. 164–209. DOI: 10.1016/j.aam.2005.12.005.
- [PW11] S. Pon and Q. Wang. “Promotion and evacuation on standard Young tableaux of rectangle and staircase shape”. In: *Electron. J. Combin.* 18.1 (2011), Paper 18, 18.
- [Rez95] F. Rezakhanlou. “Microscopic structure of shocks in one conservation laws”. In: *Ann. Inst. H. Poincaré Anal. Non Linéaire* 12.2 (1995), pp. 119–153. DOI: 10.1016/S0294-1449(16)30161-5.
- [Rom04] D. Romik. “Explicit formulas for hook walks on continual Young diagrams”. In: *Adv. in Appl. Math.* 32.4 (2004), pp. 625–654. DOI: 10.1016/S0196-8858(03)00096-4.

- [Rom06] D. Romik. “Permutations with short monotone subsequences”. In: *Adv. in Appl. Math.* 37.4 (2006), pp. 501–510. DOI: 10.1016/j.aam.2005.08.000.
- [Rom12] D. Romik. “Arctic circles, domino tilings and square Young tableaux”. In: *Ann. Probab.* 40.2 (2012), pp. 611–647. DOI: 10.1214/10-AOP628.
- [Ros81] H. Rost. “Nonequilibrium behaviour of a many particle process: density profile and local equilibria”. In: *Z. Wahrsch. Verw. Gebiete* 58.1 (1981), pp. 41–53. DOI: 10.1007/BF00536194.
- [RŚ15] D. Romik and P. Śniady. “Jeu de taquin dynamics on infinite Young tableaux and second class particles”. In: *Ann. Probab.* 43.2 (2015), pp. 682–737. DOI: 10.1214/13-AOP873.
- [Sag01] B. E. Sagan. *The Symmetric Group: Representations, combinatorial algorithms, and symmetric functions*. Second. Vol. 203. Graduate Texts in Mathematics. Representations, combinatorial algorithms, and symmetric functions. New York: Springer-Verlag, 2001, pp. xvi+238. DOI: 10.1007/978-1-4757-6804-6.
- [Sch61] C. Schensted. “Longest increasing and decreasing subsequences”. In: *Canadian J. Math.* 13 (1961), pp. 179–191. DOI: 10.4153/CJM-1961-015-3.
- [Sch63] M. P. Schützenberger. “Quelques remarques sur une construction de Schensted”. In: *Math. Scand.* 12 (1963), pp. 117–128.
- [Sep01] T. Seppäläinen. “Second class particles as microscopic characteristics in totally asymmetric nearest-neighbor K -exclusion processes”. In: *Trans. Amer. Math. Soc.* 353.12 (2001), pp. 4801–4829. DOI: 10.1090/S0002-9947-01-02872-0.
- [Śni06] P. Śniady. “Gaussian fluctuations of characters of symmetric groups and of Young diagrams”. In: *Probab. Theory Related Fields* 136.2 (2006), pp. 263–297. DOI: 10.1007/s00440-005-0483-y.
- [Śni14] P. Śniady. “Robinson–Schensted–Knuth algorithm, jeu de taquin, and Kerov–Vershik measures on infinite tableaux”. In: *SIAM J. Discrete Math.* 28.2 (2014), pp. 598–630. DOI: 10.1137/130930169.
- [Spi70] F. Spitzer. “Interaction of Markov processes”. In: *Advances in Math.* 5 (1970), 246–290 (1970).
- [Sta99] R. P. Stanley. *Enumerative combinatorics. Vol. 2*. Vol. 62. Cambridge Studies in Advanced Mathematics. With a foreword by Gian-Carlo Rota and appendix 1 by Sergey Fomin. Cambridge: Cambridge University Press, 1999, pp. xii+581. DOI: 10.1017/CBO9780511609589.
- [Sun18] W. Sun. *Dimer model, bead model and standard Young tableaux: finite cases and limit shapes*. 2018. arXiv: 1804.03414 [math.PR].

INSTITUTE OF MATHEMATICS, POLISH ACADEMY OF SCIENCES, ŚNIADECKICH 8,
00-656 WARSZAWA, POLAND

Email address: lmaslanka@impan.pl

INSTITUTE OF MATHEMATICS, POLISH ACADEMY OF SCIENCES, ŚNIADECKICH 8,
00-656 WARSZAWA, POLAND

Email address: psniady@impan.pl